

AD-A104 364

PANAMETRICS INC WALTHAM MASS
ADVANCED FUEL FLOWMETER FOR FUTURE NAVAL AIRCRAFT (U)
JUN 81 L C LYNNWORTH, N E PEDERSEN

F/G 21/4

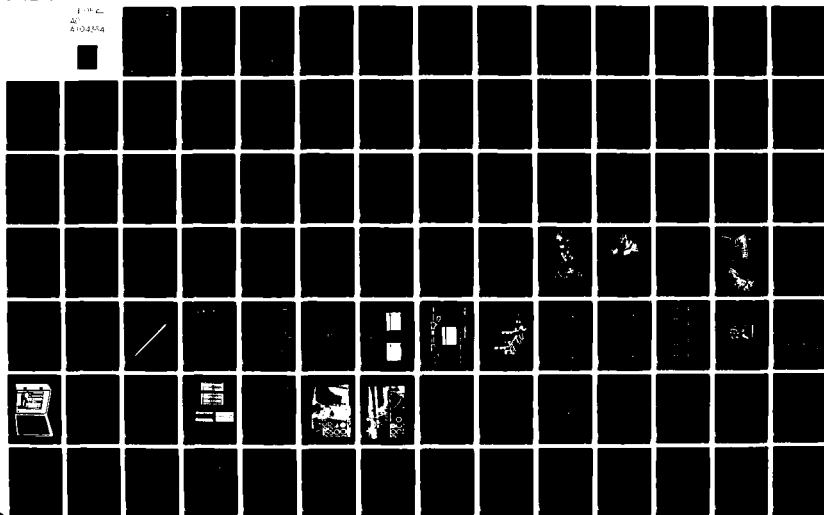
N62269-78-C-0069

UNCLASSIFIED

NADC-80254-60

NL

FORM
AD
A104514



NADC 80254-60

AD A104364

ADVANCED FUEL FLOWMETER FOR FUTURE NAVAL AIRCRAFT

(Contract N62269-78-C-0069)

L. C./Lynnworth, N. E./Pedersen, J. E./Bradshaw, J. E. Matson, E. S. Johansson/
and T. H. Nguyen

Panametrics, Inc.
221 Crescent Street
Waltham, Massachusetts 02254

28 Jun 1981

Final Report

Prepared for
NAVAL AIR DEVELOPMENT CENTER
Warminster, Pennsylvania 18974

DTIC FILE COPY

Approved for public release; distribution unlimited.

81 9 17 042

Unclassified (28 June 1981)

SECURITY CLASSIFICATION OF THIS PAGE (When Data Entered)

REPORT DOCUMENTATION PAGE		READ INSTRUCTIONS BEFORE COMPLETING FORM
1. REPORT NUMBER NABC-80254-60	2. GOVT ACCESSION NO. AD-A104364	3. RECIPIENT'S CATALOG NUMBER
4. TITLE (and Subtitle) ADVANCED FUEL FLOWMETER FOR FUTURE NAVAL AIRCRAFT		5. TYPE OF REPORT & PERIOD COVERED Final Report Dec. 1977 to April 1981
6. AUTHOR(s) L. C. Lynnworth, N. E. Pedersen, J. E. Bradshaw, J. E. Matson, E. S. Johansson, and T. H. Nguyen		7. PERFORMING ORG. REPORT NUMBER Job 138 Final Report
8. PERFORMING ORGANIZATION NAME AND ADDRESS Panametrics, Inc. 221 Crescent Street Waltham, MA 02154		9. CONTRACT OR GRANT NUMBER(s) N62269-78-C-0069
10. CONTROLLING OFFICE NAME AND ADDRESS Naval Air Development Center Warminster, PA 18974		11. PROGRAM ELEMENT, PROJECT, TASK AREA & WORK UNIT NUMBERS
12. MONITORING AGENCY NAME & ADDRESS (if different from Controlling Office)		13. REPORT DATE 28 June 1981
		14. NUMBER OF PAGES 145
		15. SECURITY CLASS. (of this report) Unclassified
		16a. DECLASSIFICATION/DOWNGRADING SCHEDULE
16. DISTRIBUTION STATEMENT (of this Report) Approved for public release; distribution unlimited.		
17. DISTRIBUTION STATEMENT (of the abstract entered in Block 20, if different from Report)		
18. SUPPLEMENTARY NOTES		
19. KEY WORDS (Continue on reverse side if necessary and identify by block number) <div style="display: flex; justify-content: space-between;"> <div> Ultrasonics Mass flowmeter Flow meter Flow profile </div> <div> Flow velocimeter Densitometer Fuel Flow Area averaging </div> <div> Zigzag flow cell Axial offset flow cell Clamp-on flowmeter </div> </div>		
20. ABSTRACT (Continue on reverse side if necessary and identify by block number) A fuel mass flowmeter was developed with the objective of accurately measuring the mass flow rate \dot{M} of various fuels and their mixtures, for flow rates from 91 to 11,364 kg/hr (200 to 25,000 lb/hr). The delivered system included (1) an area averaging zigzag flow velocimeter cell, in which the fuel was interrogated in opposite directions by an alternating sequence of ultrasonic pulses, to determine the area averaged flow velocity \bar{V} ; (2) a densitometer based on the Clausius-Mosotti law, in		

DD FORM 1 JAN 75 1473 EDITION OF 1 NOV 65 IS OBSOLETE

Unclassified (28 June 1981)

SECURITY CLASSIFICATION OF THIS PAGE (When Data Entered)

Unclassified (28 June 1981)

SECURITY CLASSIFICATION OF THIS PAGE (When Data Entered)

which the fuel density ρ is determined; (3) electronics which computed ρ and V separately, and then generated a square wave output having a frequency proportional to the product of ρ and V , namely, $\dot{M} = \rho VA$, where A = velocimeter cell cross sectional area. The transducers can operate beyond the temperature range -38 to $+150^\circ\text{C}$, and the flow cell, with transducers, at pressures up to 1500 psig and in the 3-axis, 20 g, 5 to 2000 Hz vibration environment specified by MIL Std. 810-514.1, except for noise problems at a few discrete frequencies. Ultrasonic and turbine flowmeter data were compared using a fuel substitute (Stoddard solvent) for \dot{M} between ~ 43 and 14,300 kg/hr. In water calibration tests, at V from 0.1 to 38 ft/s (water \dot{M} from ~ 150 to 60,000 lb/hr) [30 mm/s to 11.6 m/s, or ~ 70 to 27,000 kg/hr] flow velocity, linearity, and accuracy of better than 0.5% full scale was observed using the equipment delivered at the end of the program. To determine repeatability, a 10-day test was conducted with water flowing through an offset cell of 6 mm inside diameter, at a velocity between 0.5 and 4.4 ft/s (~ 150 and ~ 1500 mm/s). The velocity was controlled by the pressure of a variable height water column. Repeatability (one standard deviation) was 0.2% of reading at ~ 1500 mm/s and 2% of reading at ~ 150 mm/s. In the final Stoddard solvent (7024 B II) tests, the rms deviation from linearity was $\leq 1.7\%$ of the reading for flow rates above 5 % of the maximum \dot{M} encountered in these tests, 14,300 kg/hr (31,450 lb/hr). Based on a full scale rating of 11,364 kg/hr (25,000 lb/hr) rms deviation from linearity was demonstrated to be about 1% of full scale, with a 2 s response time. Up to 0.5% of this nonlinearity may be due to the turbine sensors' own error band. Above 9000 lb/hr, for 3 runs, the average nonlinearity is less than 0.77% of the actual flow rate. The stability of the waveforms observed for the zigzag flow cell at the maximum flow rate encountered in the fuel substitute test (14,300 kg/hr, or 31,450 lb/hr) and in the water tests ($V = 11.6$ m/s, or 38 ft/s) suggests that a longer zigzag path could be used in the future. This would improve the resolution at low rates and, together with some other modifications to the cell and transducer, ought to improve linearity in the lower part of the system's range. Alternatively, linearization may be accomplished in the software, at least for nonlinearities mainly dependent on V .

Accession For	
NTIS GRA&I	<input checked="" type="checkbox"/>
DTIC TAB	<input type="checkbox"/>
Unannounced	<input type="checkbox"/>
Justification	
By	
Distribution/	
Availability Codes	
Avail and/or	
Dist	Special
A	

DTIC
ELECTE
SEP 17 1981
D

Unclassified (28 June 1981)

SECURITY CLASSIFICATION OF THIS PAGE (When Data Entered)

M. J. ...

TABLE OF CONTENTS

	<u>Page</u>
I. INTRODUCTION	
A. Need for Mass Flow Rate Measurements	1
B. Background on Related Work	2
C. Distinctions Over Prior Work	4
D. Comparison with Present Objectives of Other Organizations	6
E. Summary of Theory	6
II. DESIGN CONSIDERATIONS AND ALTERNATIVES	8
A. Hydrodynamic Considerations/Flow Profile	8
B. Electronic Alternatives Considered	9
1. RF Burst	9
2. Phase Locked Loop	12
C. Flow Cell Alternatives Considered	12
1. Axial Path, Offset and/or Manifolded Considerations	13
a. Medium Diameter, Optionally Including Densitometer Tubes	13
b. Small Diameter, for Low Flow Rates	14
2. 45° Zigzag Path, Minimally Obstructed	14
3. Bypass and Valved Combinations - Concepts for Maximum Rangeability	15
D. Densitometer Alternatives Considered	16
1. Nuclear Densitometer	16
2. Temperature-Dependent Densitometer	16
3. Float-Type Densitometer	16
4. Resonant Vane	16
5. Reflectance-Type Acoustic Impedance Probe	16
6. Slow Torsional Wave Densitometer	17
7. Capacitance-Type Densitometer	17
III. MASS FLOWMETER FOR PRESENT PROGRAM	18
A. Selected System	18
B. Description of Electronics for Flow Velocity and Mass Flow Rate Determination	18
C. Description of Flow Velocimeter Cell and Transducers	20
D. Description of Densitometer	24

TABLE OF CONTENTS (cont'd)

	<u>Page</u>
IV. TEST PROCEDURES AND TEST RESULTS	25
A. Accuracy	25
B. Rangeability	33
C. Repeatability	33
D. Hysteresis	33
E. Linearity	34
F. Response Time	34
G. Vibration	35
H. Temperature	35
I. Pressure	35
J. Self-Testing of Flow Velocimeter Electronics: Differential Path	38
V. CONCLUSIONS	40
VI. ACKNOWLEDGMENTS	40
VII. REFERENCES	41
VIII. LIST OF ILLUSTRATIONS & ILLUSTRATIONS	42
IX. APPENDIXES	
A. OBJECTIVES/EXTRACTS FROM NADC STATEMENT OF WORK	A-1
B. LIST OF MATHEMATICAL SYMBOLS	B-1
C. DERIVATION OF V EQUATIONS	C-1
D. FLOW VELOCIMETER ELECTRONICS	D-1
E. RESPONSE TIME TEST DATA (DATA OBTAINED WHILE FLOW VELOCITY CELL WAS UNDER X-AXIS 20 g DWELL AT 2000 Hz, 17 Sept. 1980, ATL)	E-1
F. EXTRACT FROM NASA RFP	F-1
G. CLAMP-ON AND OFFSET ALTERNATIVES FOR THE FLOW VELOCIMETER	G-1
H. HYDROSTATIC PRESSURE TEST REPORT	H-1
I. TEMPERATURE TEST DATA	I-1
J. REPORT OF TEST ON ZIG-ZAG FLOW CELL SINE VIBRATION TESTING FOR PANAMETRICS	J-1
K. FINAL SYSTEM TEST IN FUEL SUBSTITUTE 7024 B II	K-1
L. NAVY MASS FLOWMETER INITIAL SET-UP	L-1

I. INTRODUCTION

A. Need for Mass Flow Rate Measurements

The purpose of the proposed development effort was to provide NAVAIRDEVCON with a highly accurate, rugged and reliable fuel mass flowmeter. The ideal flowmeter would be sufficiently versatile so that it could be employed for engine diagnostics in future engines of the type anticipated for advanced type A aircraft (subsonic) and later, type B aircraft (supersonic). Accordingly, a flowmeter was sought which had the potential for being optimized with respect to many capabilities and characteristics, including the following:

- o Accurate measurement of mass flow rate of JP-4, JP-5 and their mixtures
- o Repeatability
- o Hysteresis
- o Vibration (cell, electronics)
- o Rangeability $\geq 250:1$, possibly $\sim 800:1$
- o Flow cell materials, shape, dimensions and weight; quick disconnect type fluid connectors; and cell mounting means
- o Response time = 2s
- o Square wave (digital) signal output, capable of multiplex operation
- o Contaminated fuel: operation without clogging or degrading
- o Temperature = -38°C to $+150^{\circ}\text{C}$ (fuel), and even higher soak-back temperature (est. 200°C)
- o Pressures to 1600 psig
- o Laminar, transitional and turbulent flow profiles
- o Minimum number of conductors between flow cell and cockpit-installed electronics (≤ 4 desired)
- o Power source: 28V dc; design shall include 115V, 400 Hz option
- o Totalized volumetric (Q), or mass (M) for convenience in troubleshooting and calibration

These needs were expressed by NAVAIRDEVCON in 1977, and were addressed during the course of the contract. The relevance of these needs is apparent if one compares them (Section I-D) with needs expressed three years later by other organizations (e. g., NASA) concerned with gas turbine engine diagnostics and/or control.

Many types of flowmeters are presently available, such as, magnetic, fluidic, nuclear magnetic resonance, turbine, vortex shedder, pitot tube, orifice plate, coriolis, venturi, target., ultrasonic, etc. Some of these would have to be combined with a densitometer to yield mass flow rate. (Dowdell, 1974; Sturdivant et al., 1978). However, if one seeks a mass flowmeter which has no moving parts, minimum obstruction to the flow, small size and light weight, wide rangeability, etc. (see Appendix A) the choice narrows considerably, and in fact at the program's outset in Dec. 1977 it was obvious that no equipment that was commercially available could satisfy all the requirements and objectives. Some of the objectives are still unattained, partly due to funding and schedule constraints, and partly due to the state of the art.

Besides at least a twenty-five year diagnostic need for measuring mass flow rate in military and commercial aircraft engines (Kritz, 1955), there remains a control need which differs somewhat from the diagnostic need. While diagnostic needs exist both on the ground (engine test stands) and in the air, control needs are obviously most important in-flight. For control applications, accuracy may sometimes be relaxed slightly, perhaps to $\pm 2\%$ of range, but response time is much more stringent, 20 ms sometimes being required, i. e., 100 times faster than the present contract's diagnostic response time objective.

Aside from the need for accurate \dot{M} data per se, a totalized or time-integrated measurement of $\int_0^t \dot{M} dt$ yields the mass of fuel burned, from which fuel remaining can be calculated. In other words, a fuel mass flowmeter can serve as a fuel quantity instrument.

B. Background on Related Work

In April 1971 Panametrics responded to the Army's Eustis Directorate advertised RFP for improved diagnostic instrumentation for aircraft engines. On 28 June 1971 Eustis awarded Panametrics our first contract to develop an ultrasonic fuel mass flowmeter.

Our original proposal offered a unique combination of a doppler flow velocimeter (the doppler shift is proportional to V/c , where V = flow velocity and c = sound speed in the fuel) and an acoustic impedance (ρc) densitometer. The product of $(V/c)(\rho c) = \dot{M}/A$, the mass flow rate per unit area. As our tests and scattering analysis proceeded, it became evident from the data that clean fuel could not scatter enough sound to enable a fast response ultrasonic doppler system to provide accuracy better than a few percent, say $\sim 5\%$. N. E. Pedersen soon found an alternate way to measure flow velocity. This alternate way involved a pseudo random noise (PN) code which phase-modulated 5 MHz cw waves. The area-averaging flow cell used in this first Eustis program is shown in Fig. 1, exploded view, and Fig. 2 shows this cell assembled, and also shows the PN flowmeter block diagram.

We have continued to use modulated cw in some of our flowmeters, but for several technical reasons we now use amplitude modulation rather than phase modulation. The amplitude modulation method, now patented, is described by its inventors, Pedersen and Bradshaw in their patent (1977) and in the Proc. of the 1977 NBS/AIP/ISA Symp. on Flow. Our second Eustis contract, covering the period January 1973 to June 1975, supported the fabrication and testing of an amplitude-modulated flow velocimeter, i. e., the use of coherent rf bursts. During this second contract, we learned of the capabilities of Simmonds Precision's (SP) capacitance-type densitometer. Test data made available to us, plus published accuracy data for JP-4 and JP-5 (Stuart, 1974) showed that the capacitance densitometer was likely to be more accurate than our ρc densitometer available at that time. We therefore obtained on loan one of SP's densitometers and used it in calibration tests at Avco Lycoming in December 1974. Precision of the SP densitometer was found to be 0.1% or better. Precision of the entire \dot{M} system (Panametrics ultrasonic flow velocimeter plus SP dielectric densitometer) was 0.25% FS, and linearity $\sim 0.1\%$ FS.

In view of these results, in June 1976 we were awarded a third contract from Eustis to particularize the design for GE's T-700 engine, for the \dot{M} range 100 to 1000 lb/hr.

Fabrication and testing of the 5 MHz Eustis electronic design shown in Figs. 3 and 4a, and the cell of Fig. 4b was completed shortly before the present Navy program began in Dec. 1977.

The status of the Eustis work at the end of the third contract was reported by Lynnworth, Pedersen, Seger and Bradshaw (1978). This report described in detail how the fuel mass flowmeter system (previously demonstrated in the second Eustis program, and consisting of an ultrasonic flow velocimeter and a capacitance-type densitometer) was adapted to T-700 gas turbine engine requirements. Mechanical adaptations included the reduction in size and weight of the flow cell to fit the configuration and mounting constraints of a T-700 engine. Electronic developments included repackaging into a portable field-type case, configuration switching and digital delay equalizers, and the substitution of a microprocessor for a previously-used calculator chip, resulting in a choice of response times, or integration times, selectable from ~ 50 s down to ~ 0.5 s. Test results were presented for 7024 Type IIB calibrating fluid over the mass flow rate range $\dot{M} = 40$ to 1200 PPH, for temperature near 70°F (21°C), and for pressures up to 1500 psig. Performance of the system was discussed with respect to laminar, transitional, and turbulent flow profiles associated with Reynolds numbers from ~ 50 to $\sim 50,000$ and with respect to geometrical constraints imposed by the T-700 configuration.

C. Distinctions Over Prior Work

At the time the present work was proposed, July 1977, it was planned to modify the Eustis system to meet the Navy requirements. The differences in requirements and objectives between Eustis and NAVAIRDEVCON are summarized in Table 1. Shortly after the time the Navy program got underway, in early 1978, it became apparent to the principal investigators that a new phase locked loop electronic approach quite distinct from the Eustis rf burst system merited consideration. Accordingly, both of these approaches are reviewed in section IIB. See also, Appendix C.

Three years later, in July 1980, the new broadband phase locked loop (PLL) technique had been demonstrated over a wider range of flow rates, with numerous fluids and with a wider variety of transducer and flow cell combinations, than had been achieved with the rf burst or any other earlier Panametrics flowmeter approach. The PLL technique, however, being broadband, inherently has resolution and acoustic noise limitations which are not as good as the rf burst method. For example, the present PLL resolution limit is 1 ns, as compared to the rf burst resolution of 0.2 ns achieved previously at a carrier frequency of 5 MHz. The PLL bandwidth typically exceeds 100% of the center frequency; the rf burst bandwidth is typically 10%.

In retrospect, considering the various tradeoffs between the PLL, rf burst and other methods, we conclude that the PLL method was indeed the most appropriate method to use in this contract. The performance achieved in this contract represents results on two area averaging flow cells (zigzag path in square holed sleeve, and offset) with the first PLL velocimeter of the "Model 6000" type. It is reasonable to expect that improvements in the flow cell, the transducers, and the electronics (hardware, firmware and software) will lead to improved performance in the future.

Table 1. Comparison of Eustis and Navy Requirements and Objectives

REQT OR OBJECTIVE	EUSTIS	NAVAIRDEVCON
Fuels	JP-4, -5 mixtures; Contaminated*	Same types of fuel(s)*
M, lb/hr	100-1000	200-25,000 (80,000)
Accuracy	$\pm 0.5\%$ FS	$\pm 0.5\%$ R, 3000-25000 PPH; $\pm 5\%$ R at 100 PPH
Hysteresis	-	$\pm 0.3\%$ of reading (R)
Repeatability	-	$\pm 0.1\%$ R, 3000-25000 PPH $\pm 2\%$ R, 200 PPH
Cal. Temp. Range, °C	+10 to +46	-38 to +150
Response Time, sec.	5	2
Signal Output Format	-	Sq. wave, $f \propto \dot{M}$; muxable
Vibration	810-C, Proc. I**	810-514.1
Power	115V 60Hz	28V dc; optional design, 115V, 400Hz
Wiring	-	4 conductors, 2 pwr, 2 sig; optical option
Flow connectors	1500 psi, AN-3, -4	1600 psi, quick disconnect
Configuration	T-700	V/STOL Type A(B)
Electronic housing	Field type case for helicopter cabin	-
Flow cell weight, lb	< 5 lb if SS, < 1 lb if aluminum	-
Delivery date for complete system	October 1977	October 1979

*4 hr exposure; calibrate before and after. Navy, 300 hr; calibrate during contaminated; fuel contaminated according to Table X, MIL-E-5007 D.

**No flow, room temperature.

D. Comparison with Present Objectives of Other Organizations

The continuing need for improved \dot{M} instrumentation is reflected in needs expressed at present by government and industry. Because of the growing scarcity of fuel, and its rising cost, even minor improvements in engine efficiency are significant. Hence manufacturers of jet engines seek \dot{M} accuracy of 0.1% (i. e. , error < 0.1% of reading).

NASA RFP 3-188129, issued in early 1980, reiterated the need for \dot{M} measurements in fuels such as JP-3, -4, -5, -8 (Type A-1) and Type A with rangeability on the order of 100:1, an accuracy requirement of 0.25% of reading with 0.1% of reading as a goal, and a response time requirement of 25 ms. These and other present design guidelines and specifications are contained in Appendix F for reference and comparison purposes.

E. Summary of Theory

The theory of the present \dot{M} system may be explained in five steps:

1. The mass flow rate \dot{M} is proportional to the product of the average flow velocity \bar{V} and the fuel density ρ .
2. \bar{V} is measured ultrasonically by determining the small difference in transit times in the upstream and downstream directions. Ideally, 100% of the flowing cross section is interrogated, so that the transit times provide area-averaged values independent of the flow profile.
3. ρ is measured dielectrically (capacitively) based on the Clausius-Mosotti law that relates ρ to ϵ , the fuel's dielectric constant. A Simmonds Precision densitometer provides an analog voltage which is empirically related to ρ .
4. A microprocessor - controlled computer performs the necessary calculations to yield \dot{M} .
5. A square wave is generated at a frequency proportional to \dot{M} .

These steps are covered in detail elsewhere in this report, and in the literature. It may be useful, however, to expand on the \bar{V} and ρ ideas in the following paragraphs.

For the contrapropagating transmission method of flow measurement utilized in this program, transit time decreases in the downstream direction and increases upstream. Flow rate is proportional to $(t_1 - t_2)/t_1 t_2$, where the values of t are measured transit times. A valid approximation when $(V/c)^2 \ll 1$ is given by an equation of the form

$$V = (t_1 - t_2) P^2 / 2 L t_1 t_2$$

where P = length of liquid path and L = axial projection of path in flowing liquid.

To retain high accuracy in V despite variable flow profiles it is necessary to calibrate and/or use equipment which properly weights the flow profile. The delivered equipment utilizes an area averaging cell. In contrast to this method, meter factors for conventional flow cells are usually based on the Reynolds number Re . Theoretically, the meter factor $K = 1$ for cells with midradius paths or cells suitably interrogated over 100% of their area. For large diameter pipes interrogated conventionally (tilted diameter path) $K = 0.750$ for laminar flow ($Re < 2000$), $K \approx 0.85$ for transitional flow ($2000 < Re < 4000$) and $K = 1 / (1.119 - 0.011 \log Re)$ for turbulent flow ($Re > 4000$). For example, $K = 0.930$ at $Re = 10^4$, 0.940 at 10^5 , 0.950 at 10^6 , 0.960 at 10^7 .

The electronic approach to measuring V utilizes a modified Panametrics Model 6000 instrument. This instrument transmits pulses sequentially upstream and downstream at two phase locked repetition frequencies whose periods are proportional to the times of flight t_1 and t_2 between transducers. By timing a large number of periods, t_1 and t_2 are measurable to high precision (resolution = 1 ns). The flow velocity V is computed by an equation similar to that given above. (See Appendix C.) The adjustable interrogation rate is factory-wired to avoid errors due to reverberations in transducers, pipe wall or fluid. The number of interrogations to be averaged is chosen to maximize resolution within the allowed response time.

The dielectric constant/density relation used in SP's densitometer is given by the Clausius-Mosotti law $(\epsilon - 1)/(\epsilon + 2) = C\rho$. This is rearranged to yield density as $\rho = (\epsilon - 1) / [a(\epsilon - 1) + b]$ where a and b are empirical constants. By measuring capacitance between concentric tubes, ρ is determined.

Having determined ρ and V , the mass flow rate \dot{M} is determined from their product, taking into account the cell cross sectional area A , and using consistent units, of course.

II. DESIGN CONSIDERATIONS AND ALTERNATIVES

A. Hydrodynamic Considerations/Flow Profile

A full discussion of flow profile is beyond the scope of this report. The interested reader is referred to books by Schlichting (1968) or Streeter (1961) for tutorial coverage of this topic.

For our present purposes it may suffice to simplify or abbreviate the discussion by listing the following relationships:

<u>Reynolds Number</u>	<u>Flow Regime</u>	<u>Flow Profile</u>
< 2000	Laminar	Parabolic
2000 to 4000 (or 10000)	Transitional	Unstable
> 4000 (or > 10000)	Turbulent	Power law

Reynolds number $Re = \rho \bar{V} D / \eta$ where ρ = density, \bar{V} = average flow velocity, D = conduit diameter and η = viscosity. The ratio η/ρ is often denoted ν , the kinematic viscosity.

To obtain a general perspective on the variation of ν with temperature T for numerous fluids, and therefore a perspective on how T influences Re , refer to Fig. 5. The right-hand portion of Fig. 5 yields Re in terms of ν and VD . Thus, at a given ν , say $\nu = 0.01$ stokes (water at room temperature) if $D = 2.54$ cm, then increasing V from 4 to 40 cm/s will increase Re from 1000 to 10000, i.e., laminar to turbulent. Similarly, at $VD = 100$ cm²/s, if ν decreases from 0.1 to 0.01 stokes, Re again ranges from 1000 to 10000.

According to Fig. 6c, the value of viscosities of interest in this program ranges from about 0.3 to 30 cs, or 0.003 to 0.3 stokes. According to Fig. 7, the V range, for a 1 in. x 1 in. duct (25.4 mm x 25.4 mm), is from 1.7 to 300 in./s (4.32 to 762 cm/s). Therefore the min $VD = 4.32 \times 2.54 = 10.97$ cm²/s, and the max $VD = 1935$ cm²/s, or approximately 10 to 2000 cm²/s. Referring again to Fig. 5, we see that Re ranges from ~ 40 to $\sim 7 \times 10^5$. Thus, flow cell and/or analytic (e.g., μ processor) compensation for profile is required in order to obtain accurate results.


We may remark that in the course of contrapropagating ultrasonic flowmeter developments since the 1920's, the importance of flow profile has been recognized since ~ 1950 . A partial list of investigators who published their ideas on how to deal with flow profile is given in Table 2. These contributions are fully referenced, and several are illustrated, in Mason and Thurston (1979), pp. 407-525.

The present contract mainly utilized the eighth area averaging method of Table 2. The principal investigators have used this area averaging method in three previous \dot{M} contracts with satisfactory results. Depending on requirements, however, other cell designs may be preferred for reasons of size, weight, resolution, ease of installation and maintenance, absence of cavities in which gas could be trapped, or cost. See, for example, Fig. 9, especially offset (1B) and clamp-on (8A) designs.

B. Electronic Alternatives Considered

In this section we briefly discuss the rf burst system as originally proposed, e. g., based on the Eustis system reported in 1978, and then we briefly discuss the newer phase locked loop (PLL) approach. By early 1978 the PLL flowmeter approach had been developed as a Panametrics product to the point of demonstrating stability and reasonable linearity. By May 1978 it became apparent that the PLL was likely to emerge as the superior approach to meet the velocimetry objectives, and in fact this approach was eventually selected and utilized in the delivered mass flowmeter system.

1. RF Burst

The rf burst flow velocimeter due to Pedersen and Bradshaw transmits coherent rf bursts () of 50 μ s duration upstream, and then downstream. Each received burst is narrowband filtered. The phase difference between upstream and downstream directions, $\Delta\phi$, is proportional to the flow velocity divided by c^2 . In the Eustis system, to eliminate undesired effects of sound speed c , we also filtered at the am frequency, 2 kHz, and the phase of the 2 kHz component provided the c compensation. (In another version of this system, developed for measuring the flow velocity of natural gas, the rf burst center frequency is 100 kHz. See Pedersen et al., 1977).

A μ processor combines ρ , V , and the flow cell geometry to yield the desired mass flow rate \dot{M} , in the Eustis system.

The flow velocity V may be shown to be proportional to $\Delta T / (T_1 + T_2)^2$ where $\Delta T = T_1 - T_2$ and the T 's are transit times measured upstream and downstream.

A block diagram of the Eustis fully coherent electronic system which measured $T_1 - T_2$ and T_1 and T_2 is shown in Fig. 3. It operated as follows. Flow related parameters were measured by using a fully coherent electronic system which operated synchronously from a 5 MHz crystal-controlled oscillator. The transmitted waveform was generated by means of synchronously gating the output of the 5 MHz oscillator for a 50 μ s interval at a 2 kHz repetition rate. Upstream and downstream common-path transmissions were consecutive and spaced 250 μ s apart. Independent measurements were made of the phase difference between the upstream and downstream 5 MHz spectral components of

Table 2. Contributors to ultrasonic area averaging flowmeters using contra-propagating transmission (upstream-downstream transit time) methods.

<u>Inventor(s) or Author(s)</u>	<u>Year(s)</u>	<u>Approach</u>	<u>Remarks</u>
Swengel	1950- 1956	100%	Waveguide antennas communicate over sheet-like unfolded path; $f \approx 25$ kHz; rectangular duct dimensions up to $\sim 5 \times 8$ m.
Kritz	1955 a, b	K	Tilted diameter path; $f \approx 10$ MHz; pipe diameter = 100 mm; graph of K vs Re; questioned whether a path other than the tilted diameter could provide better immunity to flow profile.
Katzenstein & Katzenstein	1961	100% axial	Axial interrogation illustrated for small tube.
Knapp	1964	4- chord	Proposed (but did not demonstrate) use of 4-chord Gaussian quadrature method.
Noble	1968	100%	Demonstrated axial interrogation method; $f \approx 6$ MHz; acrylic tube diameters = 2.38 and 6.35 mm.
Malone & Whirlow	1971	4-chord	Quadrature methods of Gauss, Chebycheff and Lobatto.
Lynnworth etal.	1972- 1979	100% zigzag	Zigzag interrogation over square- or rectangular-enveloped path; $f = 0.5$ to 5 MHz; duct dimensions from 12.7 to 25.4 mm.
Pfau	1973	\sim Midradius path	Computed optimal distance to be 0.493 of the radial distance for both laminar and turbulent flows.
Lynch and Brown	1974	K	Suggested K be modified electronically as a function of flow velocity V.
Baker & Thompson	1975	\sim Midradius path	Errors calculated for chordal paths at and near midradius; tested in air at $f \approx 40$ kHz in 100 mm duct.
Lynnworth	1975, 1977a	100% axial	Transmitter and receiver transducers in acoustically isolated parts of flow cell.

Table 2. (Cont'd)

<u>Inventor(s) or Author(s)</u>	<u>Year(s)</u>	<u>Approach</u>	<u>Remarks</u>
Lynnworth	1977b, 1978	~ Midradius	Meter factors calculated for narrow-beam chordal paths at and near midradius; folded path along inscribed equilateral triangle ($r \approx 0.5 a$).
Lynnworth	1977	100% axial	Reflectors installed in enlarged bore.
Johnson et al.	1977 a	Tomography	Analysis of multiple chord data allows algebraic reconstruction of three dimensional fluid flow.
Pedersen et al.	1977	K	\bar{V} computed from V and Re based on power law.
Lynnworth	1980	Axial sample	Reflected path at $\sim 3/4$ of radial distance ($r = 0.76 a$).
Lynnworth et al.	1980	K	K switch-selectable; K varied electronically as a function of V or Re.
Meisser	1980, 1981	100% axial	Heat meter uses fixed offset geometry with cylindrical tee manifold, 1 MHz transducers.
Pedersen	1981	Tomography	Volumetric flow rate determined in conduit of arbitrary shape by integration over conduit area using linear equation combinations.

the received waveforms and the phase sum of the 2 kHz modulation components of these waveforms. These two independent measurements were combined to yield the Mach number V/c and V , where V = flow velocity and c = sound speed. High signal-to-noise ratio was achieved by means of narrowband receivers and fully coherent detection, thereby providing distinct advantages in precision and stability over conventional flowmetering techniques which utilize broadband pulses.

One of the limitations on the single frequency (e. g., 5 MHz) rf burst system as just described, is that at high flows, the phase shift may exceed 180° or even 360° , causing ambiguity unless remedies are introduced. If a low carrier frequency is used, to prevent $\Delta\phi$ from exceeding 180° , then at low flows, adequate resolution of $\Delta\phi$ becomes exceedingly difficult. The phase ambiguity problem is aggravated by the present contract's wide temperature range which leads to over a 2:1 sound speed range from ~ 750 to ~ 1600 m/s.

We considered using two different carriers, say 0.5 and 5 MHz, with some overlap, to avoid phase ambiguity at high flow yet retain adequate phase resolution at low flows. However, implementation of this dual-frequency rf burst velocimeter appeared more difficult than the PLL method, which avoids these problems of ambiguity and resolution.

2. Phase Locked Loop

The phase locked loop (PLL) method as utilized in our flow velocimeter originated with N. E. Pedersen. In some respects it resembles singaround circuits that have been used for some thirty years in sound velocimeters and later, flow velocimeters. The basic idea in these systems is to launch upstream and downstream waves at repetition frequencies whose difference Δf is proportional to flow velocity V . Pedersen's concept, which was demonstrated prior to its use in this program, included the use of a VCO which, at steady flow, would normally control the launching of pulses at frequencies f_1 and f_2 having periods equal to twice the time of flight in the two directions. The phase lock technique assured that lock, once achieved, would maintain the desired relationship. In operation two quasi-dc control voltages V_1 and V_2 corresponded to f_1 and f_2 . Their difference ΔV was an analog measure of the flow velocity V . The initial PLL sequentially interrogated upstream and downstream for equal intervals, e. g., 0.1 s each way.

Two problems with the early model PLL flowmeter were lack of interchangeability of nominally identical VCO's, and repetition frequencies that in some cases were so high that cell reverberations and/or transducer ringdown interfered with obtaining high precision. These problems were solved in the delivered equipment as described in Section IIIB and Appendix C.

C. Flow Cell Alternatives Considered

Figure 9 provides a general perspective on flow cell alternatives that may be considered for contrapropagating transmission ultrasonic flowmeters. In any particular application, the choice is usually governed by pipe size (flow rate), accuracy, geometrical, installation and maintenance constraints, cost and delivery schedule.

If we separate applications according to small, medium and large size pipe (defined dimensionally as 1/8" to 1/2", 1/2" to 2", and 2" to 2m, respectively) then the flow cell designs that will commonly be selected are those depicted in Fig. 10. It will be recognized that the flow cell finally selected for this program basically resembles the "medium" style of Fig. 10, with the "small" style recommended for higher accuracy at the lowest flow rates of interest. See Table 3.

Table 3. Calculated Δt in nanoseconds in small and medium size conduits at $T = -50^\circ\text{C}$ ($\rho = 0.9 \text{ g/cm}^3$, $c = 1600 \text{ m/s}$) and at $T = 150^\circ\text{C}$ ($\rho = 0.65 \text{ g/cm}^3$, $c = 750 \text{ m/s}$, for $L = 4"$ (10 cm).

\dot{M} , PPH	Small Design		Medium Design	
	1/8" Schedule 80 Pipe, ID = 0.3"		1" x 1" Square Hole	
	-50°C	+150°C	-50°C	+150°C
200	48	302	3	19
3000	722	4549	51	321
25000	-	-	425	2678

The Δt values in Table 3 are calculated for the "worst case" lowest temperature condition from the equation $\Delta t = 2LV/c^2$ where V is replaced by $\dot{M}/\rho A$. That is to say, $\Delta t = 2LM/\rho A c^2$, where A = conduit cross sectional area. At the high temperature, the Δt values increase over the low temperature values by a factor of $(\rho_{\text{max}}/\rho_{\text{min}})(c_{\text{max}}/c_{\text{min}})^2 = (0.9/0.65)(1600/750)^2 = 6.3$.

1. Axial Path, Offset and/or Manifolded Configurations

This category includes "medium diameter" designs having an internal dimension on the order of 1" (25.4 mm), and also, "small diameter" designs, with a conduit size in the range of standard 1/8" to 1/2" pipe, for low flow rates. As early as 1954, Kalmus reported on a method for interrogating effectively along a substantially axial path in a plastic tube. Practical axial interrogations, however, awaited later methods, i. e., offset designs.

a. Medium Diameter, Optionally Including Densitometer Tubes

The concept of interrogating along the axis of an offset section of conduit has been considered by several investigators since Katzenstein and Katzenstein (1961). Some of these investigators have pointed out the area-averaging advantage of a conduit whose full cross section is interrogated.

In May 1978, N. E. Pedersen suggested using an axial interrogation cell in which transducers would be installed at each end of a pipe section, and communicate right through the Simmonds Precision (SP) densitometer. Pedersen also suggested using symmetrical streamline inlet and outlet

transitions, and possibly additional flow control surfaces. Because the flow cell design had to be frozen before this concept could be fully investigated, the delivered cell design resembles the Eustis velocimeter cell of Fig. 4. However, we tested the axial path right through the SP tubes, shortly after they were received in July, 1979. Results at no flow were encouraging: good signal, little reverberation (see Fig. 11). Accordingly, more work with this concept may prove worthwhile, whether the subsequent densitometer is based on dielectric constant or torsional wave principles (Lynnworth, 1977b, Fig. 13). See also, Appendix G.

b. Small Diameter for Low Flow Rates

For a constant volumetric flow rate Q , Δt is inversely proportional to A . Therefore, the use of small diameter tubes to increase the flow velocity, and hence increase Δt , has been considered by several flowmeter manufacturers. Some designs were reported by Lynnworth (1977a and 1979), including contributions from Bradshaw. Examples of such cells are given in Fig. 12. (See also, Fig. 10, top, and Appendix G.)

The cells of Fig. 10 (top) and some of those in Fig. 12 have several features apparently unavailable from other manufacturers of ultrasonic flowmeters:

- o 45° inlet and outlet fittings, for less pressure drop than 90° tees provide (Bradshaw, ca. 1977, unpublished).
- o Acoustically isolated transmitter and receiver parts in which the transducers are installed (Lynnworth, 1975).
- o Metallurgically-sealed transducer housings, optionally containing an acoustic impedance matching member between the piezoelectric transducer and the stainless steel front layer (Lynnworth, Fowler and Patch, 1979, unpublished).

Limits due to the pressure drop at high V , nonlinearity due to end effects, asymmetrical flow profile, and potential cavitation are drawbacks to this design.

2. 45° Zigzag Path, Minimally Obstructed

This design is based on the area-averaging principles used in all three Eustis contracts. See, for example, Figs. 1, 2, 4 and 10 (middle). Collimated beams interrogate the entire cross section of fluid passing through the square holed sleeve within the cell. The square holed sleeve also makes it easy to interrogate along an axially-extended in-line low-pressure-drop path by bouncing the collimated beams in zigzag fashion, achieving $L = 4D$ in the delivered cell. Thus, the square holed sleeve provides 100% in-line area averaging to minimize profile effects, and, in contrast to a round pipe, also provides for distortion-free multiple reflections to increase sensitivity, since Δt is proportional to L . The deliverable flow cell design finally selected for this program is shown in the photograph of Fig. 13, and in outline form, in Fig. 14. This cell includes optional ports for a torsional wave densitometer, as will be

described in Sections IID2 and IIIC. In simpler form, without these optional ports, the selected flow velocimeter cell for this program is shown in outline form in Fig. 15. This simplified illustration also shows the positions of the square holed sleeve and transducers.

The delivered cell uses the longest (6" or 15 cm) square-holed one-piece stainless steel sleeve that was commercially available without involving special tooling. This square-holed sleeve has an axial hole 1" x 1" (25.4 mm x 25.4 mm) through which all the flowing fuel passes. The conically chamfered inlet and outlet desirably reduce turbulence and pressure drop, but undesirably reduce the maximum axial distance over which zigzag interaction can occur to $L = 4"$ (10 cm). Ports for transducers are screened to reduce eddy formation at or near the ports.

The only practical problem encountered so far with this design is that air bubbles are occasionally trapped in the transducer ports. To avoid this potential problem, the cell should be installed with the transducer ports below the horizontal plane passing through the sleeve axis, e. g., transducer ports on bottom. If the cell axis can not be maintained in a horizontal or nearly-horizontal plane, then the alternative geometry of Fig. 16 may be necessary.

If a longer cell were desired, so as to increase L , one could elongate the housing and install two (or more) relatively standard square holed sleeves, each having a maximum length of 6" (15 cm).

3. Bypass and Valved Combinations - Concepts for Maximum Rangeability

The flow velocity range is given by $(\dot{M}_{\max}/\dot{M}_{\min})(\rho_{\max}/\rho_{\min}) = (25000/200)(0.9/0.65) = 173$, or nearly 200:1. Initially it had been desired to cover \dot{M} down to 100 PPH, which would have doubled the rangeability (turndown ratio) to nearly 400:1.

Two concepts have arisen which might be useful in some circumstances. M. McDonald suggested using a bypass, so that at low flow, all the fuel would pass through the single sensing region. At high flow only a small and presumably known fraction would be sensed.

A second and somewhat related concept is to use two flow cells, one small, one medium (Fig. 10), and an electronically actuated diverter valve. Here, all the fuel is to be sensed either in one cell or the other. For example, the small cell would cover \dot{M} up to perhaps 500 PPH, and the medium cell, \dot{M} from 500 to 25000 PPH. Provision would have to be made to divert automatically but not toggle when \dot{M} was right near the switch point, 500 PPH in this example.

D. Densitometer Alternatives Considered

Seven types of densitometers were considered. The advantages and limitations are summarized below, including reasons for rejecting all but the last type, the SP capacitance - type.

1. **Nuclear Densitometer.** Measures fuel density substantially independent of composition or temperature. Rejected because: radioactive source required; high activity required for fast response; development cost considered prohibitive.
2. **Temperature-Dependent Densitometer.** Measures fuel temperature, computes "nominal" or average density for a specified fuel type. Rejected because: errors could exceed 5% due to density variations in a specified fuel even at room temperature.
3. **Float-Type Densitometer.** Might be usable in fuel tank or in ground testing. Rejected because: does not measure ρ in flow cell; cannot measure ρ transients; sensitive to vibration and acceleration, especially in-flight conditions.
4. **Resonant Vane.** Response derived from Newton's law, $F = ma$. Provides a resonant frequency output signal which is nonlinearly related to the fuel density surrounding the probe. Linearized electronically. Manufactured by Agar, ITT-Barton, Solartron, others. Rejected because: size was too large; it required a 2 inch pipe, the vane's support ring alone being 1.5 inch diameter.
5. **Reflectance-Type Acoustic Impedance Probe.** Responds to characteristic acoustic impedance (ρc) of fuel, where c = sound speed in fuel. In principle, ρc could be combined with a "velocimeter" measurement of V/c (the Mach number). This combination could provide a flush-mounted, noninvasive measurement of fuel \dot{M} . Investigated by Panametrics in previous contracts but abandoned in favor of capacitance type. [More recent designs of shear wave impedometer probes, such as those illustrated in Fig. 16 which provide a number of bounces between transmission and reception, may prove useful in the future. However, 1% or better accuracy has not yet been demonstrated. (Lynnworth, 1979; Lynnworth, Seger and Bradshaw, 1980.)] Rejected because: initial designs were not sufficiently ρc -sensitive or stable, but were sensitive to temperature effects in probe; accuracy may degrade if contaminant builds up on surface.

6. **Slow Torsional Wave Densitometer.** New device based on discovery in 1976 by one of the principal investigators that the speed of a torsional wave at a frequency of ~ 0.1 MHz that is guided in a noncircular waveguide, is inversely proportional to the density of the surrounding liquid. Requires only 2 electrical conductors, which could be the same ones used for the V measurements. Under development for nuclear application in two-phase water/steam mixture (Lynnworth, 1977b; Arave, 1978, 1979.) [See Recommendation IV A.] Rejected because: accuracy not yet demonstrated to be good enough; probe requires temperature compensation; mounting may be difficult.
7. **Capacitance- Type Densitometer.** Based on Clausius-Mosotti relationship between fuel density and dielectric constant (Stuart, 1974). Hardware manufactured by several vendors. Simmonds Precision (SP) provides the best, to our knowledge, and their equipment has been calibrated and used extensively in aircraft and in JP-4, JP-5, etc. The SP equipment was used in our previous Eustis program and performed satisfactorily. It was therefore selected by us for use in our present program, despite the size and intrusiveness of the coaxial tubes and supports required for responding to the fuel's dielectric constant, and potential problems with water in the fuel, and some shift in calibration with different fuel types, and high temperature nonlinearity. This densitometer was selected because: it appeared to meet all accuracy, rangeability, fuel types and other requirements, and was compatible with the rest of our M system.

III. MASS FLOWMETER FOR PRESENT PROGRAM

A. Selected System

Figure 18 shows in block diagram form the selected \dot{M} system. It consists of a "spoolpiece" containing the SP densitometer at the inlet or outlet end, the Panametrics ultrasonic flow velocimeter, and optionally, quick-connect valved fittings. The electronics consists of a modified model 6000 flow-meter instrument connected to a SP densitometer electronic module, the system providing a square wave output proportional to \dot{M} . If it is desired to operate the V part with clamp-on transducers, or other cells, this can be accommodated in the software (Appendix G).

B. Description of Electronics for Flow Velocity and Mass Flow Rate Determination

The ultrasonic flow velocimeter electronics consists essentially of two basic parts: the phase locked loop controlled signal section (Section 1) and the digital computer section (Section 2). The first section generates, transmits and receives the ultrasonic signals. It also produces outputs that are fed to the second section. The computer section accepts the output of the first section and calculates the flow velocity. The computer also runs any displays or outputs, and can be optionally formatted in different units and scales. See Fig. 8. (Appendix C contains a more detailed description.)

The first section consists of a modified phase locked loop (PLL). The output of the voltage controlled oscillator (VCO) is used to generate 15V transmit pulses that are sent to the upstream or downstream transducer, depending upon the state of the configuration switch (CS). The CS determines which transducer acts as transmitter and which acts as receiver. The CS changes state (from upstream to downstream and vice versa), when a fixed number of transmit pulses have occurred. This way both upstream and downstream configurations always involve the same number of transmitted pulses. After propagating over the liquid fuel in the flow cell, the received pulses are detected and amplified by an automatic gain controlled (AGC) amplifier. The amplified received pulse is detected by a zero crossing detector (ZCD). The output of the ZCD is fed to the phase detector along with the original VCO output. The 50% duty cycle point of the VCO's output and the output of the ZCD (receive signal) are compared (phase detected) and any difference in time between them is used to correct the VCO's frequency so that the output of the phase detector is maintained as close as practical to zero. This ensures that the time between transmit pulses is essentially twice the transit time of the ultrasonic pulse from transmitter to receiver transducer. (Typical received signals obtained using JP-5 at various flow rates are shown in Fig. 22.)

Since the time of transit of the ultrasonic pulse from transmitter to receiver transducer is increased when the ultrasonic wave propagates against the flow, but decreased when propagating with the flow, the output frequency of the VCO will be changed accordingly as the PLL tracks the changing transit times t_1 and t_2 . (Various pulse widths, blanks, filters and thresholds are selected to optimize system performance and minimize interference from spurious pulses or noise.) This means that when the CS is in one configuration, say upstream, the frequency will be less than the no flow condition. When this CS is in the downstream configuration, the VCO frequency will be greater than the no flow frequency. Since both upstream and downstream configurations use exactly the same number of pulses, N , the total time that the CS is in either configuration will proportionately increase or decrease in response to the flow velocity. As the flow increases the total upstream time $2Nt_1 = T_1$ increases and the total downstream time $2Nt_2 = T_2$ decreases. The output of the CS is fed to the second section where each configuration time T_1 and T_2 (number of pulses times period of VCO output) is measured.

The computer section consists of two 24 bit counters, a 10 MHz oscillator and some arbitration logic. The arbitration logic receives the input times from the first section (the output of the CS) and switches the 10 MHz clock back and forth between the two 24 bit counters for the duration of each configuration time. The arbitration logic also tells the computer which time (upstream or downstream) it is measuring and when the measurement is done. The computer then takes the two times T_1 and T_2 (total upstream, total downstream) and performs calculations on them based upon the number of pulses in each direction, the physical dimensions of the flow cell and any scale factors necessary (see Appendix 2). The calculation yields the flow velocity V . The computer can then use the flow velocity to derive the volumetric or mass flow rate Q or \dot{M} respectively using additional information about the cell or the fluid. The computer then outputs the result in a given format and resets the system for the next measurement. In the present program the desired format is a square wave whose frequency is proportional to the mass flow rate.

The response time of the digital portion of the electronic system, if defined as the maximum time required to fully respond to a step change in flow rate, is essentially $2(T_1 + T_2)$. For example, if the average transit time were $250\mu s$, and $N = 1024$, the response time would be $4 \times 250 \times 10^6 \times 1024 = 1.024$ second, or approximately 1s.

The mass flowmeter electronics multiplies ρ and V as follows. The flow velocity V is available in the computer from the previous calculation. The computer is also provided with A , the cross sectional area of the flow cell so that the computer multiplies V times A to obtain Q , the volumetric flow rate, in gallons/sec. The density ρ is obtained from the SP densitometer electronics. The output of the SP electronics is a voltage that is related to density and that voltage is used to calculate actual density in lb/gal by the following relation:

$$\rho = 2.505 \text{ lb/gal} + (19.05 \text{ lb/gal} \cdot \text{volt})(R \text{ volts})$$

where $R = V_{out}/V_{ref}$ and V_{out} is the output voltage of the SP electronics and V_{ref} is the supply voltage for the SP electronics (15V). The output voltage V_{out} is fed to a 12 bit analog to digital converter that is controlled by the computer. The program in the computer tells the A/D to make a conversion and upon completion of the conversion the computer uses the resulting digital code to calculate V_{out} . The computer solves the above equation for ρ and then multiplies the calculated ρ times the calculated Q to yield the mass flow rate \dot{M} in lb per second. This number is then scaled and used as a divisor for a computer using a 1 MHz clock so that the resultant square wave output of the counter is the frequency output proportional to mass flow rate. This square wave output is thus the required measure of \dot{M} .

C. Description of Flow Velocimeter Cell and Transducers

The flow velocimeter (V) cell has been partially described in an introductory manner in Section II C2. Size, weight and other characteristics are as follows:

	SP <u>Densitometer Cell</u>	Panametrics <u>Flow Velocimeter Cell</u>
Length	5" (127 mm)	10-7/8" (276 mm)
Diameter and/or other dimensions	2" diam + elec. connectors	2.5" diam x 5" high
Inlet	1-1/2" NPT male	1-1/2" NPT female
Outlet	1-1/2" NPT male	1-1/4" NPT female
Weight	2.2 lb (1 kg)	10 lb (4.5 kg)
Wetted metals	SS 304	SS 304
Drwg. No.	SP # Rev 473279	Panametrics 138-401

The V cell is functionally equivalent in principle to the design shown in Fig. 10, middle. However, to reduce the weight of standard laterals, the cell body was welded using SS 304 pipe sections, nominally 1.5" schedule 80. A 1.5" 3000 # half coupling, SS 304, was welded to its inlet to adapt to the SP ρ cell. The outlet is tapped 1-1/4" NPT, into which a nipple and Snap-Tite quick-connect valved fitting may be installed.

The axial portion of pipe, in the simplest case (Fig. 15) would be tapped for 1/4-20 set screws which hold the square holed sleeve in place. For permanent installation the set screws could be welded in place.

The square holed sleeve has two transducer ports milled on one side, collimating the interrogating beam to provide the desired square or rectangular beam envelope which then zigzags along the square holed sleeve. The collimating ports are covered with 40 mesh SS 304 wire cloth (0.005", or ~ 0.1 mm wire diameter), spot-welded in place.

We had also considered using a membrane of metal or other material instead of the wire cloth, to further reduce the tendency of the transducer ports to generate eddies. Figure 19 is a plot of the calculated attenuation vs thickness for several candidate membranes. However, it was decided to use screens, as they had been used in previous Eustis contracts without any problem other than bubble retention. It was thought that this problem could be aggravated if a membrane tended to seal the collimating ports. The screen has the further advantage of being transparent, so if the transducers are removed, visual inspection of part of the square hole channel is possible, without removing the entire V cell from a flow loop.

The initial transducer design used 1.25" (31 mm) diameter 2 MHz discs made of a lead zirconate titanate composition with a curie point above 300°C. They were sandwiched between a thin (< 0.1 mm) corrosion-resistant metal shim and an insulated graphite backing. The backing was rigid enough to withstand the 1600 psig design pressure, yet attenuating enough to not limit the pulse repetition frequency. The transducer/backing portion was contained in an all-metal-sealed container or well which was electron beam welded to the end of a conventional 1.25" threaded SS 304 hex head plug. The plug was modified to accommodate a Microdot electrical connector and a gas tight Swagelok fitting and 3/8" (~4 mm) tube which seals and protects the coaxial cable.

The hex head pipe plugs screwed into scooped couplings which had been tungsten inert gas (TIG) welded to the cell body. When the flowmeter is in use, the transducers should be oriented so that air does not get trapped in the transducer ports, i. e., transducers should be downward at least until all gas is removed from the liquid under test.

For extended-well thin-window flow cell geometric parameters were as follows:

fuel path length $P = 7.5$ (~ 525 mm) nominal
axial path length $L = 4.020$ " (~ 100 mm)
duct area $A = 1.010$ in.² (~ 6.3 cm²)

Transducer and cable delays were approximately $t_w = 40 \text{ ns (shims)} + 20 \text{ ns (2 cables)} = 60 \text{ ns}$. If a thick window or buffer rod were placed between the piezoelectric element and the fuel, t_w would increase by $2X/c_1$ where X = window or buffer dimension and c_1 = speed of sound therein.

In the delivered system, 2 MHz, 25 mm diameter lead metaniobate transducers were installed in SS 316 hex head 1.25" pipe plugs. These were bored to provide windows of thickness $X = 30 \text{ mm}$. Transducers were installed in the delivered flow cell, the appropriate constants being:

$$P = 10.8 \text{ in. (274.3 mm)}$$

$$L = 4.020 \text{ in. (102.1 mm)}$$

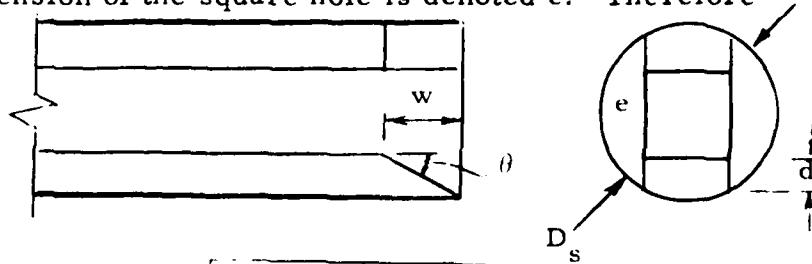
$$A = 1.010 \text{ in.}^2 (6.581 \text{ cm}^2)$$

$$t_w = 10 \mu\text{s}$$

These values were entered in the delivered "constants prom."

Compared to the initial thin window design, the thick window SS plug design sacrifices a few dB of signal (due to impedance mismatch) in exchange for simpler, more rugged construction and ease of self-testing. Regarding the latter advantage, each thick window transducer can be self-tested in the pulse-echo mode as a function of temperature, e. g., in liquid nitrogen at -196°C , boiling water at $+100^\circ\text{C}$, oven at $+150^\circ\text{C}$, etc. The thick window transducer is more resistant to corrosion, impact, abrasion and pressure, and its wetted face can be contoured to reduce the amplitude of triple transits within the fuel path to shorten the response time or to allow more interrogations within a given response time.

Some additional remarks on the square holed sleeve follow. In Fig. 16, if the recessed reflecting face is to extend the full width of the square hole (i. e., 1 inch or 25.4 mm) then the minimum diameter of the square holed sleeve, D_s , may be calculated as follows. Referring to the accompanying sketch wherein the axial projection of the reflecting face is denoted w , its maximum depth d is given by $d = w \tan \theta$. (For a 45° zigzag path, $\theta = 22.5^\circ$.) The edge dimension of the square hole is denoted e . Therefore



$$D_s = 2\sqrt{(e/2)^2 + (e/2 + d)^2}$$

$$= 2\sqrt{\left(\frac{e}{2}\right)^2 + \left(\frac{e}{2} + w \tan \theta\right)^2}$$

Now if $w = e/2$ this simplifies to

$$D_s = 2w\sqrt{w + (1 + \tan \theta)^2}$$

For a square holed sleeve having $2w = e = 1$ inch and $\theta = 22.5^\circ = \pi/8$ radians,

$$D_s = \sqrt{0.5 + (1 + 0.4142)^2} = \sqrt{0.5 + 2} = 1.58 \approx \pi/2 \text{ inches}$$

$$= 40.1 \text{ mm}$$

D. Description of Densitometer

This discussion is adapted from Stuart's 1974 paper in which the SP densitometer is described. The well-established relationship between density and dielectric constant for aviation fuels has long been used in aircraft fuel gaging systems.

The hydrocarbons in aircraft fuels are non-polar liquids. For a non-polar liquid, a theoretical relationship between dielectric constant and density is the Clausius-Mosotti law

$$(\epsilon - 1)/(\epsilon + 2) = Cp$$

where ϵ = dielectric constant, ρ = density, and C = polarizability. This relationship is rearranged and called the "fuel regression line" in capacitance fuel gaging literature. One fuel regression line is:

$$(\epsilon - 1)/\rho = b + a(\epsilon - 1)$$

where $b = 0.12192$, $a = 0.04112$, and ρ in lb/gal. The polarizability varies only slightly from one hydrocarbon to another hydrocarbon for the principal constituents of aircraft fuels. Thus, the dielectric constant, as expressed by the Clausius-Mosotti law, is a good measure of fuel density. Stuart's paper contains a plot of density vs dielectric constant for some typical samples of JP-4. Stuart illustrates what is commonly called "fuel error." This fuel error is the deviation of a given sample from the theoretical best average straight line which is called the "JP-4 line of regression." Further statistical analysis of this and also JP-5 data is also given in Stuart's paper. The interpretation of this plot is that 95.5% of the samples measured (JP-4 and JP-5) fall within 1.3% of the JP-4 line of regression. From these data it is thus possible to predict a 2σ error of 1.3% or less. The data has been further analyzed and 1σ and 3σ errors are included.

To more certainly establish the constancy of this relationship for normal commercial fuels, more recent data was collected by Air Canada and United Air Lines. This data show that of 55 samples, 51 are within $\pm 1\%$ of variation from the JP-4 line. This tends to confirm the previous prediction.

It is known that the Clausius-Mosotti law is nonlinear, statistically corresponding to 0.5% for fuels at $+70^\circ\text{C}$ and -45°C (range, 115°C). For the range -38°C to $+150^\circ\text{C}$ the corresponding nonlinearity needs to be determined.

The particular ρ cell fabricated for this program was tested by SP in JP-5, varying the temperature to change fuel density. According to SP's Owen Clay (priv. comm., July 1979) the data were used to establish an equation of the form

$$\rho = 2.505 \frac{\text{lb}}{\text{gal}} + [19.05 \frac{\text{lb}}{\text{gal}\cdot\text{V}}] \times [R]$$

where R (volts) is obtained by a ratio meter to read the output of the SP signal conditioner in reference to a +15V power supply: $R = \text{output voltage} \div 15$.

IV. TEST PROCEDURES AND TEST RESULTS

A. Accuracy

The principal investigators judge the flow velocity tests to be the most important from among the several different tests specified in the contract. The reason for this judgement is that the densitometer has been proven elsewhere; hydrostatic tests are easily satisfied if adequate thicknesses of flaw-free engineering materials are used; transducers and coupling methods are now available which exceed the temperature objectives of the contract; noise due to vibration should be filterable, given the 2 s response time. Accordingly, except for electronic tests conducted throughout the program, more effort was placed on flow velocimeter tests than on any other test. Nevertheless, due to funding limits and piggy-back schedule constraints, we were unable to conduct as many flow tests as desired; more flow testing is therefore recommended, especially for temperature and/or viscosity ranges not experienced in the present contract.

Because of the inconvenience and high cost of conducting fuel flow calibration tests throughout the development of this contract's flowmeter, we used water for most of the flow velocimeter tests. The complete \dot{M} system, however, was tested at GE-Lynn on several occasions using JP-5 and, finally, the fuel substitute 7024 Type II (Stoddard solvent). In these tests, the reference \dot{M} was based on turbine readings for \bar{V} and ρ which was computed from the temperature of the known fuel or fuel substitute. Density had been checked occasionally with a hydrometer, so the reference \dot{M} determination was considered to be in error by less than 1/2% of reading, from ~ 1000 to ~ 25000 PPH (~500 to ~ 10,000 kg/hr).

The flow cell and flow velocimeter electronics unfortunately did not function properly on the final occasion when the fuel substitute calibration test was conducted at GE. A circuit deficiency, discovered after that test, handicapped the receiver gain by 18 dB. An additional transducer handicap of 12 dB occurred, apparently due to a partial delamination. Therefore, the complete and final delivered system was tested on the fuel substitute only up to 16000 PPH. After this final fuel substitute test, however, the circuit was repaired, the transducers were replaced, and the flow velocimeter was demonstrated at Panametrics in water to over 25000 PPH, the contract \dot{M} objective. (Fuel substitute data are given in Table 4.) Weigh tank water calibration tests were later conducted to 38 ft/s (11.6 m/s) or 60,000 PPH (Table 6, Fig. 30).

To determine the 10-day repeatability of the equipment, a closed-loop system of water flow using gravity feed was utilized. Although water has different density and viscosity than fuel, its fluid dynamics are adequate with respect to the goal of this test. Because of the low flow rates achievable with the gravity feed tester, a different flow cell (offset type) was used in this repeatability test.

Following Bernoulli's theory the velocity of fluid flow in a piping system is proportional to the square root of the gravitational difference in head, and inversely proportional to the square root of the sum of the friction factors due to friction loss in pipe and pipe fittings between any two points. For the system described below the velocity is represented by the equation

$$V_{\text{cell}} (\text{ft/sec}) = \left[\frac{2g (\Delta H - \Delta H_{\text{manometer}})}{0.586 + 93.17 f_{\text{tube}} + 53.4 f_{\text{ss}}} \right]^{1/2} \quad (4-1)$$

where ΔH (feet) = difference of height between inlet and outlet of the tubing connecting the flow cell

$\Delta H_{\text{manometer}}$ (feet) = pressure loss in flow cell

f_{tube} = factor for friction loss in flexible tubing (for $\frac{e}{d} = 0.000001$)

f_{ss} = factor for friction loss in stainless steel tubing (for $\frac{e}{d} = 0.003$)

$$g = 32.158 \frac{\text{ft}}{\text{sec}^2}$$

Figure 26 shows details of the system. The recirculating pump kept water overflowing from the top container. Constant head was therefore maintained at the inlet of the tubing leading to the flow cell. By siphoning action, water left the top container and followed the inlet tubing to the flow cell. After traveling through the system, the fluid returned to the big container in which its temperature was monitored and kept constant by a temperature controller. The importance of controlling both the room and fluid temperature is to maintain the viscosity of water at one particular value during the duration of the test (the factors for friction losses in the flexible tubing and the flow cell depend on the viscosity of water) so that the repeatability of the flow rate of water can be obtained from day to day at each different height of head (ΔH). The applicability of Eq. (4-1) to the test arrangement of Fig. 26 was verified by timing the interval required to collect 100 ml samples of water. Test data are plotted in Fig. 28 and reported in Table 5.

The inside diameter of the offset flow cell was 5/16" (79 mm) and had the following characteristics:

$$L = 5-3/16" (132 \text{ mm})$$

$$P = 6-5/8" (168 \text{ mm})$$

$$t_w = 1 \mu\text{s}$$

The measured velocity is determined by

$$V_{\text{measured}} \text{ (ft/sec)} = \frac{\left(\frac{\text{Volume of container}}{\text{Time to fill container}} \right) \times \frac{1}{\left(\frac{\text{Cross-sectional area of flow cell}}{\text{ft}^2} \right)}}{\frac{1}{12 \text{ in.}}} \quad (4-2)$$

where volume of container = $1000 \text{ ml} \times \frac{61.02 \text{ in.}^3}{10^6 \text{ ml}}$; time to fill container = elapsed time (seconds) for water to fill the 1000 ml container; cross sectional area of flow cell = $\frac{\pi (.3125 \text{ in.})^2}{4}$.

The water temperature was kept at a temperature within 1°C of room temperature. Room temperature was 22°C at each head setting. The measured velocity in Table 5 is the average velocity measured over 10 days; and the measured velocity for each day is the average value as 6 measurements. Each measured velocity has an overall uncertainty of $\pm 0.050 \text{ ft/sec}$ (15.239 mm/sec) based on a standard error of 0.008 ft/sec (2.438 mm/sec) and an allowance of 0.026 ft/sec (7.925 mm/sec) for systematic error (Eisenhart, 1969).

From the data in Table 5 the velocimeter portion of the mass flow-meter is found to have the following specifications:

Repeatability ^a	$\pm 0.010 \text{ ft/sec}$ ($\pm 3.048 \text{ mm/sec}$)	} Using Offset Cell
Linearity ^b	$\pm 0.008 \text{ ft/sec}$ ($\pm 2.438 \text{ mm/sec}$)	

Later, using the delivered cell in the Foxboro water calibration tests, where $V_{\text{max}} = 38 \text{ ft/s}$ (11.6 m/s), the following results were obtained (Table 6):

Zero flow repeatability	$\pm 0.01 \text{ ft/s}$ (offset = 0.06 ft/s)
Repeatability at full scale	0.06% of reading

$$a \text{ Repeatability} = \sqrt{\left(\frac{\text{One standard deviation of 10 days electronics reading}}{\text{ft/sec}} \right)^2 + \left(\frac{\text{One standard deviation of 10 days measured velocity}}{\text{ft/sec}} \right)^2}$$

(Abernethy, 1980).

b Linearity = Largest difference between electronic reading and best fit regression curve at a measured velocity reference.

Table 4 . Calibration test using Stoddard solvent. Data listed in order observed: first run down, first run up, second run down. Most \dot{M}_c values are averages of 2 readings; \dot{M}_p values, average of 2 to 4 readings.

\dot{M}_c KPPH	\dot{M}_p KPPH	T °F	P PSIG	$\frac{\dot{M}_p}{\dot{M}_c}$
16.37	17.20	77.2	170 \pm 15	1.051
12.01	12.85	78.8	100 \pm 10	1.070
10.00	10.65	78.8	75 \pm 10	1.065
7.06	7.45	79.0	35 \pm 10	1.055
5.00	5.30	79.4	25 \pm 5	1.060
3.04	3.30	81.0	20 \pm 3	1.086
2.00	2.23	83.5	10 \pm 2	1.115
1.00	1.10	91.1	10 \pm 2	1.100
2.505	2.93	83.2	11 \pm 1	1.170
3.988	4.33	80.9	23 \pm 3	1.086
5.990	6.43	80.1	34 \pm 10	1.073
7.956	8.37	80.1	50 \pm 15	1.052
10.95	11.75	80.2	-	1.073
13.85	14.87	80.5	120 \pm 25	1.074
15.95	16.95	81.3	160 \pm 20	1.063
14.95	16.10	81.3	140 \pm 20	1.077
12.90	13.85	81.8	115 \pm 15	1.074
11.50	12.37	81.8	85 \pm 15	1.076
9.00	9.59	81.7	60 \pm 12	1.066
5.51	5.98	82.1	30 \pm 10	1.085
3.50	3.78	83.3	20 \pm 2	1.080
1.27	1.51	87.4	13 \pm 3	1.189
1.00	1.22	90.1	10 \pm 1	1.220

\dot{M}_c = Reference value for \dot{M} measured with Cox system.

\dot{M}_p = Measured with Panametrics system.

P = Pressure of test fluid adjacent the flow cell.

Date of test: March 1980

Table 5. 10-Day Repeatability Test Data.

Head Difference (in.)	Manometer Reading (in.)	ELECTRONICS AVERAGE READING OF EACH DAY (ft/sec)										Ave. of 10 Day Elect. Reading (ft/sec)	Measured Velocity (ft/sec)	Calculated Velocity (ft/sec)	σ_R (ft/sec)	σ_M (ft/sec)	σ (ft/sec)
		1	2	3	4	5	6	7	8	9	10						
40	20-3/0	4.338	4.389	4.388	4.324	4.398	4.391	4.402	4.394	4.400	4.407	4.396	4.396	4.398	0.006	0.005	0.008
20	10	3.012	3.015	3.014	3.010	3.013	3.002	3.016	3.014	3.015	3.013	3.013	3.017	3.015	0.002	0.003	0.004
10	4-15/16	2.047	2.049	2.046	2.048	2.048	2.046	2.045	2.044	2.045	2.045	2.046	2.053	2.042	0.002	0.004	0.004
5	2-7/16	1.369	1.384	1.377	1.380	1.385	1.382	1.383	1.379	1.382	1.381	1.380	1.397	1.387	0.005	0.002	0.005
2	27/32	0.804	0.807	0.804	0.804	0.804	0.802	0.806	0.802	0.808	0.802	0.804	0.812	0.848	0.002	0.006	0.006
1	7/16	0.513	0.511	0.510	0.519	0.513	0.515	0.515	0.522	0.525	0.504	0.515	0.529	0.522	0.006	0.008	0.010

*The calculation is based on 10 degrees of freedom (10 days). (Ref. Abernethy, Thompson 1980)
 σ_R = standard deviation of A; σ_M = standard deviation of B; σ = repeatability of electronics = $\sqrt{(\sigma_R)^2 + (\sigma_M)^2}$

Water calibration tests were conducted at the Foxboro Company, Foxboro, MA, on 23 and 24 September 1980. Here, the delivered cell and the V part of the electronics were calibrated between 0.1 and 38 ft/s using a weigh tank. The fluid was water between 80 and 90 °F.

Data were obtained starting at the maximum velocity available for this test, 38 ft/s (~11.6 m/s). At this velocity, the K switches in the modified model 6000 were set to 0.9999 and the ultrasonic V essentially equaled the actual flow velocity. [Theoretically, $K = 1.000$. The maximum Re was $\sim 3 \times 10^5$. The maximum mass flow rate was $\dot{M}_{max} = \rho VA = (62.4 \text{ lb/ft}^3)(38 \text{ ft/s})(1.005 \text{ in.}^2/144 \text{ in.}^2/\text{ft}^2) = 16.49 \text{ lb/s} \approx 60,000 \text{ lb/hr}$ (7.5 kg/s or 27,000 kg/hr). However, since the delivered SP densitometer is designed for fuels, not water, it and the corresponding \dot{M} computation were not used; instead, only V was computed and displayed in this calibration test.] Other than the K switch setting, the only further electronic adjustment made during the test was the response time, which was switch-selected in the model 6000 by Foxboro personnel to average the flow readings over intervals approximately proportional to the time required to collect a pre-determined mass of water. Thus, at lower flow rates, longer response times were used to average 128 readings, 256 readings, etc.

To conduct the test, V was decreased from 38 ft/s down to 0.1 ft/s, a range of 380:1, thereby encompassing turbulent, transitional (~1/2 to 1/4 ft/s), and laminar flow. A few data points were also obtained on increasing flow back up to 20 ft/s. The data, given in Table 6 and Fig. 30, show that V zero repeatability, accuracy and linearity of better than 1/2% full scale were achieved.

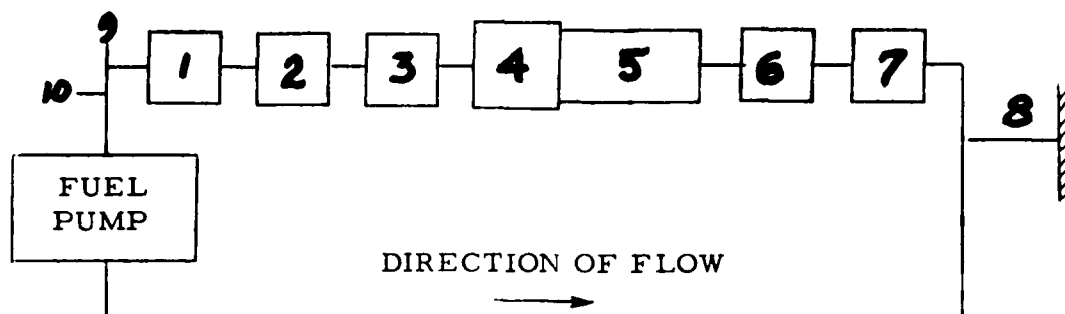
These water flow calibration or scale error data may be considered as an extension of the Stoddard solvent tests at GE (Table 4) where the maximum \dot{M} was 16,370 lb/hr. In other words, the water flow data in Table 6 and Fig. 30 show that the V part of the system operates properly at velocities which correspond to fuel mass flow rates at least up to 50% beyond the contract-specified value of 25,000 lb/hr. Later, on 31 March and 1 April 1981, it was demonstrated that the zigzag cell and \dot{M} electronics could operate in a fuel substitute (7024 BII) at flow rates up to at least 31,450 lb/hr. Data in Appendix K show that operation to the limit of the test stand under the test conditions was achieved without signal degradation.

Table 6. Water calibration test at the Foxboro Company.

Date of tests: 23 and 24 September 1980.

Flow Rate ft ³ /s	Temp. °F	\bar{V} actual ft/s	V ultra ft/s	Error	
				% Reading	% Full Scale
.2668	86.4	38.045	37.90	-.38	-.38
.2672	87.1	38.096	37.93	-.44	-.44
.2109	87.4	30.075	30.00	-.25	-.20
.1797	87.7	25.620	25.58	-.16	-.11
.1412	88.2	20.128	20.20	+.36	+.19
.1047	88.6	14.923	15.00	+.52	+.20
.07136	89.2	10.173	10.20	+.27	+.07
.03517	90.0	5.014	5.071	+1.14	+.15
.007844	90.2	1.118	1.094	-2.15	-.06
.004008	89.6	.5715	.540	-5.51	-.08
.001916	88.8	.2732	.217	-20.6	-.15
.00000	--	.0000	-0.07	--	-.002
.001198	80.5	.17073	.126	-26.2	-.12
.01416	80.7	2.018	2.033	+.74	+.04
.03530	86.8	5.033	5.150	+2.32	+.31
.07890	85.5	11.249	11.40	+1.34	+.40
.1072	85.6	15.284	15.40	+.76	+.31
.1406	85.6	20.039	20.169	+.65	+.34
.00000	--	0.000	-0.06	--	-.002

Test Mode 1: FUEL FLOW CALIBRATION TEST PLAN



- | | |
|---------------------------------|-----------------------------------|
| 1. Turbine flow meter | 6. Sight port (optional) |
| 2. Flow straightener (optional) | 7. Kenics static mixer (optional) |
| 3. Sight port (optional) | 8. Anti-vibration mount |
| 4. SP densitometer | 9. Temperature sensor |
| 5. Panametrics flow velocimeter | 10. Pressure Tap |

JP-5 DATA TO BE RECORDED

Temp, °F	Pressure, psig	GE Mass Flow Rate, PPH		Panametrics Mass Flow Rate, PPH			
		Turbine	Corrected for T	ρ	V	Calc. \dot{M}	Meas. \dot{M}

Test Mode 2: WATER FLOW CALIBRATION TEST PLAN

Test arrangement as above except include only items 5, 9, 10; use water as fuel substitute.

Record data on actual flow velocity (determined from weigh tank or volumetric measurement) and on ultrasonically-determined flow velocity.

Test Mode 3: 10-DAY REPEATABILITY TEST PLAN

Test arrangement like in Mode 2 except use head difference ΔH instead of fuel pump, and use axial path offset cell instead of zigzag cell as item 5. Record data as in Mode 2.

B. RANGEABILITY

The maximum (water) flow rate at which the flow velocimeter was tested in this program was 38 ft/s (11.6 m/s). (Higher flows could probably be measured since the received signals at 38 ft/s show no large jitter. See, for example, oscillograms in Fig. 22 for JP-5 at 20 kPPH and water at 60 kPPH.) The minimum flow rate was zero. However, the zero offset observed prior to testing, during testing, and again after the equipment was returned from Foxboro to Panametrics, was 0.06 ft/s. This zero offset error, V_e , corresponds to a Δt_e offset error of

$$\begin{aligned}\Delta t_e &= 2 L V_e / c^2 \\ &= (2)(0.33 \text{ ft})(0.06 \text{ ft/s}) / (5 \times 10^3 \text{ ft/s})^2 \\ &= 1.6 \text{ ns}\end{aligned}$$

which is close to the ± 1 ns resolution limit of the flow velocity electronics.

The fuel mass flow rate zero offset error, \dot{M}_e , corresponding to this V_e and Δt_e , is 60 PPH.

The \dot{M} objective in this contract was from 200 to 25000 PPH, a rangeability of 125:1. However, due to the density range, ~ 0.65 to 0.9 g/cm^3 , the corresponding velocity range objective is thus $(0.9/0.65)(125) = 173:1$. Now in the Foxboro calibration test (Table 6; Fig. 30), the nonzero flow range was 0.1 to 38 ft/s, demonstrating a velocity rangeability of 380:1. Due to the zero offset, accuracy over this entire range is not adequate for all purposes; hence, the useful rangeability depends on the required accuracy. It appears that, within the limits of one zigzag cell, useful rangeability in excess of 100:1 was achieved. For better accuracy at the lower flow rates, a longer L is required, e.g., as provided by an offset axial path flow cell (Appendix G).

C. REPEATABILITY

Reference to Table 6 shows that repeatability at zero flow was 0.06 ft/s, or 0.2% full scale based on the 38 ft/s maximum velocity, or 0.24% based on a full scale flow velocity of 25 ft/s (fuel $\dot{M} = 25$ kPPH).

D. HYSTERESIS

Reference to Table 6 shows that hysteresis was less than 1.2% of reading (5 - 20 ft/s) and less than 0.25% full scale. (The values listed below are extracted from Table 6, for the convenience of the reader.)

Nominal Flow Velocity <u>ft/s</u>	<u>% of Reading Error</u>		<u>Hysteresis (Difference)</u>	
	<u>Flow Decr.</u>	<u>Flow Incr.</u>	<u>% of Reading</u>	<u>% Full Scale</u>
-	+1.14	+2.32	1.18	.24
+ .27	+ .27	+1.34	1.07	.11
+ .52	+ .52	+ .76	.24	.02
+ .36	+ .36	+ .65	.29	.02

E. LINEARITY

The linearity is 1% full scale. Note that the "meter factor" was set to 0.9999 in the water flow calibration tests and agreement between the ultrasonic measurement of flow velocity, and that determined independently by the weigh tank method, was within 0.5%. This demonstrates the area-averaging property of the square duct when 100% interrogated as described elsewhere in this report. No flow straighteners or static mixers were used in this water test. In the water calibration tests, and in the final fuel substitute tests, the deviation from linearity, expressed as percent of actual flow, is larger at the bottom portion of the system's range. See for example, p.40 or Appendix K.

F. RESPONSE TIME

In the delivered instrument, the \dot{M} response time is fixed at 2 s. However, for V only, a board is available for the instrument to provide switch-selectable averages of 1, 2, 4, 8 . . . , 128 readings. In the vibration tests at ATL, the response time of 2 seconds was demonstrated by rapidly changing a valve setting. See Appendix E. Referring to the chart recording on p. E-1, note that deflections for each cell are measured from a " $V = 0$ " no-flow reference axis. The deflection sensitivity is 0.3 inches (30 mV) per English unit of flow velocity. That is, 30 mV corresponds to $V = 1$ ft/s (0.3 m/s). When the water flow control valve is suddenly opened or closed, the response time of the velocimeter electronics can be determined by measuring how long the output takes to steady down (equilibrate) at the new flow. At a chart speed of 1 inch per minute, 1 minor division = 6 seconds. Note that the quasi-step changes in the output are completed in $T \leq 2$ s, as when flow increased from 1 to 2.5 ft/s, or when the valve was rapidly opened by three turns. In other laboratory tests at Panametrics, quasi-step changes in water flow rate, produced by closing a ball valve in less than 1 s, lead to the same value of T , even when \dot{M} changes over the 50:1 range from 25,000 down to 500 lb/hr. If the flow is turned off suddenly, the output reading nearly reads zero immediately, but does not fully settle until the eddies subside. See also, pages G-10 and G-11.

G. Vibration

ATL's vibration test report comprises most of Appendix J. This is followed by a drawing to define x, y and z axes of vibration and recordings of the flow velocity data during vibration. It will be understood that for another flow cell configured to and mounted on a particular engine, results will be different.

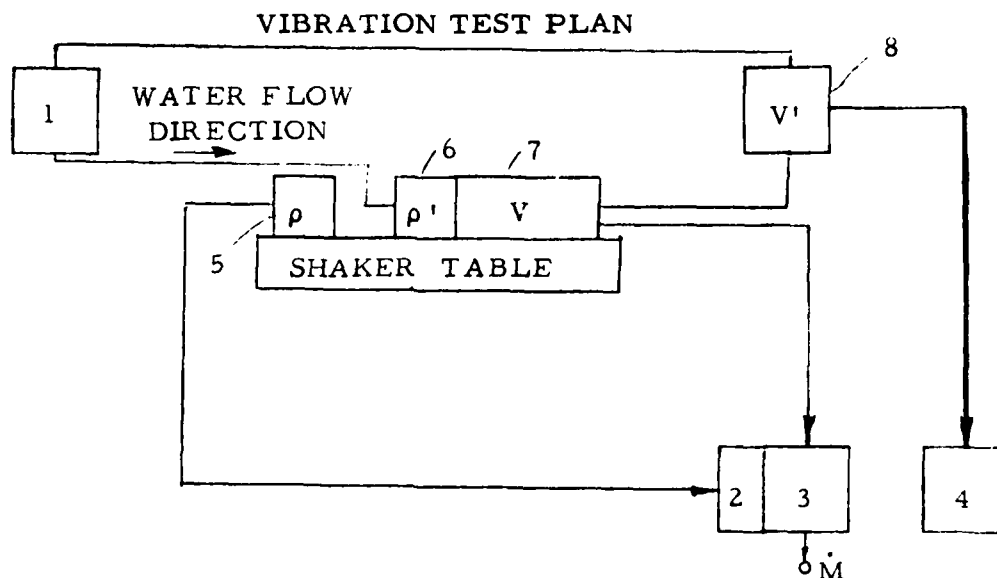
Vibration testing at ATL, Burlington, MA, utilized two cells in series as shown in the Test Plan. Cold water, at the maximum flow rate available from the tap, up to 3 ft/s (~ 1 m/s), flowed first through the cell being vibrated and then through a second cell at rest (Mode 1). Flow velocimeter electronics monitored the velocities V_1 and V_2 respectively in the two cells. The influence of vibration on the measured V_1 was found to be small, in general. Besides resonances and noise, the only effect of vibration to be expected from theoretical considerations occurs when the vibration frequency f_v in the axial direction is approximately equal to the frequency at which upstream and downstream interrogation directions alternate electronically. Such vibratory synchronism produces an additional component of relative velocity V_g between the cell and the fluid, directly proportional to g and inversely proportional to f_v . That is, the peak relative velocity $V_g = \pi f_v S = 61.44 g/f_v$ where the units of V_g are in./s, f_v , Hz; S , μ in. (double amplitude displacement); and g is the gravitational constant ($g = 0.0511 f_v^2 S = 0.0162 V_g f_v$). For example, at $f_v = 2000$ Hz, and 20 g's, $S = 100 \mu$ in. (2.54μ m) and $V_g = 0.64$ in./s (~ 16 mm/s). Further details on the vibration test performed on the delivered flow velocimeter cell are given in the Vibration Test Plan and in Appendix J. No damage was observed due to the vibration test. However, at a few discrete frequencies, e.g. $f_v \approx 1250$ Hz, noise was so intense that flow data had to be discarded. Some future work could be devoted to eliminating such undesirable resonant behavior.

H. Temperature

A transducer identical in construction to the two in the delivered flow cell was tested in an environmental chamber in the pulse-echo mode from -196 to $+175^\circ\text{C}$. Testing included cycling and dwells of several hours at the extremes. Both low and high extremes are beyond the contract-specified values of -38 to $+150^\circ\text{C}$. The oscillograms in Appendix I show that the tested transducer exceeded the temperature objectives of the contract.

I. Pressure

The flow velocimeter cell was hydrostatically tested at 1500 psig for one hour and was found to be leak tight (see Appendix H).



1. Water pressure source and drain
2. SP ρ electronics
3. Panametrics electronics (V and \dot{M})
4. Optional Panametrics flow velocimeter electronics
5. SP ρ cell filled with fuel or fuel substitute**
6. SP ρ cell through which water flows**
7. Panametrics V cell
8. Optional V cell not under vibration

* Test mode 1: compare V and V' as function of vibration, at constant water flow conditions.

* Test mode 2: compare ρ and V and/or \dot{M} readings, under vibration and flow, and then when vibration and/or flow is momentarily turned off.

DATA, MODE 1: V, V' & H₂O flow conditions

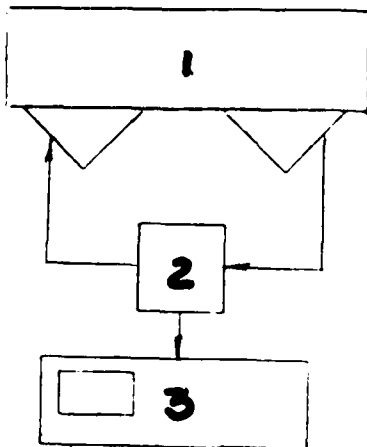
DATA, MODE 2: ρ , V and/or \dot{M} for vibration and/or flow = zero and \neq zero.

*Test mode 1 was selected for the ATL tests conducted Sept. 1980.

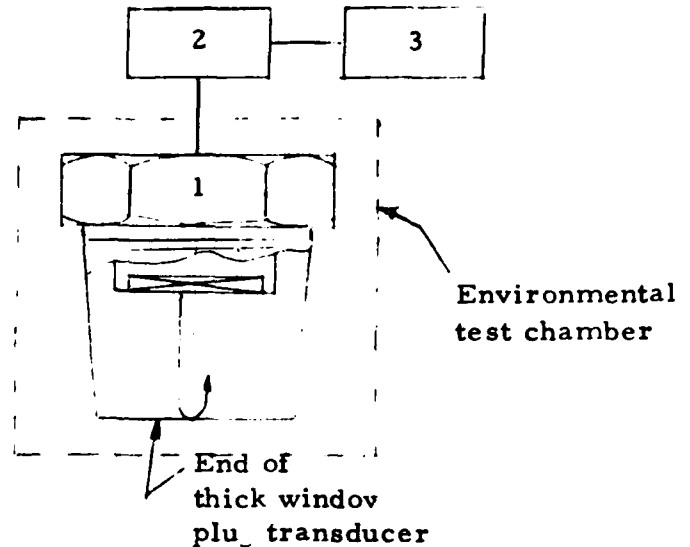
**SP cells may be eliminated from tests to avoid water damage; SP density signal may be simulated using dc power supply to represent $\rho = 1 \text{ g/cm}^3$.

TEMPERATURE TEST PLAN

Test Mode 1:



Test Mode 2:



Test Mode 1

1. Flow cell full of liquid (water or hydrocarbon)
2. Pulser/receiver, Panametrics model 5055, or flow velocimeter electronics.
3. Oscilloscope

Procedure: measure received signal before and after exposure to contractually-specified temperature extremes.

DATA: Received signal (mV), before _____; after -65°F _____; after 304°F _____

Test Mode 2

1. Thick window transducer tested individually, not in flow cell.
- 2,3. Electronics same as for the items for Test Mode 1.

Procedure: measure relative amplitude of echo from end of thick window at room temperature and then during exposure to contractually-specified temperature extremes, or at temperatures beyond these extremes.

HYDROSTATIC PRESSURE TEST PLAN

1. Plug flow cell outlet.
2. Pressurize from inlet, using water, at 1600 psig. Hold for one hour. Report any leaks. If necessary, re-seal and test again.

J. Self-Testing of Flow Velocimeter Electronics: Differential Path

There are a number of approaches to self-testing parts of the flow velocimeter electronics. Among the more obvious approaches may be mentioned the electronic simulation of a particular flow condition as represented by a preset Δt or Δf injected into the system, and/or the use of numerous diagnostic trouble lights (led's) to indicate malfunction of particular circuits. The problem with the former is that the transmitter and perhaps parts of the receiver are not included in the test. An objection to the latter is that if the operator in the field is unable to repair the equipment based on the led indications, then the detailed troubleshooting information provided by them may be superfluous.

In order to self-test the complete flow velocimeter electronics independent of the actual flow cell, and, as desired, independent of or including the actual transducers, consider the following differential path or interferometric type self-test cells. These cells may use two or four transducers which are generally fixed in a standard pipe fitting housing. The housing itself, or a reflector therein, is arranged to provide different fixed or variable paths simulating upstream vs downstream interrogations. Pipe section extensions may be connected to the housing to increase the fluid paths to closely approximate the delays encountered in any specific application. The self-test cell may be filled with water or other fluid of interest, provided, of course, that the necessary precautions are taken if fuel or other hazardous fluid is used.

We briefly explain four self-test cells as follows. Referring first to Fig. 23a note the use of two fixed transducers and a reflector between them. The transducers are operated each in pulse echo mode, the reflector blocking transmission between the transducers. Displacement of the reflector by a small distance Δx increases the "upstream" simulated delay by $2\Delta x/c$ and decreases the "downstream" simulated delay by the same amount. Therefore, the simulated upstream minus downstream time difference changes by $4\Delta x/c$.

Depending on the nature of the pulser and receiver, it is not always convenient to operate the electronics in pulse echo mode. For a through transmission mode self-test, one can consider the self-test cells of Fig. 23b and c. In Fig. 23b, the differential path is again denoted Δx , the path difference simply being the difference in fixed distances between transmitters and receivers. The time difference is simply $\Delta x/c$.

Reference to Fig. 23c shows that displacement of the reflector along the x-axis by Δx changes each 45° folded path by $2\sqrt{2}\Delta x$. If the test fluid is water, the flow-simulated Δt is about $2\mu\text{s}/\text{mm}$ or $50\text{ ns}/\text{mil}$ ($1\text{ mil} = 10^{-3}\text{ inches}$).

It may be of interest to note that if the pulse echo idea of Fig. 23a is combined with the "geometry" of Fig. 23c in the sense of having the reflector face at 45° to the displacement axis, then the same Δt 's are generated with this cell in pulse echo or through transmission, namely, $2\sqrt{2} \Delta x/c$. See Fig. 23d.

With respect to Δt , the simulation of flow may be understood by equating actual and simulated time differences:

$$\Delta t = \frac{2LV}{c_a^2} = \frac{2\sqrt{2} \Delta x}{c_s}$$

where c_a = sound speed in actual fluid (e. g. JP-5) and c_s = sound speed in simulation fluid (e. g. water).

Solving for the displacement corresponding to a given V and L ,

$$\Delta x = \frac{c_s}{c_a^2} \frac{LV}{\sqrt{2}}$$

As a numerical example corresponding to the delivered flow cell and the maximum flow velocity of interest (at 25000 lb/hr), $L = 4$ inches = 0.333 ft (10 cm), $V = 25$ ft/s (~ 8 m/s), $c_s = 5000$ ft/s (~ 1500 m/s) and $c_a = 2500$ ft/s (~ 750 m/s). Then

$$\Delta x = \frac{(5000)(0.33)(25)}{(2500)(2500)\sqrt{2}} = 0.057 \text{ inches} = 1.4 \text{ mm}$$

A rapid change in reflector position could be used to check the transient response of the electronics. For example, a rapid change of $\Delta x = 1.4$ mm in 0.1 s could simulate $\Delta V = 8$ m/s in 0.1 s, equivalent to a fuel acceleration of $\Delta V/\Delta t = 8 \text{ m/s}^2$ or about 0.8g. Similarly a rapid path change of $\Delta X = 17$ mm (~ 0.7 inches) in 0.1 s would simulate a fuel acceleration of 10g.

V. CONCLUSIONS

The complete delivered \dot{M} system was tested at GE in the fuel substitute 7024 BII to 14,300 kg/hr (31,450 lb/hr). The V part of the system was also tested in water to $V = 11.6$ m/s (38 ft/s) or $\dot{M} \approx 27000$ kg/hr (60,000 lb/hr). Based on a full scale rating of 11,364 kg/hr (25,000 lb/hr) rms deviations from linearity in both tests were demonstrated to be about 1% of full scale, with a 2 s response time. Over approximately the upper 95% of the \dot{M} range, in the fuel substitute tests at GE, the rms deviation from linearity is at most 1.7% of the actual flow rate. Up to 0.5% of this nonlinearity may be due to the turbine sensors' own error band. Above 9000 lb/hr, for 3 runs, the average nonlinearity is less than 0.77% of the actual flow rate. The performance of the mass flow rate system is believed to be substantially independent of fuel composition (at least for JP-4, -5, their mixtures, or 7024 BII), and substantially independent of temperature from -55 to +300°F, pressure to 1600 psig and vibration (MIL Std. 810-514.1), except at a few discrete frequencies. Ten-day repeatability testing between ~ 0.5 and ~ 5 ft/s (~ 0.15 to 1.5 m/s) demonstrated system repeatability of ± 0.01 ft/s (± 3 mm/s). The flow velocimeter part of the electronics can be operated with a variety of flow cells such as clamp-on or axial offset or conventional diagonal traverse, in addition to the square hole zigzag design with which the present contract was mainly concerned. The stability of the waveforms observed for the zigzag flow cell at the maximum \dot{M} encountered in the fuel substitute test, and in the water tests, strongly suggests that a longer zigzag path could be used in the future. This would improve the resolution at low \dot{M} , and, together with some other modifications to the cell and transducer, ought to improve linearity in the lower part of the system's range. Alternatively, linearization may be accomplished in the software, at least for nonlinearities dependent on V alone.

VI. ACKNOWLEDGMENTS

The authors gratefully acknowledge the patience and guidance of the sponsors, and especially the contributions of William G. Cole and Marshall McDonald, during the conduct of this program. The cooperation of the General Electric Company, Lynn, MA is sincerely appreciated, especially the cooperation of J. Jacobson, D. Hebert, S. Werbikas, G. V. Titterington, and A. Page. At Panametrics, K. Fowler, D. Patch and B. Crandell contributed to the transducer design and fabrication, and W. B. Studley contributed to the delivered hardware. J. L. Korba programmed the electronic look-up table referred to on p. K-3, and also programmed parts of the main-line program. K. E. McFarland drafted the drawings and PC layouts. Helpful discussions with R. L. Bryant, E. H. Carnevale and D. Chleck are also acknowledged. June Bennett carefully typed the entire manuscript, and her attention to detail is sincerely appreciated.

VII. REFERENCES

1. Lynnworth, L. C., N. E. Pedersen and E. H. Carnevale, Ultrasonic Mass Flowmeter for Army Aircraft Engine Diagnostics, USAAMRDL Technical Report 72-66, Contract DAAJ02-71-C-0061 (January 1973).
2. Pedersen, N. E., L. C. Lynnworth and J. E. Bradshaw, Improved Ultrasonic Fuel Mass Flowmeter for Army Aircraft Engine Diagnostics, USAAMRDL Technical Report 75-8, Contract DAAJ-73-C-0061 (June 1975).
3. Lynnworth, L. C., N. E. Pedersen, J. L. Seger and J. E. Bradshaw, Advanced Technology Fuel Mass Flowmeter, USARTL Technical Report 78-45 (October 1978).
4. Lynnworth, L. C., Slow Torsional Wave Sensors, pp. 29-34 in 1977 Ultrasonics Symp. Proc., IEEE Cat. #77CH1264-1SU (1977).
5. Lynnworth, L. C., Ultrasonic Flowmeters, Chap. 5 in Physical Acoustics-Principles and Methods, pp. 407-525, edited by W. P. Mason and R. N. Thurston, Academic Press, New York (1979).
6. Stuart, R. B., An Advanced Turbine Flowmeter System with Density Compensation, p. 695 in Flow: Its Measurement and Control in Science and Industry, ISA (1974).
7. Eisenhart, C., Expression of the Uncertainties of Final Results, Section 1.6 in Precision Measurement and Calibration: Statistical Concepts and Procedures, 11/69-72, Edited by H. H. Ku, National Bureau of Standards Special Publ. 300 - Vol. 1, Washington, D. C. (February 1969).
8. Abernethy, R. B., Thompson Jr., J. W., Handbook - Uncertainty in Gas Turbine Measurements, a reprint of NTIS AEDC-TR-73-5, Reproduced by NTIS, U.S. Dept. of Commerce, Springfield, VA 22161 (1980).
9. Meisser, Claudio, Control Engineering 28 (5) 87-89 (May 1981).
10. Lynnworth, L. C., A. J. Berry and R. Allen, Selecting An Ultrasonic Flowmeter, in: Inst. Public Health Engineers Year Book, List of Members and Buyers Guide 1981, pp. 369-374, Sterling Publ. Ltd., London (1981).
11. Pedersen, N. E., Method and Apparatus for Determining Fluid Flow, U.S. Patent (1981); ser. no. 82,820 (Oct. 9, 1979).

VIII. LIST OF ILLUSTRATIONS

- Fig. 1. Ultrasonic mass flowmeter cell shown in exploded view. Cell consists of aluminum housing milled to provide $1/2''$ (2.54 mm) square duct and interrogation path at 45° , 5 MHz transducers for sensing flow velocity, another ultrasonic transducer for sensing the speed of sound by a pulse echo technique, and a reflection coefficient densitometer probe using a 10 MHz transducer. Sponsor: Eustis Directorate, 1971-1973.
- Fig. 2. Assembly view of ultrasonic mass flow cell and block diagram of flow velocimeter electronics utilizing a pseudo random noise code generator which permitted the fuel to be interrogated simultaneously upstream and downstream at the same carrier frequency, 5 MHz, using only one pair of transducers.
- Fig. 3. Block diagram of 5 MHz rf burst system used for measuring flow velocity in third Eustis program.
- Fig. 4. (a) Flow cell configured for GE's T-700 engine including passage-ways for the ultrasonic measurement of flow velocity and the capacitance-based measurement of fuel density. (b) Field-type case which housed the electronics for mass flow rate determination. Source: USARTL-TR-78-45 (October 1978).
- Fig. 5. Reynolds number nomogram for determining Re as a function of kinematic viscosity and the product of area averaged flow velocity \bar{V} and duct diameter D . Curves at left show the temperature dependence of kinematic viscosity for a number of liquids and gases. Adapted from Physical Acoustics - Vol. 14, p. 490 (1979) including adaptations from Streeter (1961) and Moody (1944) cited therein. Dashed box indicates scope of present contract.
- Fig. 6. Graphs showing (a) sound speed vs temperature, (b) density vs temperature, (c) kinematic viscosity vs temperature, and (d) kinematic viscosity vs sound speed, for JP-4 and JP-5
- Fig. 7. \bar{V} vs \dot{M} for $\rho = 0.65$ and 0.9 g/cm^3 .
- Fig. 8. Block diagram of phase locked loop flow velocimeter, operating in conjunction with SP densitometer to measure mass flow rate.

VIII LIST OF ILLUSTRATIONS (cont'd)

- Fig. 9. Comparison of various types of ultrasonic flow cells.
- Fig. 10. Small, medium and large flow cells.
- Fig. 11. (a) Axial path interrogation of liquid contained within SP concentric tube densitometer cell. (b) Oscillographic test results for SP cell and (c) Comparison with unobstructed axial path. Liquid: water, room temperature. Electronics: Panametrics Pulser/Receiver 5055 PRM + Krohn-Hite Filter 3202, 1.5 MHz high pass.
- Fig. 12. Flow cells made of standard tubing pipe and compression fittings.
- Fig. 13. Navy flow velocimeter cell photograph showing optional ports for set screws holding square holed sleeve and for optional slow torsional wave densitometer.
- Fig. 14. Outline drawing of equipment shown in Fig. 13 in which the key components are identified.
- Fig. 15. Outline drawing of basic flow cell in which optional ports are omitted. The position of the square holed sleeve and the two ultrasonic transducers are indicated by dashed lines.
- Fig. 16. Alternate design for flow velocimeter cell portion of the system, using transducer ports orthogonal to flow axis and reflectors to control 45° zigzag interrogation path.
- Fig. 17. Photograph showing examples of pc reflectometer probes similar in principle to flush-mounted pc densitometer probe investigated in first and second Eustis contracts.
- Fig. 18. M system block diagram.
- Fig. 19. Photograph of prototype flow velocimeter electronics similar to the instruments which were used to test the reference (at rest) flow velocimeter cell in the vibration tests and the final offset flow cell tests at GE.
- Fig. 20. Graph of insertion loss vs thickness of sheets that were considered as eddy reducers in vicinity of transducer ports. Curves are based on calculations for normal incidence longitudinal waves at 5 MHz and assume that the sheet is fully immersed and wetted by water at room temperature.

VIII. LIST OF ILLUSTRATIONS (cont'd)

- Fig. 21. Accuracy nomogram.
- Fig. 22. Test oscillograms of received signals transmitted through JP-5 at various flow rates.
- Fig. 23. Flow simulators comprised of differential path cells. (a) Pulse echo. (b) Through transmissiion. (c) Folded transmission, or "pitch-and-catch," arrangement. (d) Pulse echo with reflector motion at 45° to interrogation axis.
- Fig. 24. General view of flowmeter under preliminary test at GE-Lynn. Photo courtesy GE.
- Fig. 25. Close-up of mass flowmeter cell in preliminary test. In subsequent tests, distance from elbow to cell was increased, allowing room for either flow straightener or static mixer to be installed in-line upstream. Photo courtesy GE.
- Fig. 26. Schematic of test at GE-Lynn, March 1980
- Fig. 27. Mass flow rate calibration data using fuel substitute. Reference \dot{M} obtained using Cox ANC-24, S/N 23803, calibrated from 990 to 59000 pounds per hour, accuracy $\pm 1/4\%$ of reading.
- Fig. 28. ΔH flow loop with offset flow cell used in repeatability test.
- Fig. 29. Data for 10-day repeatability test, using water in offset flow cell, July 1980.
- Fig. 30. Water calibration test data obtained by the Foxboro Company, Foxboro, MA, on 23 and 24 September 1980.



Fig. 1. Ultrasonic mass flowmeter cell shown in exploded view. Cell consists of aluminum housing milled to provide 1/2" (2.54 mm) square duct and interrogation path at 45°. 5 MHz transducers for sensing flow velocity, another ultrasonic transducer for sensing the speed of sound by a pulse echo technique, and a reflection coefficient densitometer probe using a 10 MHz transducer. Sponsor: Eustis Directorate, 1971-1973.

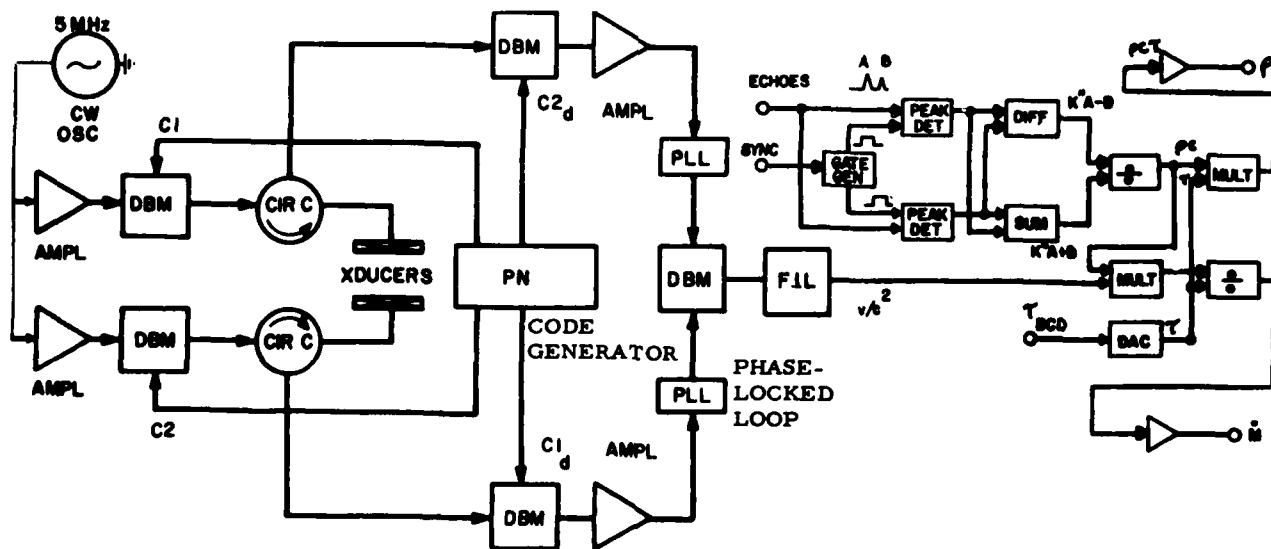


Fig. 2. Assembly view of ultrasonic mass flow cell and block diagram of flow velocimeter electronics utilizing a pseudo random noise code generator which permitted the fuel to be interrogated simultaneously upstream and downstream at the same carrier frequency, 5 MHz, using only one pair of transducers.

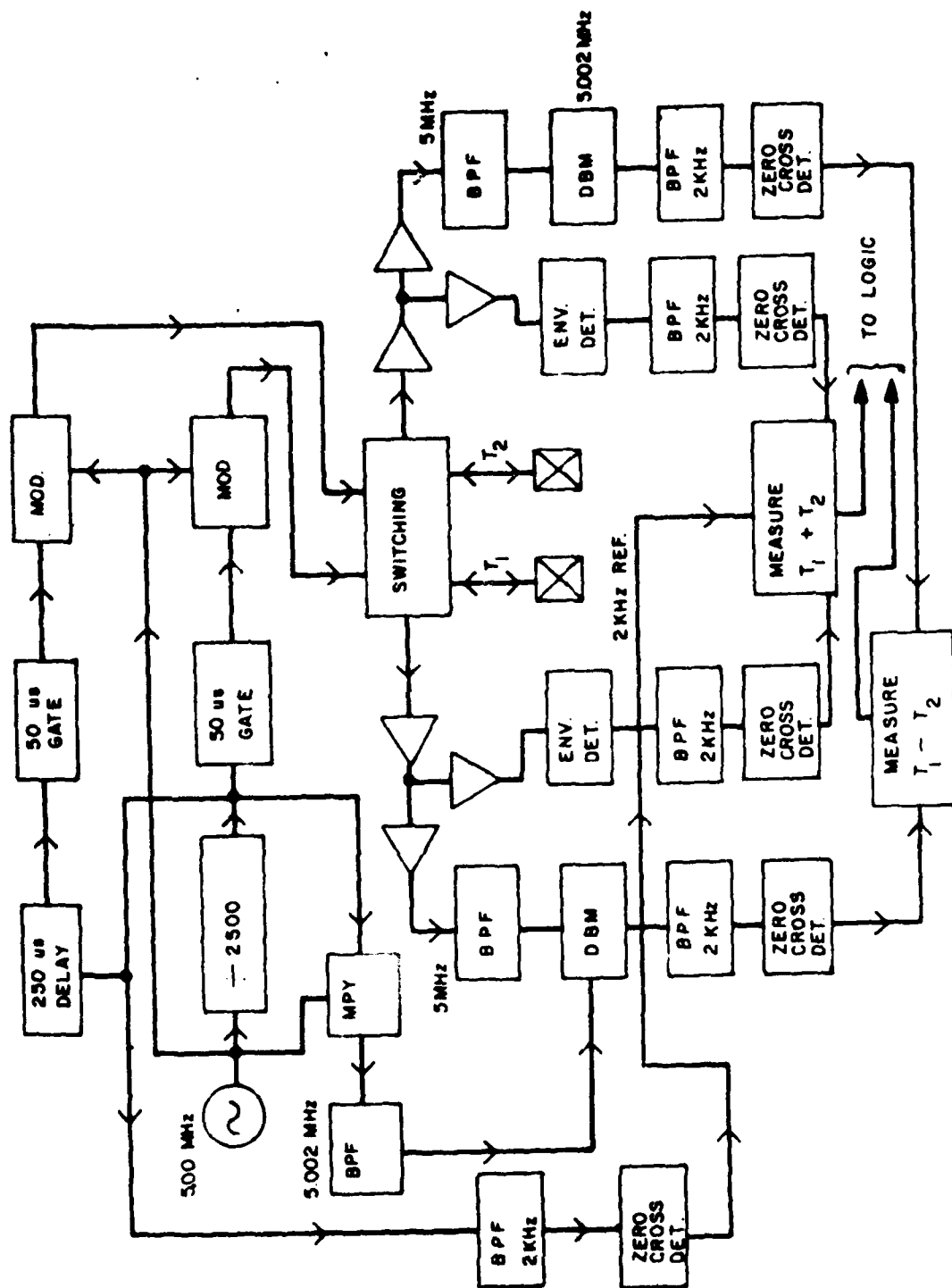


Fig. 3. Block diagram of 5 MHz rf burst system used for measuring flow velocity in third Eustis program.

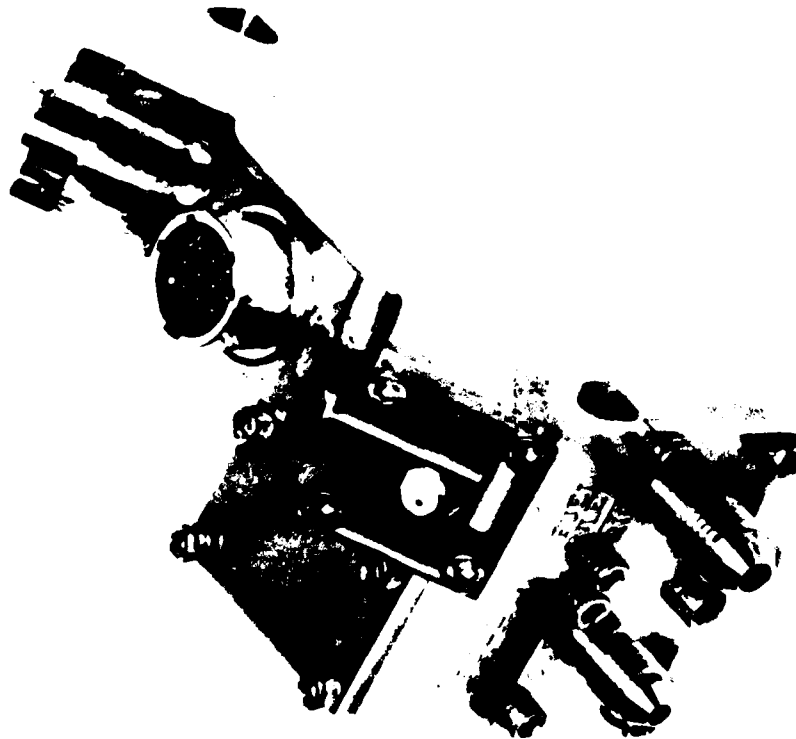
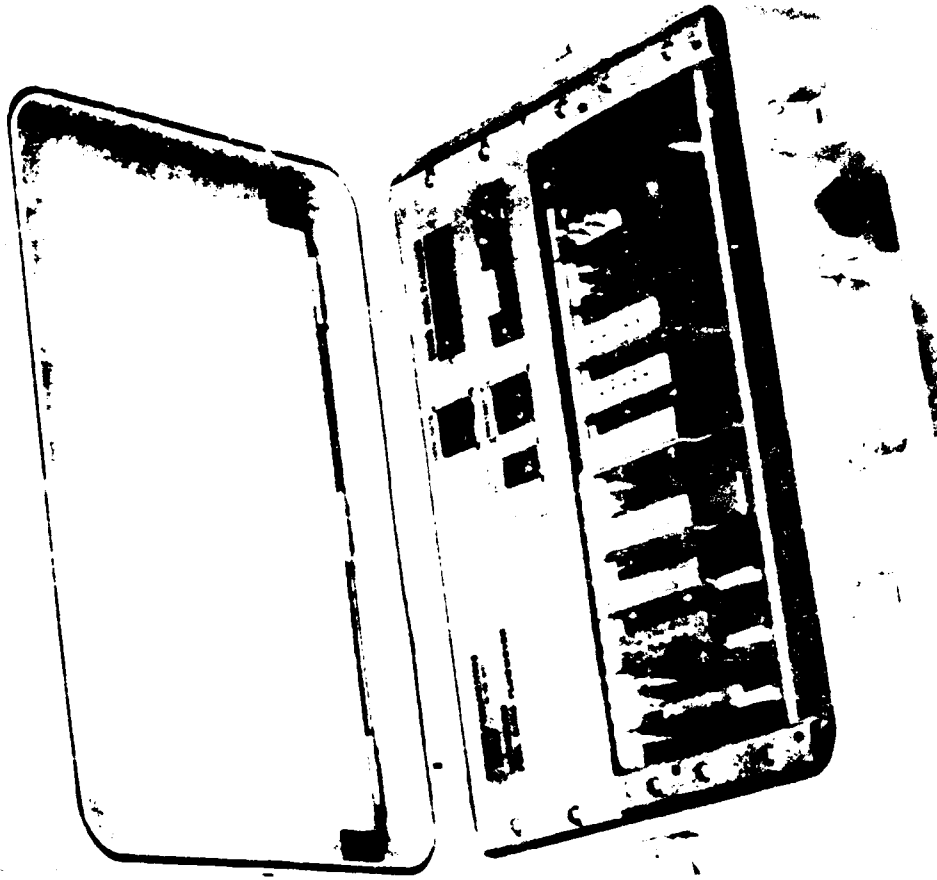


Fig. 4. (a) Flow cell configured for GE's T-700 engine including passageways for the ultrasonic measurement of flow velocity and the capacitance-based measurement of fuel density. (b) Field-type case which housed the electronics for mass flow rate determination. Source: USARTL-TR-78-45 (October 1978).

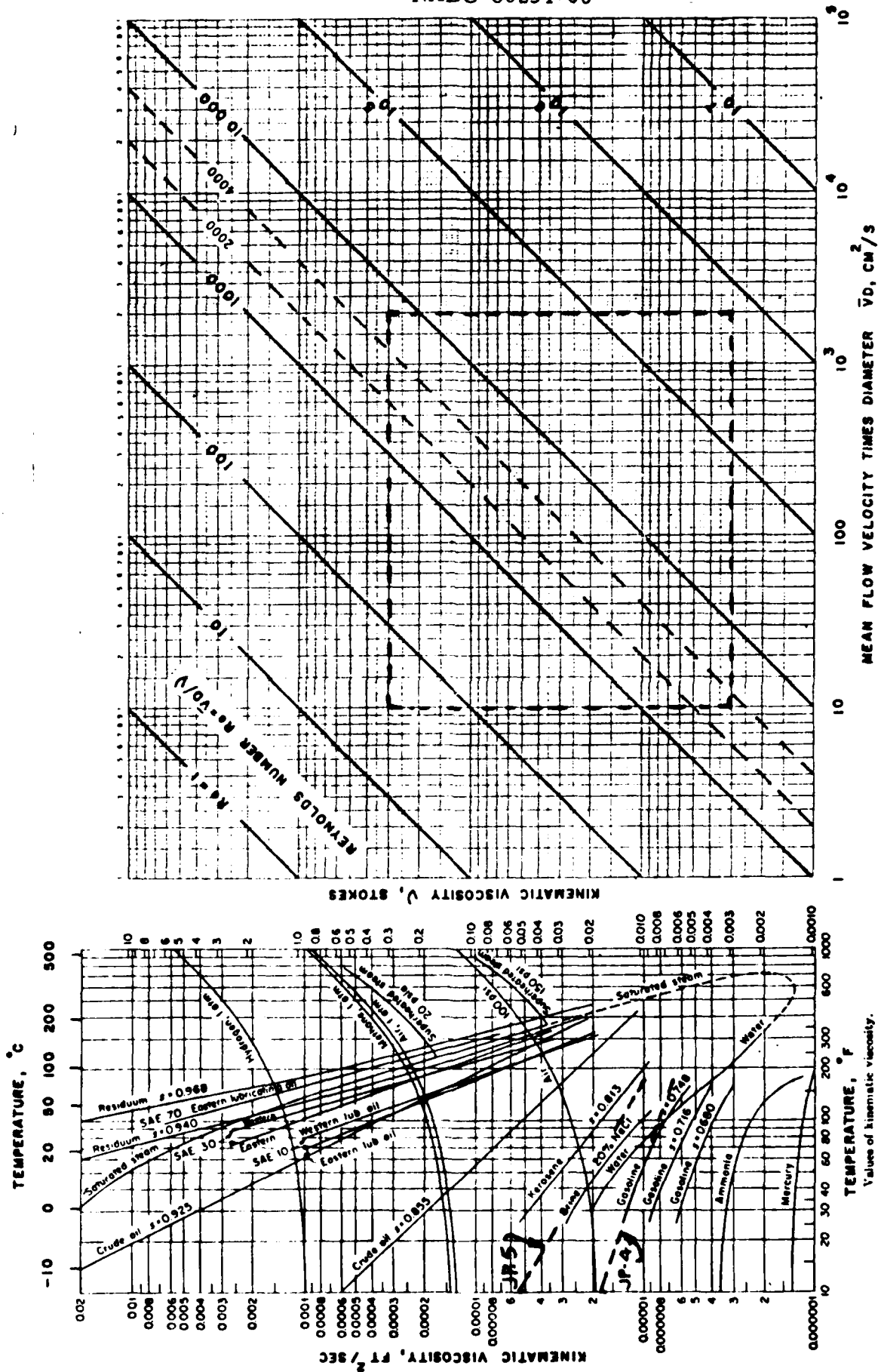


Fig. 5. Reynolds number nomogram for determining Re as a function of kinematic viscosity and the product of area averaged flow velocity \bar{V} and duct diameter D . Curves at left show the temperature dependence of kinematic viscosity for a number of liquids and gases. Adapted from Physical Acoustics - Vol. 14, p. 490 (1979) including adaptations from Streeter (1961) and Moody (1944) cited therein. Dashed box indicates scope of present contract.

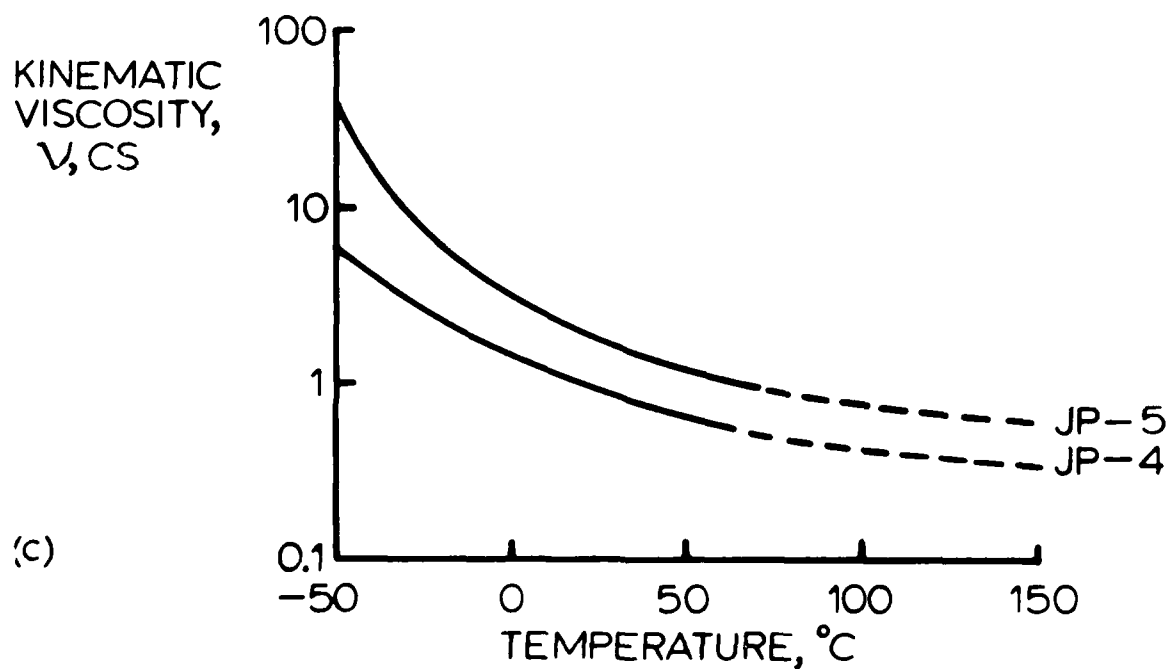
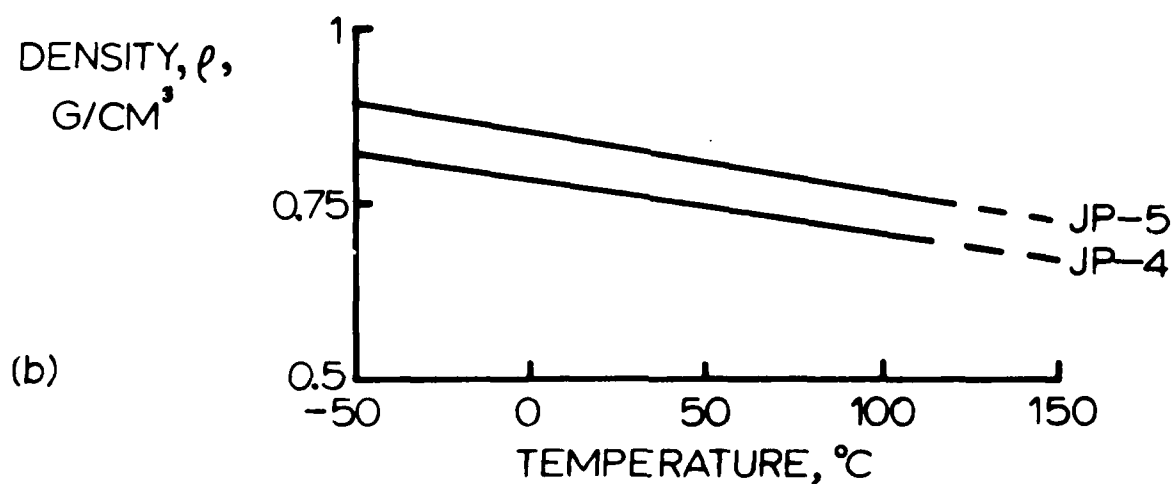
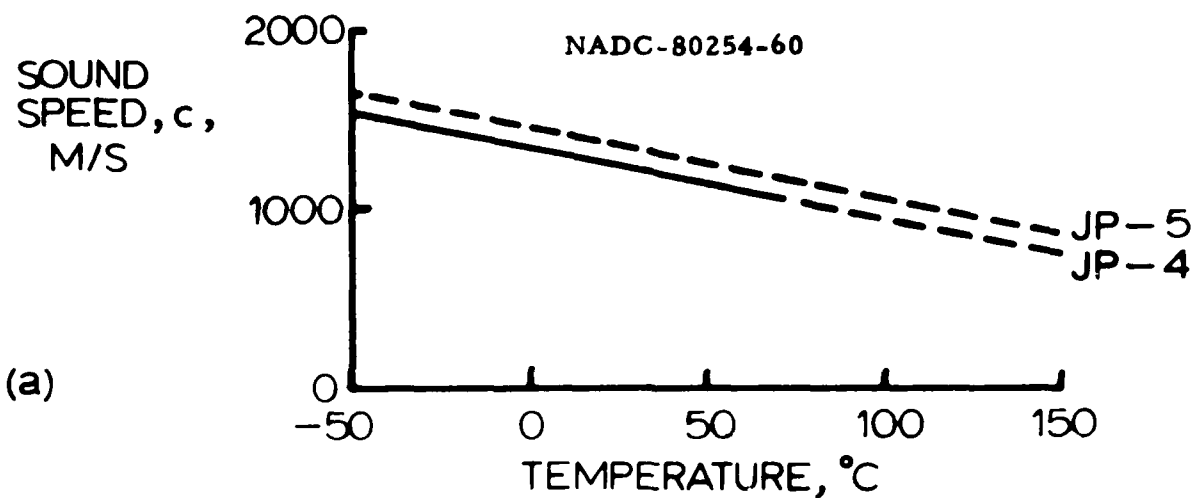


Fig. 6. Graphs showing (a) sound speed vs temperature, (b) density vs temperature, (c) kinematic viscosity vs temperature and (d) kinematic viscosity vs sound speed, for JP-4 and JP-5.

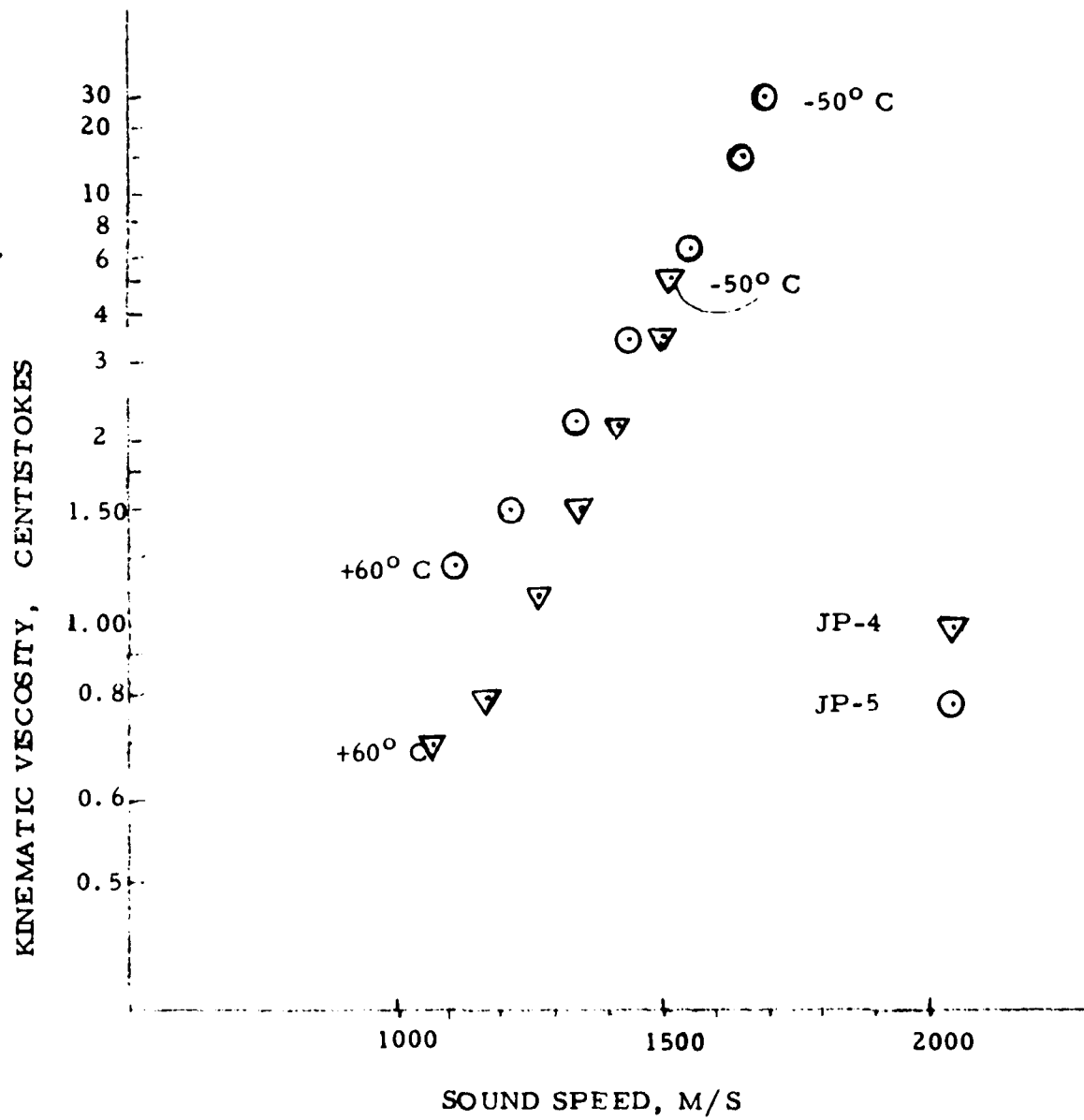


Fig. 6(d)

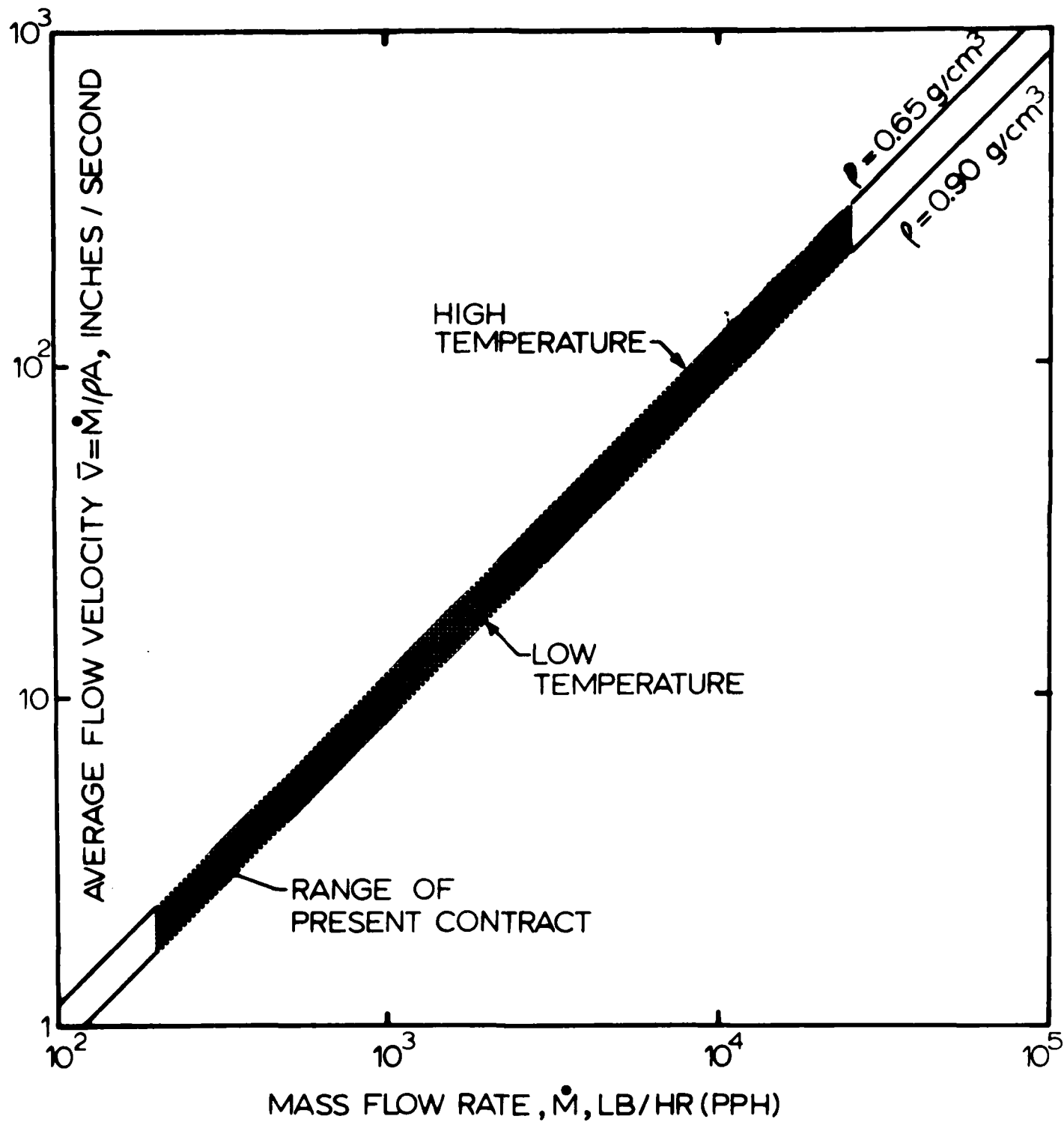


Fig. 7. \bar{V} vs \dot{M} for $\rho = 0.65$ and 0.9 g/cm^3 .

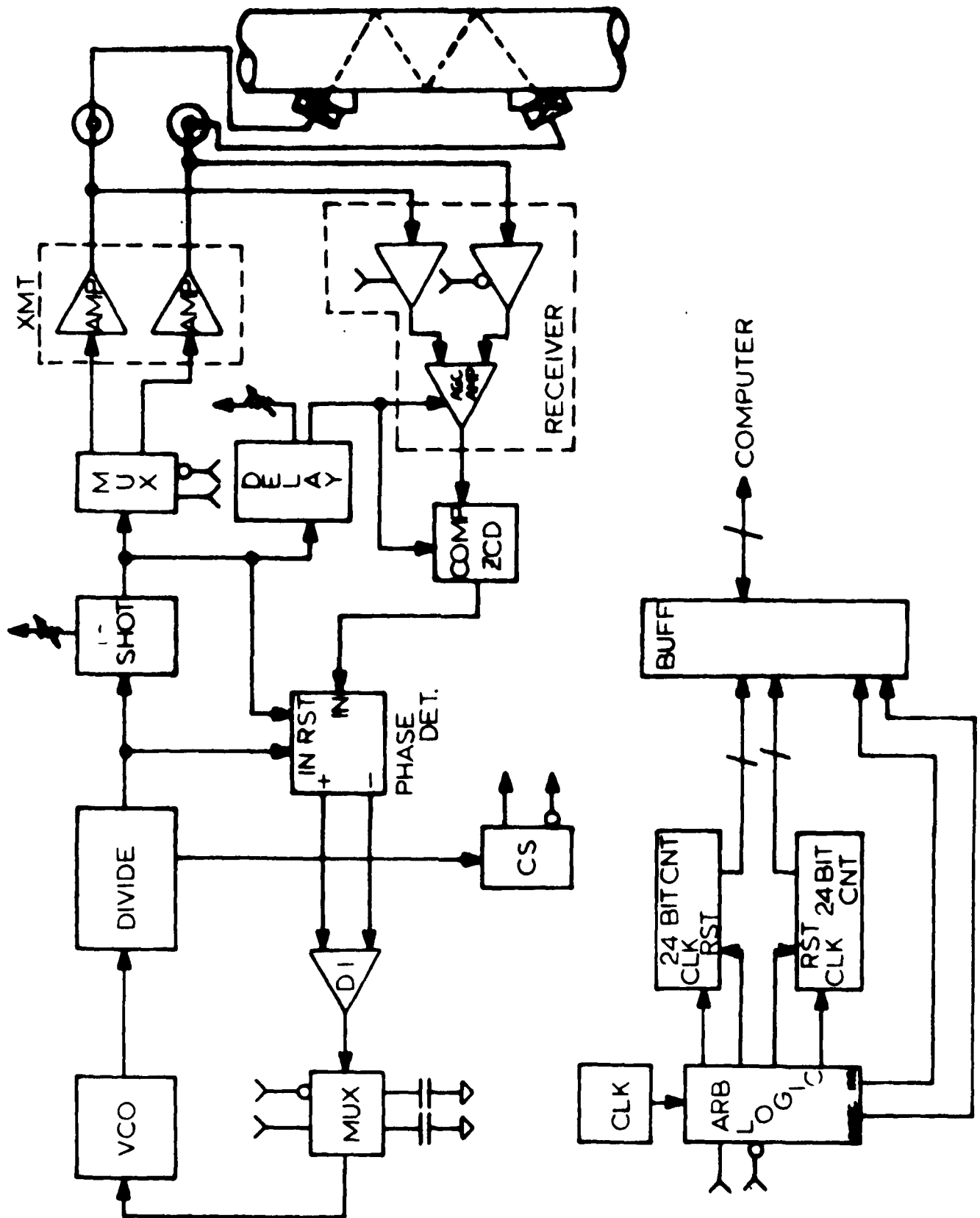


Fig. 8. Block diagram of phase locked loop flow velocimeter, operating in conjunction with SP densitometer to measure mass flow rate.

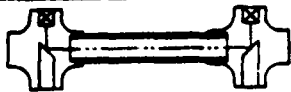




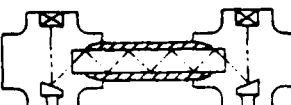
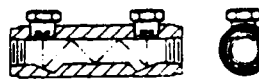




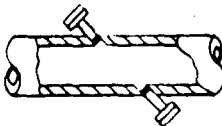
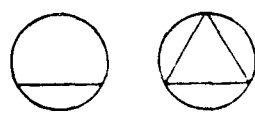

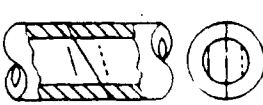
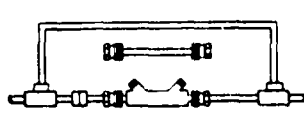

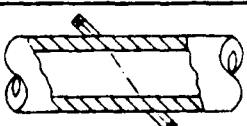


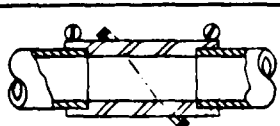

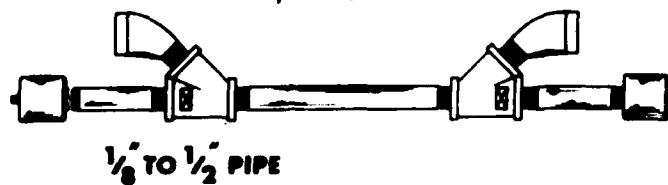
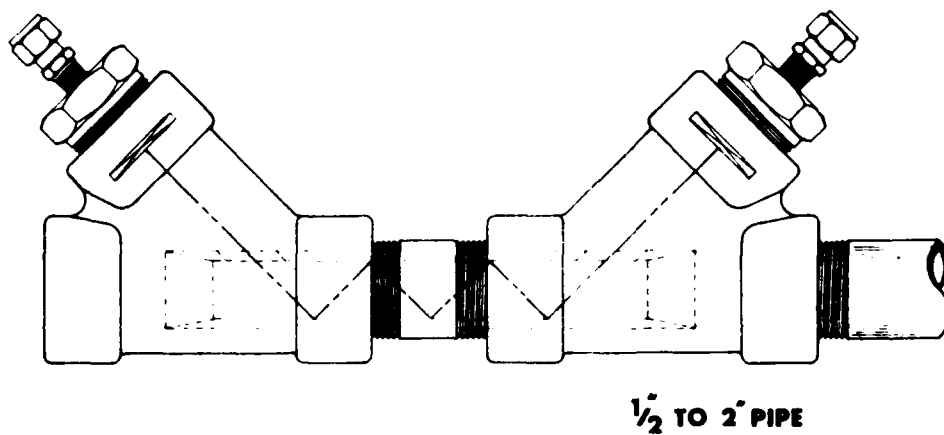
CELL TYPE	NADC-80254-60 SCHEMATIC	ADVANTAGE/ DISADVANTAGE	PIPE DIAMETER										
			3mm 1/8in	6 1/4	12 1/2	25 1	50 2	100 4	200 8	400 16	800 32	1600 64	
1. AXIAL PATH A. IN LINE REFLECTOR		Expensive. High sensitivity to V. Isolates transducers. No area reduction. Approximately area-averaging. Reflector projects into flow stream.	<div>ON AXIS</div>  <div>OFF AXIS</div> 										
	B. OFFSET-NO REFLECTOR	Uses standard compression or pipe fittings. No area reduction. Offset due to 45° elbow or tee causes some ΔP, some stagnation.											
2. JACKET+SQ. HOLED SLEEVE		No obstruction. In line. Area-averaging. Inexpensive. Can use threaded laterals to iso- late transducers. Can use 36 sch 80 sleeve and welded couplings.											
		Can use standard high pressure SS crosses (30000).											
	B. SQ. PIPE	Long zigzag path. Light weight. Relatively inexpensive. Pressure limited.											
C. MACHINED DUCT		Cells interchangeable with mini- mal as no need for recalibration. No obstruction. In line. Choice of ends. Area-averaging. Relatively expensive.											
													
3. FLANGITRON®		Flange-mounted transducers. No obstruction. Short splice piece. Can use customer's pipe or customer's splice piece with Para- metric flanges.											
4. CONVENTIONAL WETTED XDCR		Flange or screwed transducers. Long history of successful use in industry, for similar hardware made by various manufacturers.											
5. MIDRADIUS		Theoretically provides area- average for laminar and turbulent flow. Requires off-diameter ports, which increases machining difficulty.											
6. THREE CHORD GAUSSIAN, L- WEIGHTED FOR Δt OR Δf		Area-averaging. Simpler than 4-chord, especially for pipe dia- meter less than 12" (300 mm).											
7. QUICK CONNECT OR SURVEY		Meter in place only when data is being taken. Meter easily cali- brated and used at n locations.											
8. A. CLAMP-ON		Easy to use. Low cost. Safe, no penetration required. No shut- down required for installation. Accuracy best on large diameter, thin-walled pipes.	<div>PLASTIC DUCTS</div>  <div>THIN WALL SS</div> 										
	B. CLAMP-IN	Smooth bore. Uses standard fiberglass sleeve coupler. 1.0 psi maximum.											
													

Fig. 9. Comparison of various types of ultrasonic flow cells. Features or characteristics of these different types of cells, plus a few others, and identification of types 1B, 2A and 8A as the most commonly used types at this time, are discussed in ref. 10.

**AXIAL PATH, OFFSET SEGMENTED
SPOOLPIECE, 100% INTERROGATION***



ZIGZAG PATH, 100% INTERROGATION*



**TRANSDUCER: WETTED, BUFFERED
OR SHEAR WAVE CLAMP-ON***

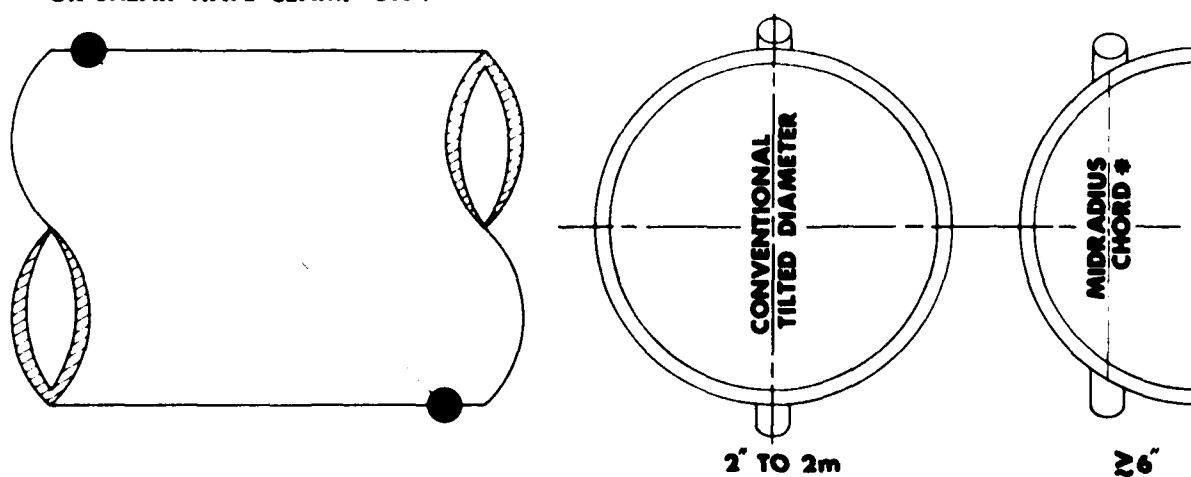
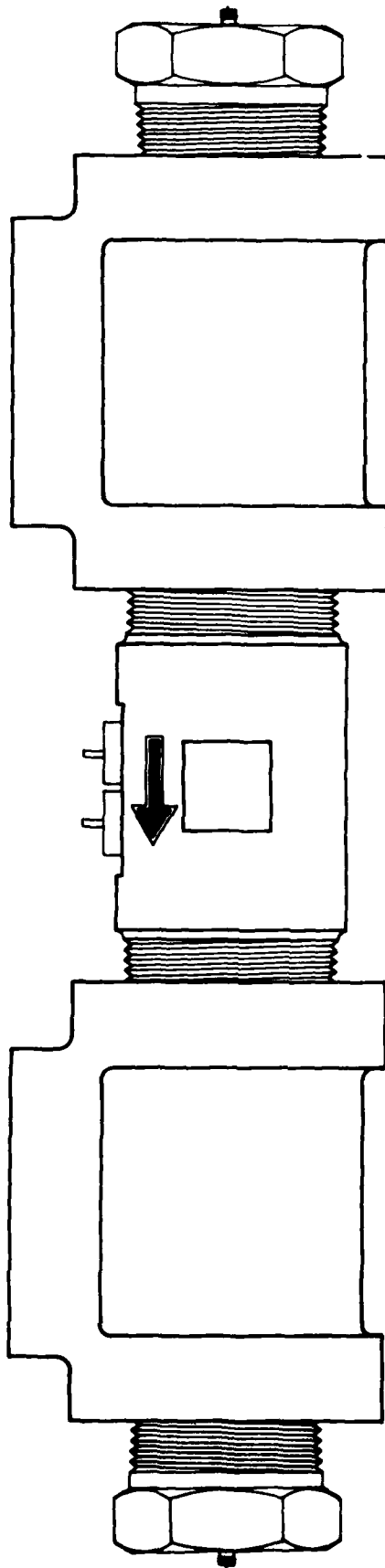
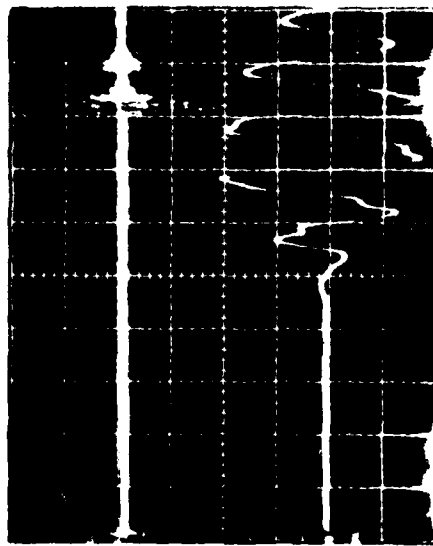


Fig. 10. Small, medium and large flow cells.
55

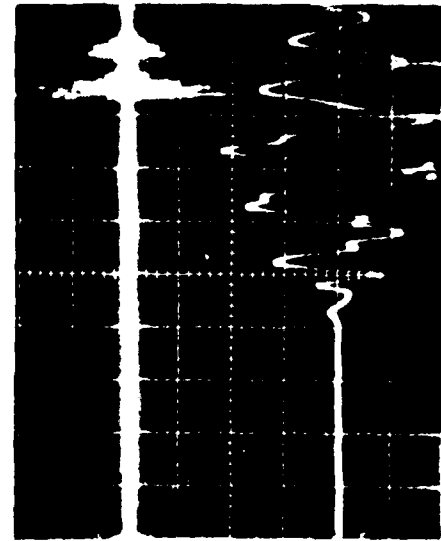
* PATENTED



(a)



(b)



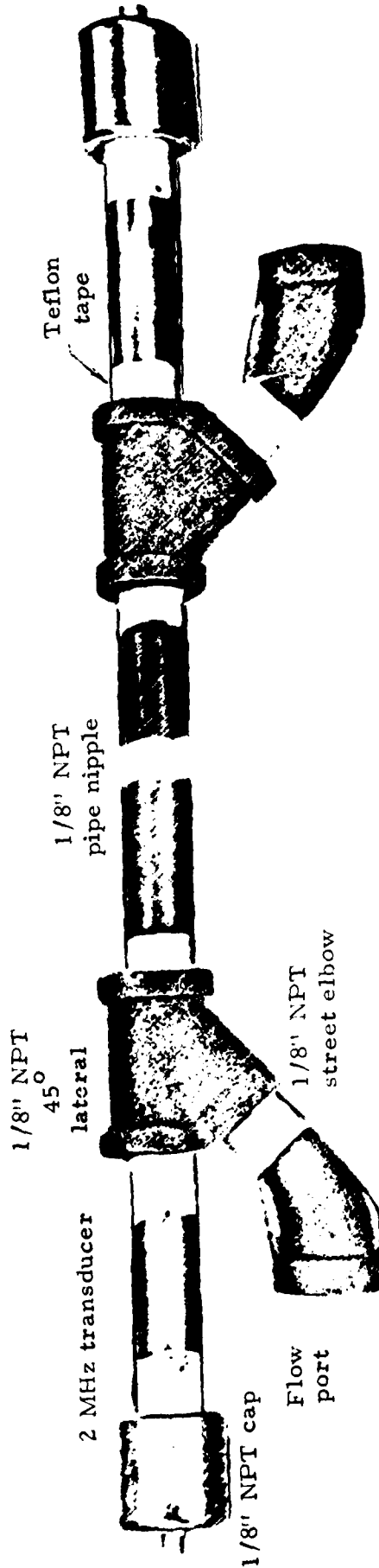
(c)

Compressed sweep:
20 $\mu\text{s}/\text{div}$

Expanded sweep:
2 $\mu\text{s}/\text{div}$

Date of
Test:
June 1978

Fig. 11. (a) Axial path interrogation of liquid contained within SP concentric tube densitometer cell. (b) Oscillographic test results for SP cell and (c) Comparison with unobstructed axial path. Liquid: water, room temperature. Electronics: Panametrics Pulsar/Receiver 5055 PRM + Krohn-Hite Filter 3202, 1.5 MHz high pass. Experimental arrangement illustrates possible use of tubes in offset flow cell as flow control surfaces, to reduce turbulence. The densitometer "flow straighteners" do not degrade the ultrasonic signal significantly in this no-flow test.



Top trace shows first received signal, and the triple transit, which is 20 dB smaller.

Bottom trace shows zero crossing of first received signal.

Electronics used in test:
Panametrics pulser/receiver,
model 5055 PRM, gain = 20 dB,
1 MHz high pass filter. Date
of test: June 7, 1979.

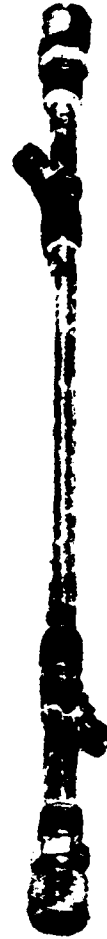


Fig. 12. Flow cells made of standard tubing, pipe and compression fittings. Design at top (with its oscillogram) was fabricated of standard brass pipe fittings. It is an example of a small diameter offset flow cell for which $D = 1/4"$ (6 mm) and $L = 4"$ (100 mm). Transmitter and receiver parts are acoustically isolated with teflon tape, according to the method due to Lynnworth, U.S. Patent No. 4,004,461 (Jan. 25, 1977).

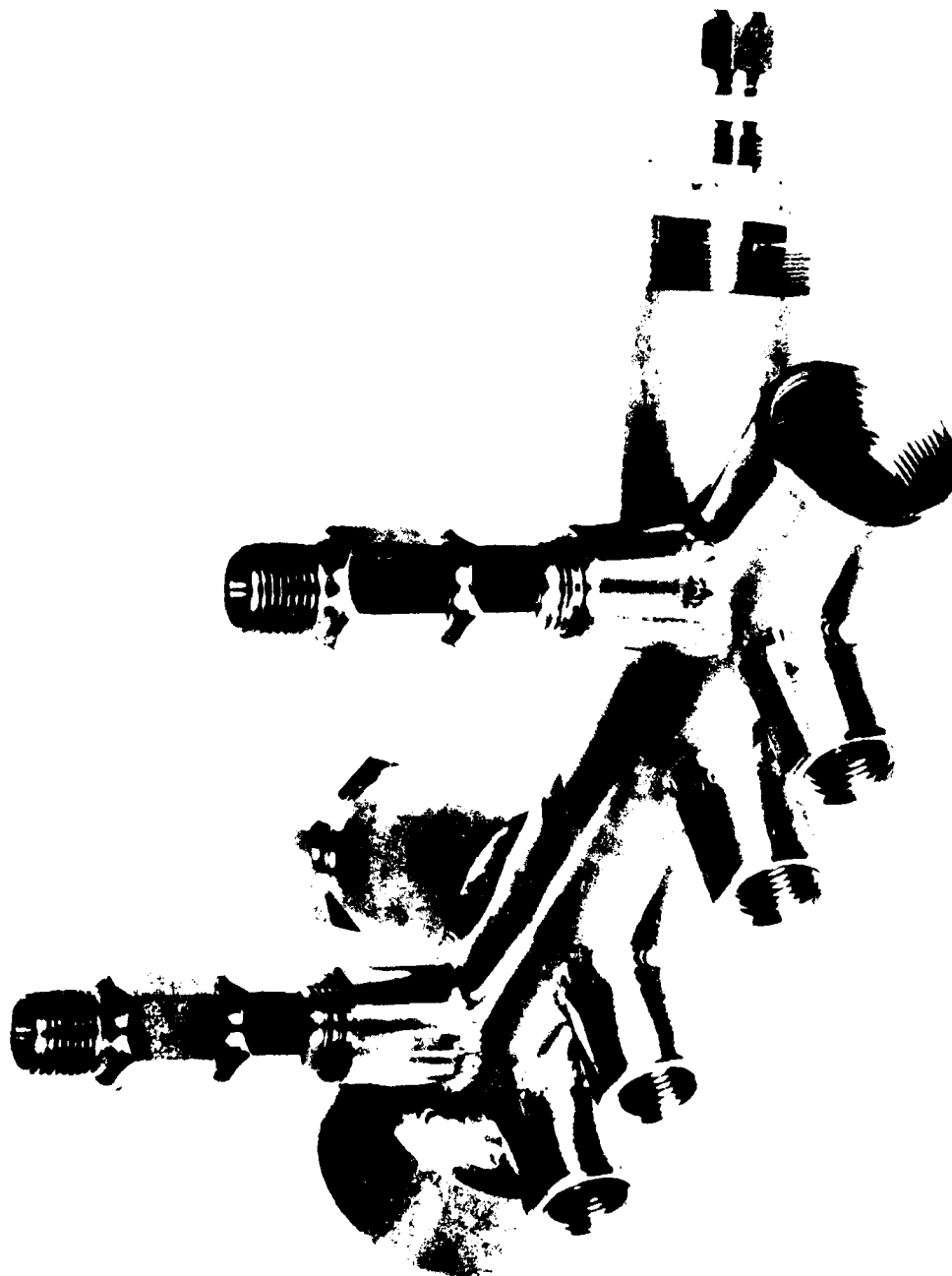


Fig. 13. Navy flow velocimeter cell photograph showing optional ports for set screws holding square holed sleeve and for optional slow torsional wave densitometer.

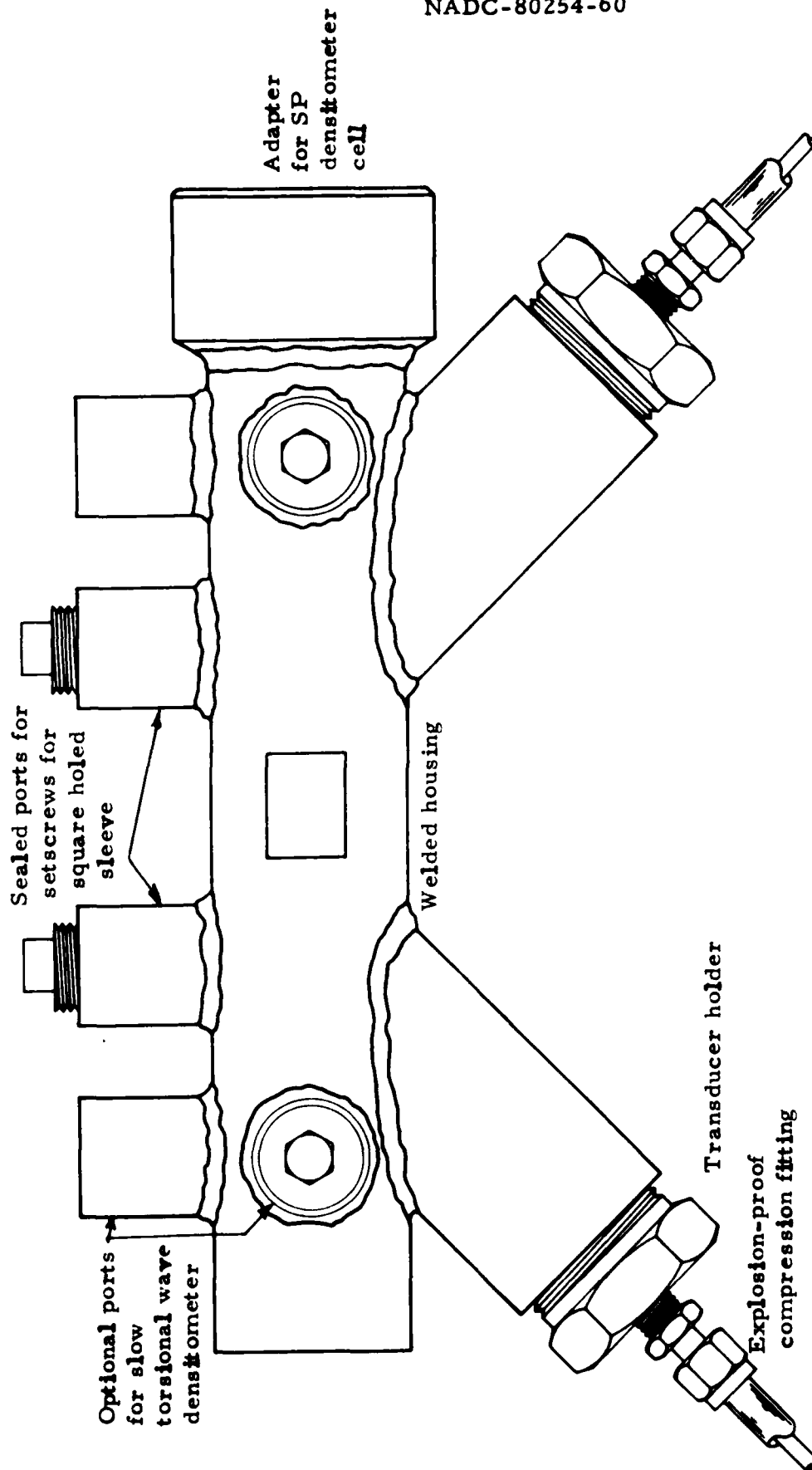


Fig. 14. Outline drawing of equipment shown in Fig. 13 in which the key components are identified.

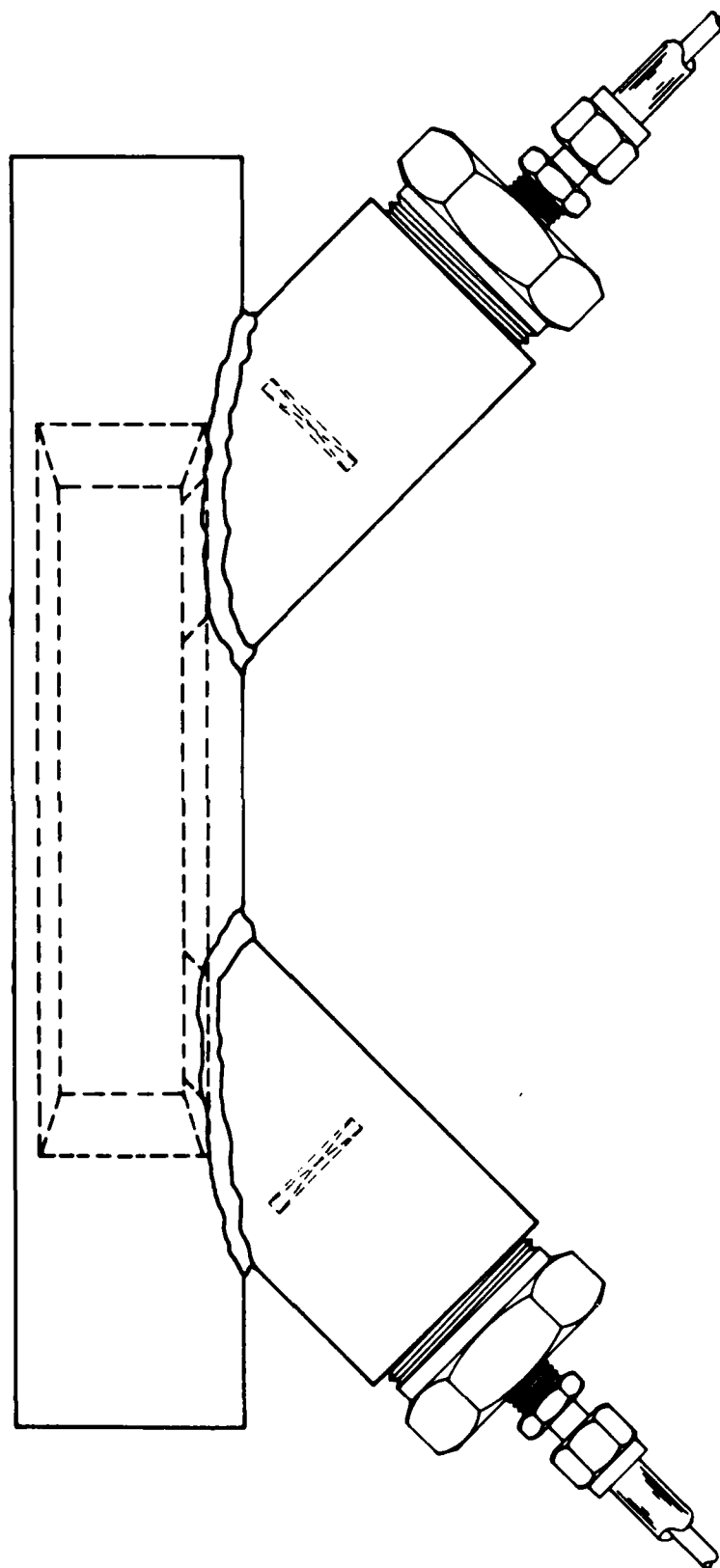
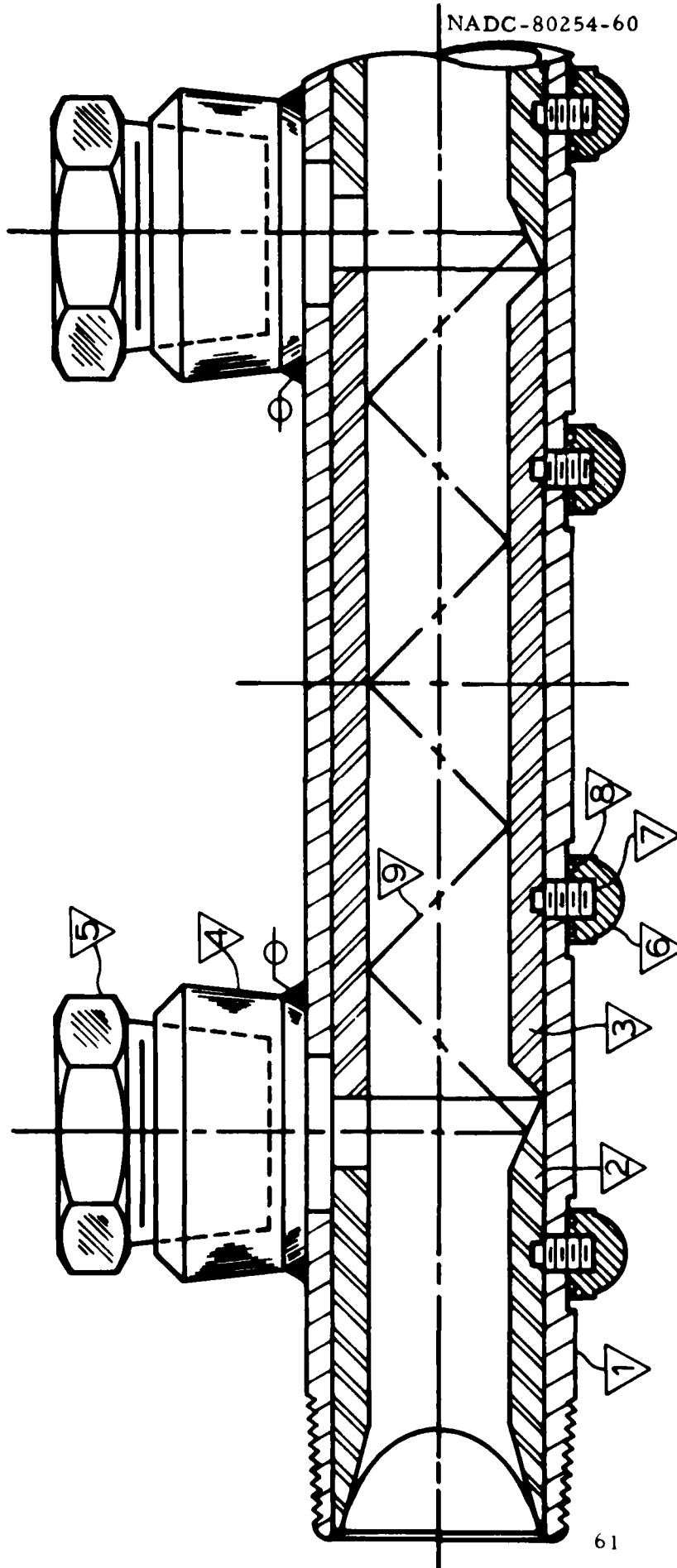


Fig. 15. Outline drawing of basic flow cell in which optional ports are omitted. The position of the square holed sleeve and the two ultrasonic transducers are indicated by dashed lines.



NOTES:

- 1 Pipe nipple, 1.5" sch 80 x 12" long
- 2 Square hole sleeve 1" x 1" x 3" long x 1.5" OD, typical 2 places
- 3 Square hole sleeve 1" x 1" ~ 6" long x 1.5" OD, or 2 segments, each ~ 3" long.
- 4 Thredolet, 3000#, 1.5" x 1.25" NPT, typical 2 places
- 5 Hex head threaded plug transducer housing, typical 2 places.
- 6 Acorn nut, typical, 4 places
- 7 Set screws, 1/4-20 typical, 4 places
- 8 O-ring seal, typical 4 places
- 9 Interrogation path, zigzag, 45°

Fig. 16. Alternate design for flow velocimeter cell portion of the system, using transducer ports orthogonal to flow axis and reflectors to control 45° zigzag interrogation path. This cell may be used with flow axis horizontal, or vertical or oblique if transducers are located on bottom.

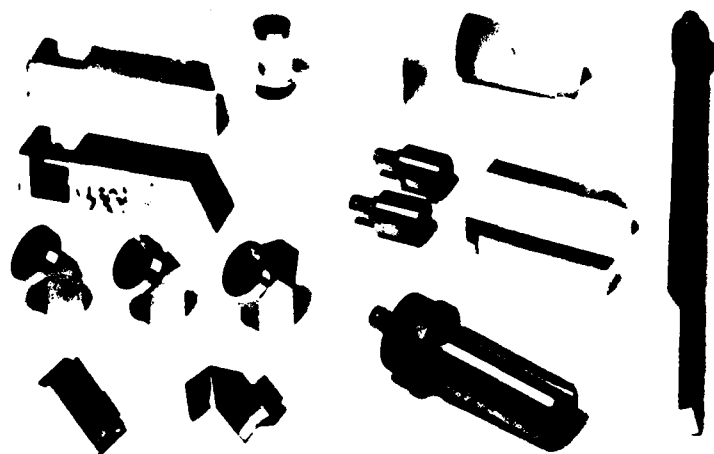
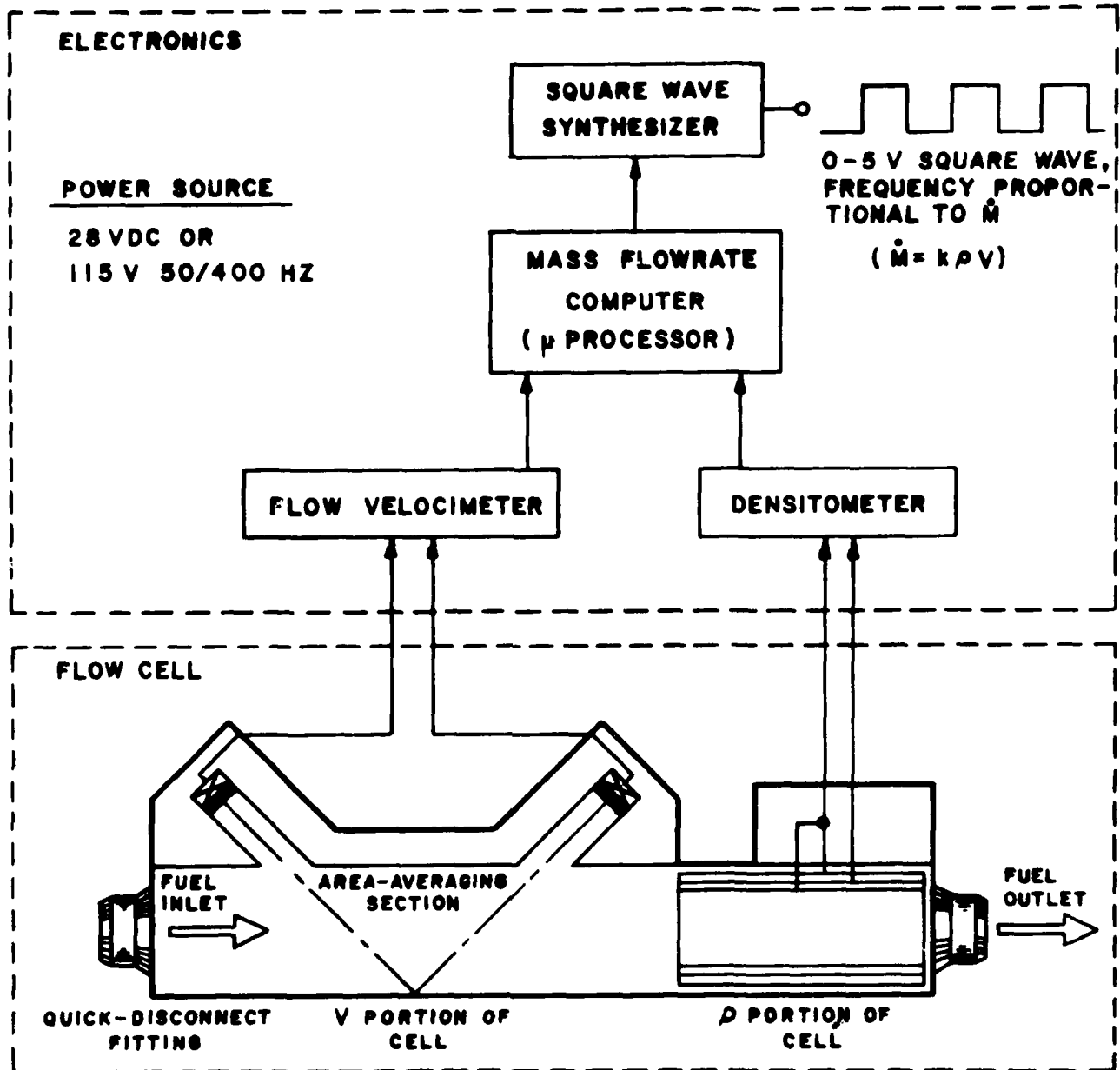


Fig. 17. Photograph showing examples of ρc reflectometer probes similar in principle to flush-mounted ρc densitometer probe investigated in first and second Eustis contracts.



SCHEMATIC OF PANAMETRICS FUEL MASS FLOWMETER

CONTRACT N00009-78-C-0000

Fig. 18. \dot{M} system block diagram.

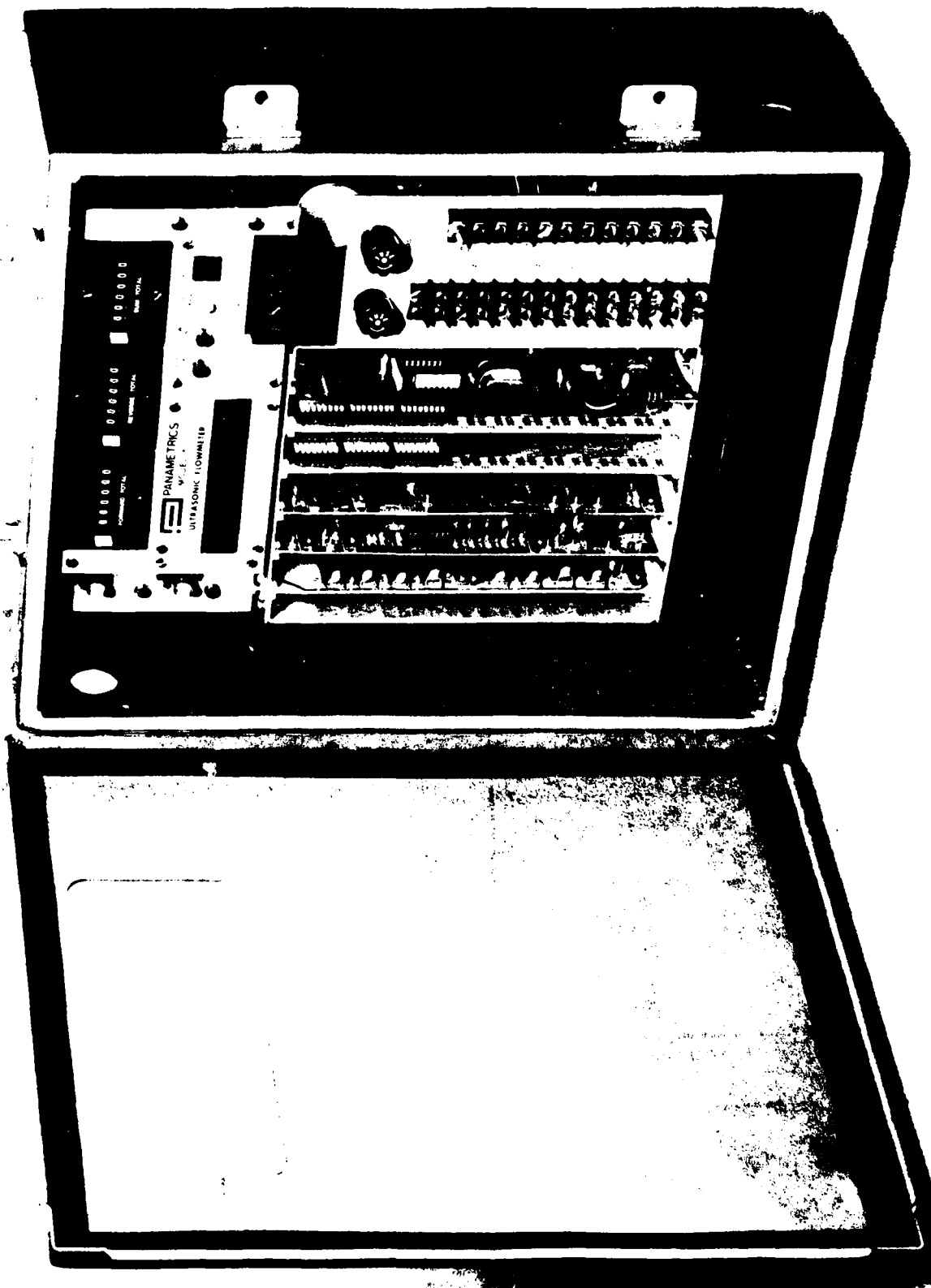


Fig. 19. Photograph of prototype flow velocimeter electronics similar to the instruments which were used to test the reference (at rest) flow velocimeter cell in the vibration tests at ATL and the axial path offset flow cell in the final fuel substitute tests at GE.

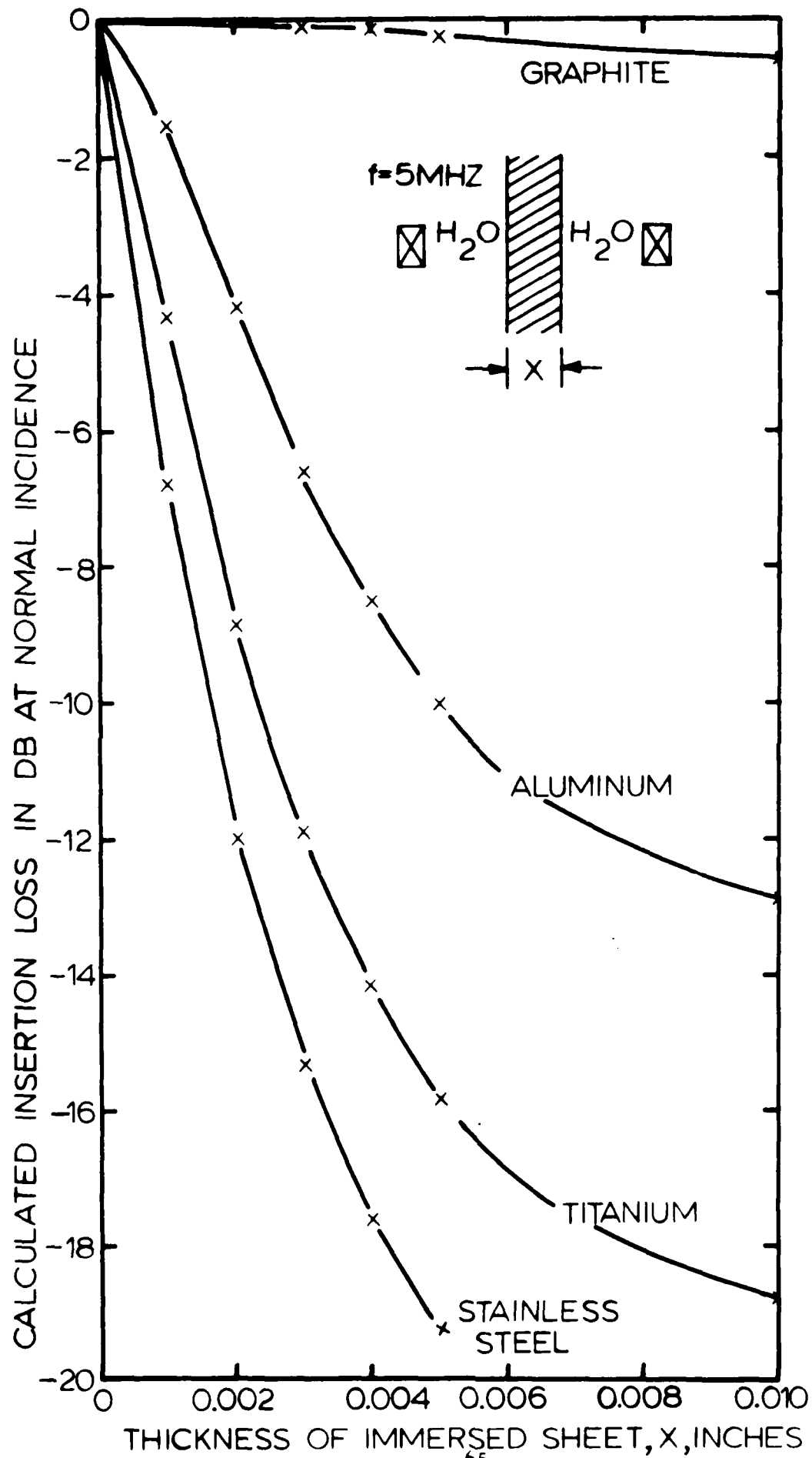
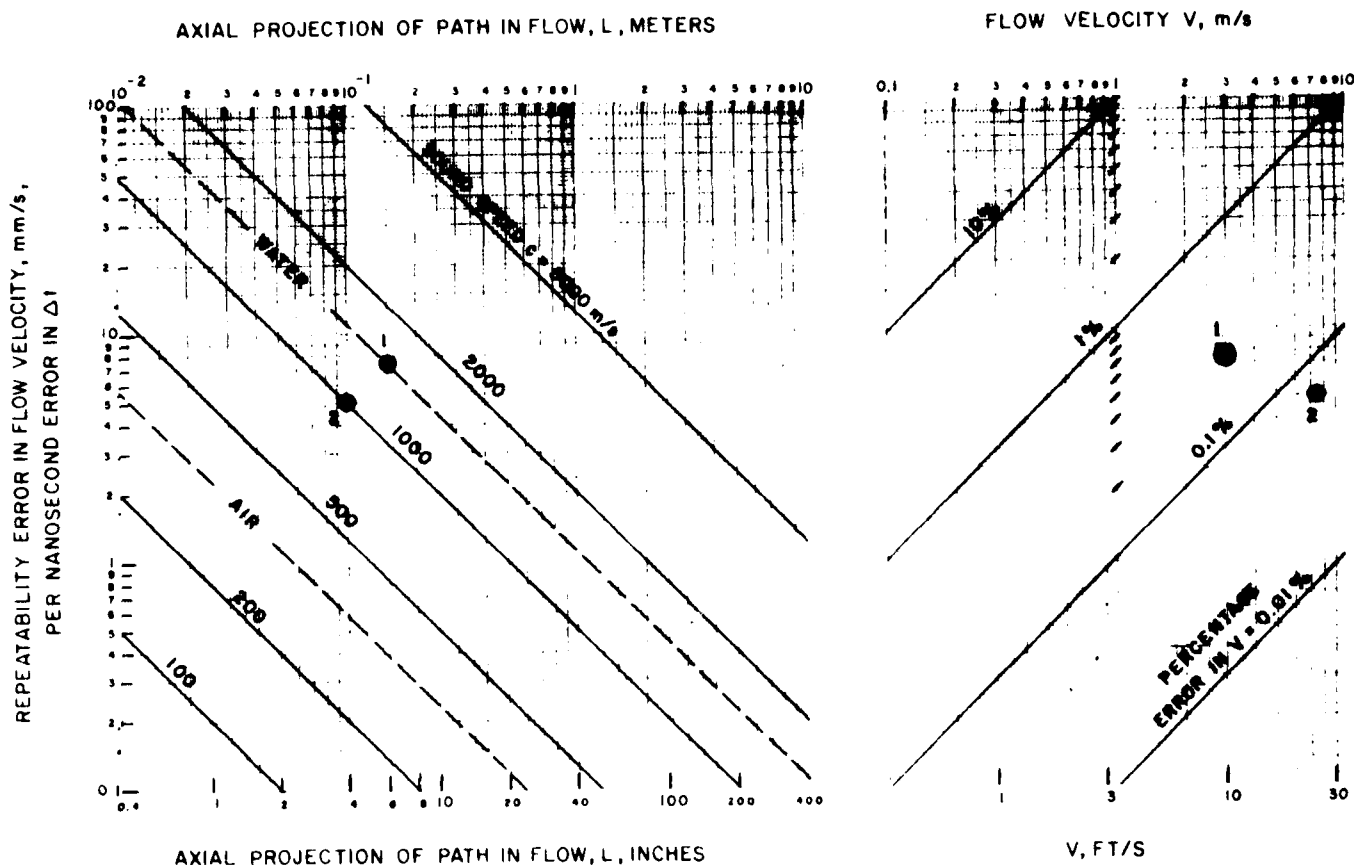


Fig. 20. Graph of insertion loss vs thickness of sheets that were considered as eddy reducers in the vicinity of transducer ports. Curves are based on calculations for normal incidence longitudinal waves at 5 MHz and assume that the sheet is fully immersed and cooled by water at room temperature.



It is virtually impossible to characterize the performance of an ultrasonic flowmeter with just one number. Even if one agrees on terminology for accuracy, repeatability response time, etc., the performance still may depend on factors beyond the control of the manufacturer. Conditions upstream or downstream, type of fluid(s), and the temperature and pressure range, and other application factors such as pipe size, wall material, thickness and roughness differ from case to case to case.

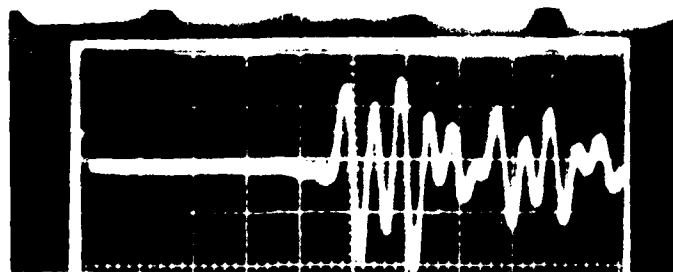
In most cases the ultimate limit on performance is imposed by the repeatability error. In the standard Model 6000 electronics, this limit is typically 1 ns. But to be meaningful this must be translated into a flow error. The above graph was constructed so the user can quickly and easily determine the flow repeatability error to be expected from a Model 6000 flowmeter, for a given set of conditions.

Enter the left-hand graph at c and L . On left ordinate read error in V , per nanosecond error in Δt .

Right-hand graph yields the percentage error, such as % of reading, % of span or % full scale, according to the V (abscissa) value selected. Example 1: water, $c = 1500$ m/s, $L = 0.15$ m (6"), $V \approx 3$ m/s (≈ 10 ft/s). Assuming error in Δt is 1 ns, read error in V as 7.5 mm/s $\approx 0.25\%$ of reading. If full scale were 10 m/s read error in V as 0.075% full scale. Example 2: JP-5, $c = 1000$ m/s, $L = 10$ cm (4"), $V = 7.62$ m/s (25 ft/s). On left-hand graph read error in V as 5 mm/s per ns. On right-hand graph estimate error as 0.07% of reading, per ns error in Δt . If error in $\Delta t = 15$ ns, then error in V would be about 1% of reading. Note use of graduations to assist logarithmic interpolation.

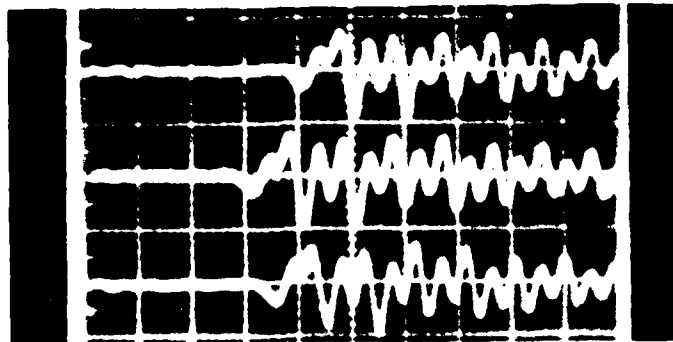
Figure 21.

JP-5

 \dot{M} , PPH T , °F

0 100

JP-5



5000 99.5

10000 93.4

20000 90.6

Above: Delayed sweep: $1 \mu\text{s}/\text{div}$
 Transit time: $\sim 200 \mu\text{s}$

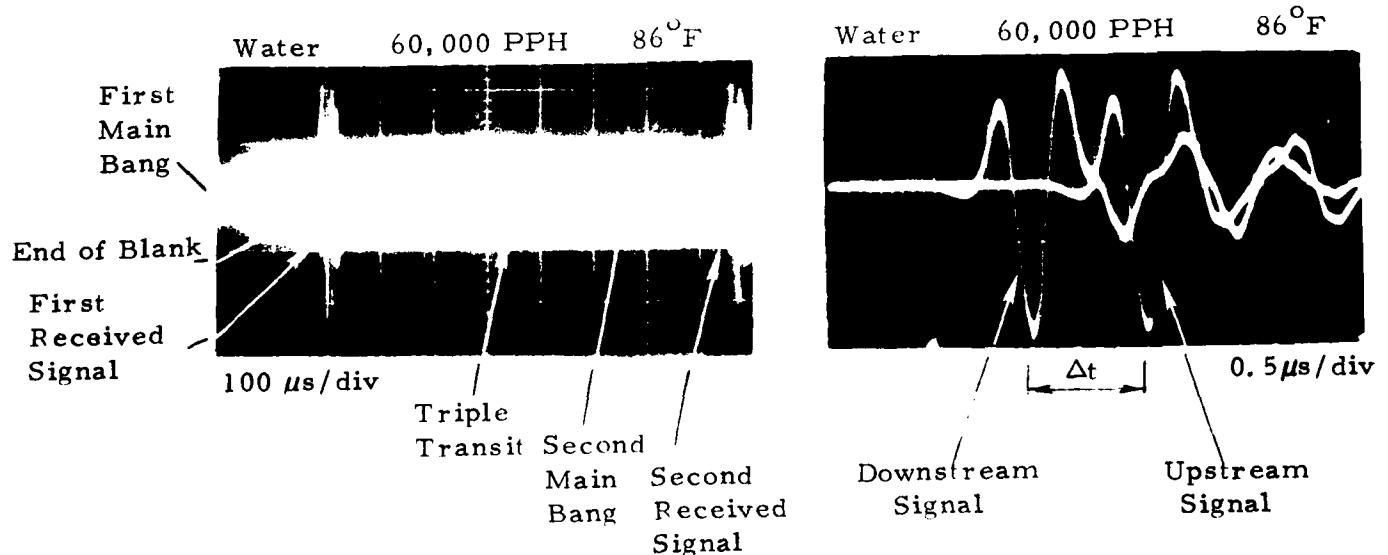
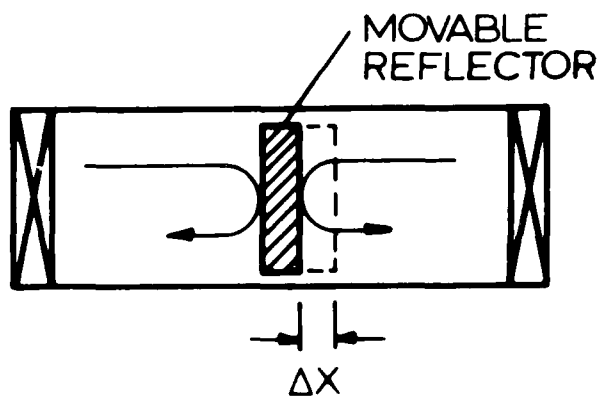
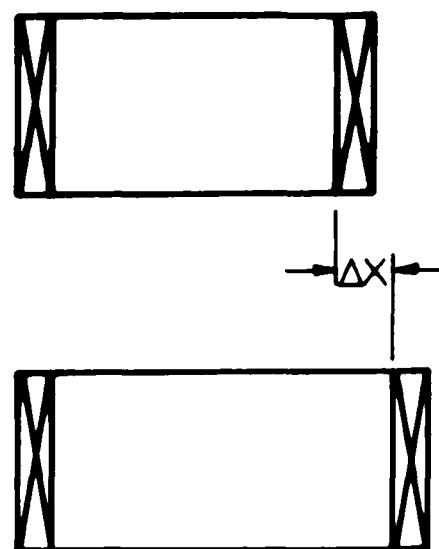


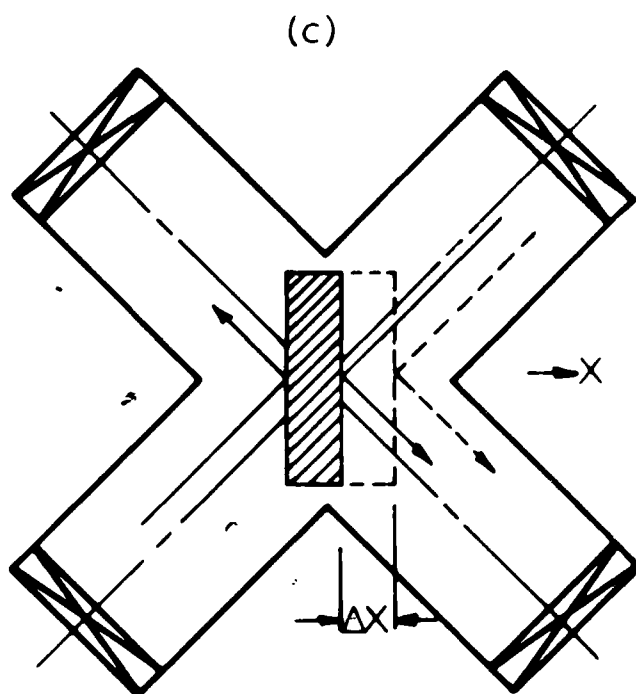
Fig. 22. Test oscillograms of received signals transmitted through JP-5 at GE at various flow rates are shown in top two recordings. Bottom two recordings were obtained at the beginning of the water calibration tests at the Foxboro Company, 23 September 1980, at a velocity of 38 ft/s ($\dot{M} = 60,000$ lb/hr). Observe that $\Delta t = 1.1 \mu\text{s}$ for $L = 100$ mm and $V = 38$ ft/s. Jitter appears negligible in the "double exposure" of the upstream and downstream received signals. Compare with Fig. K4, top oscillogram, bottom trace, obtained using the fuel substitute 7024BII at 31,450 lb/hr (14,309 kg/hr).



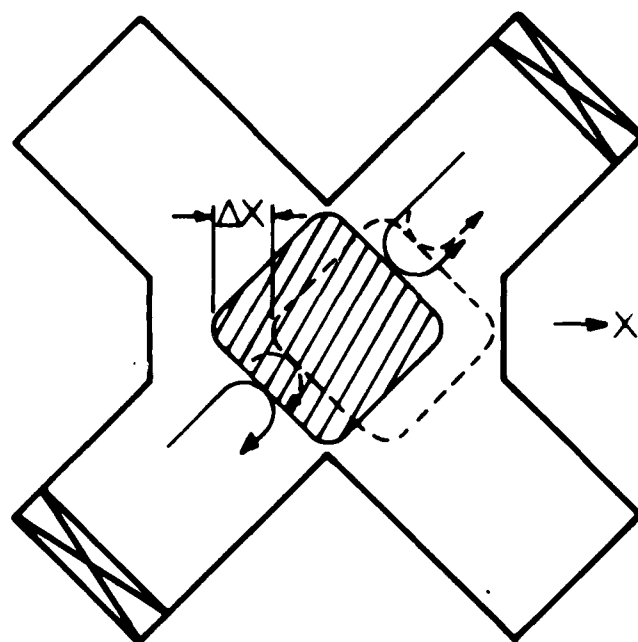
(a)



(b)



(c)



(d)

Fig. 23. Flow simulators comprised of differential path cells. (a) Pulse echo. (b) Through transmission. (c) Folded transmission, or "pitch-and-catch," arrangement. (d) Pulse echo with reflector motion at 45° to interrogation axis.

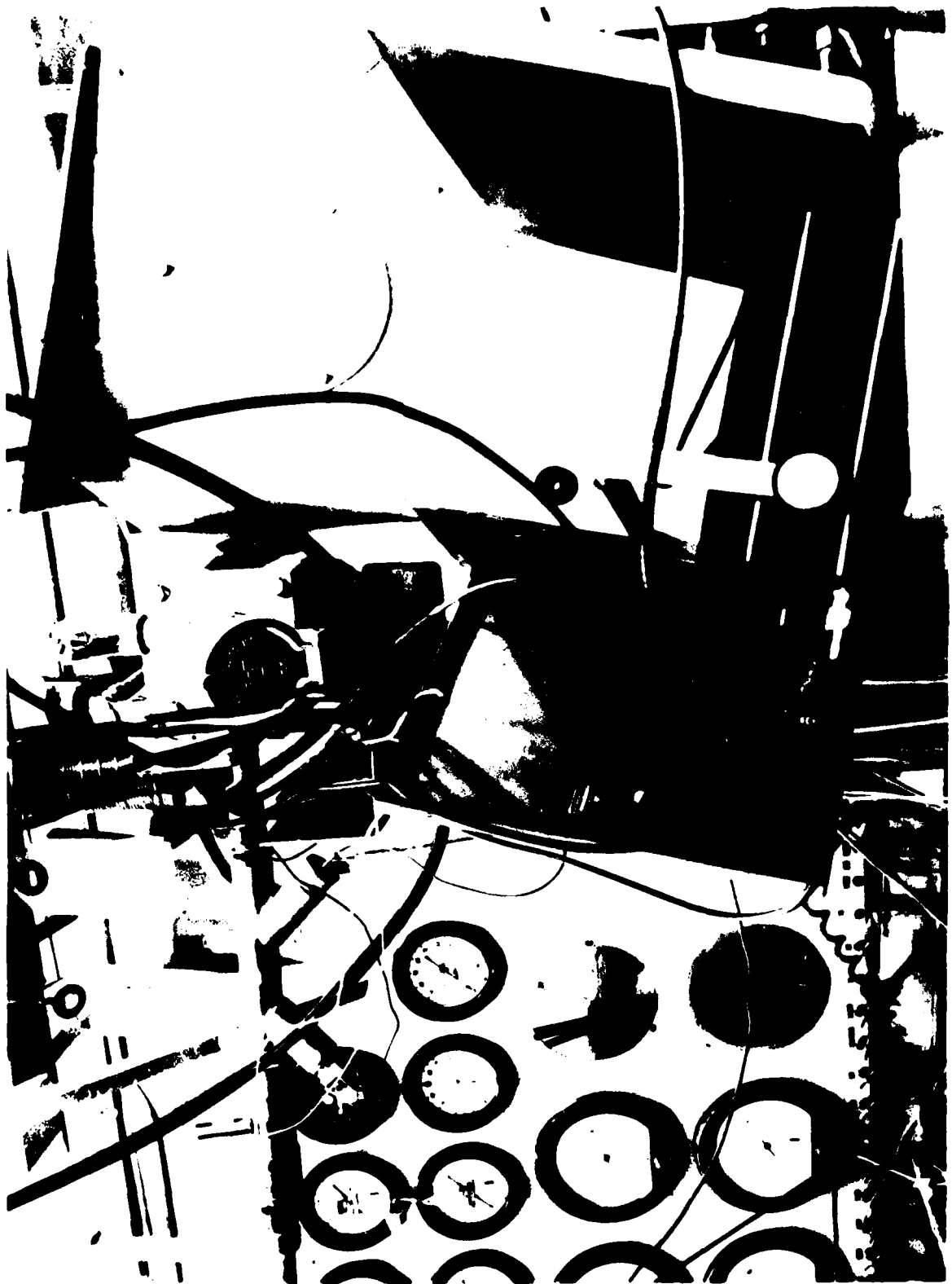


Fig. 24. General view of flowmeter under preliminary test at GE-Lynn. Photo courtesy GE.

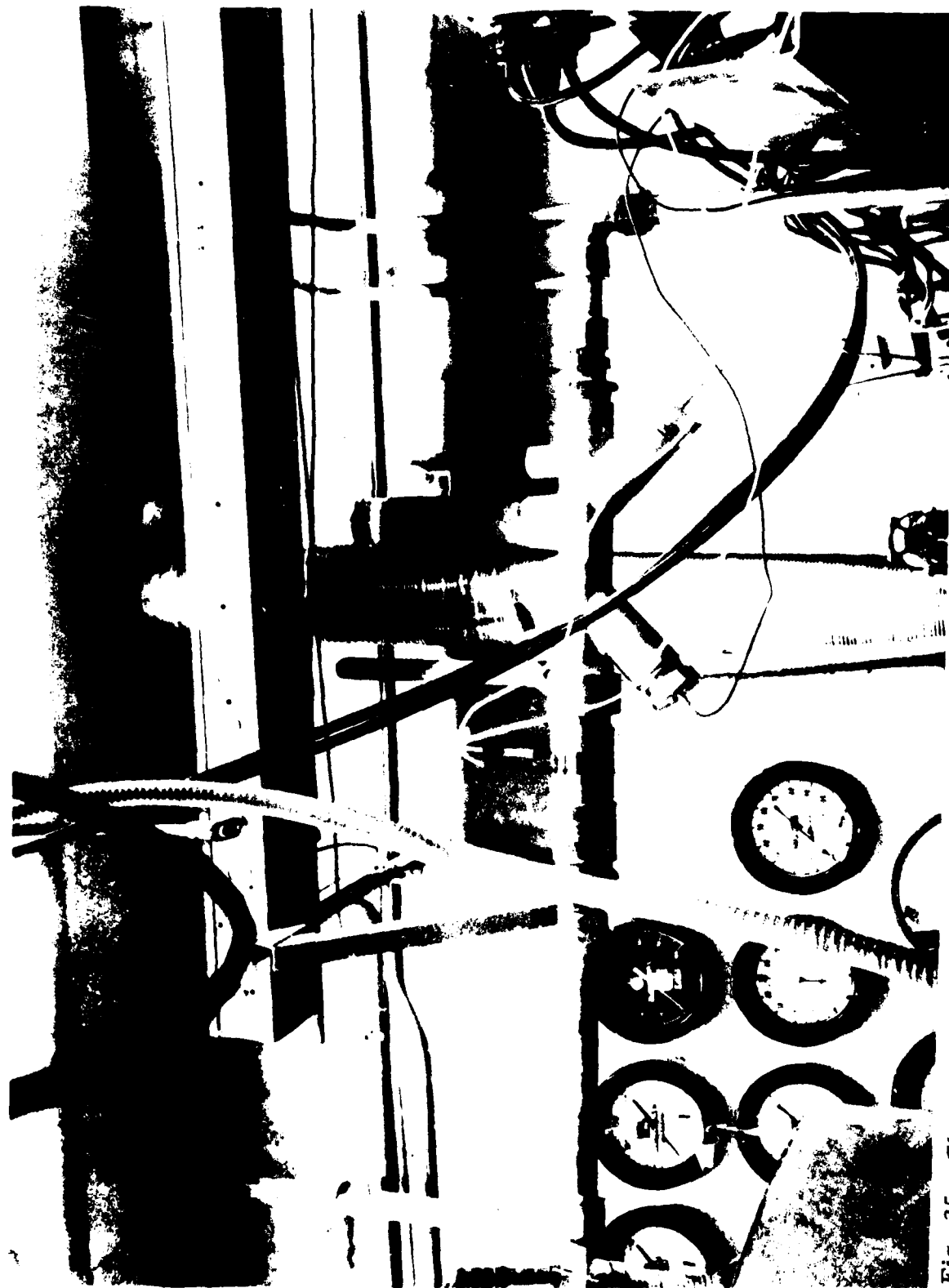


Fig. 25. Close-up of mass flowmeter cell in preliminary test. In subsequent tests, distance from elbow to cell was increased, allowing room for either flow straightener or static mixer to be installed in-line upstream. Photo courtesy GE.

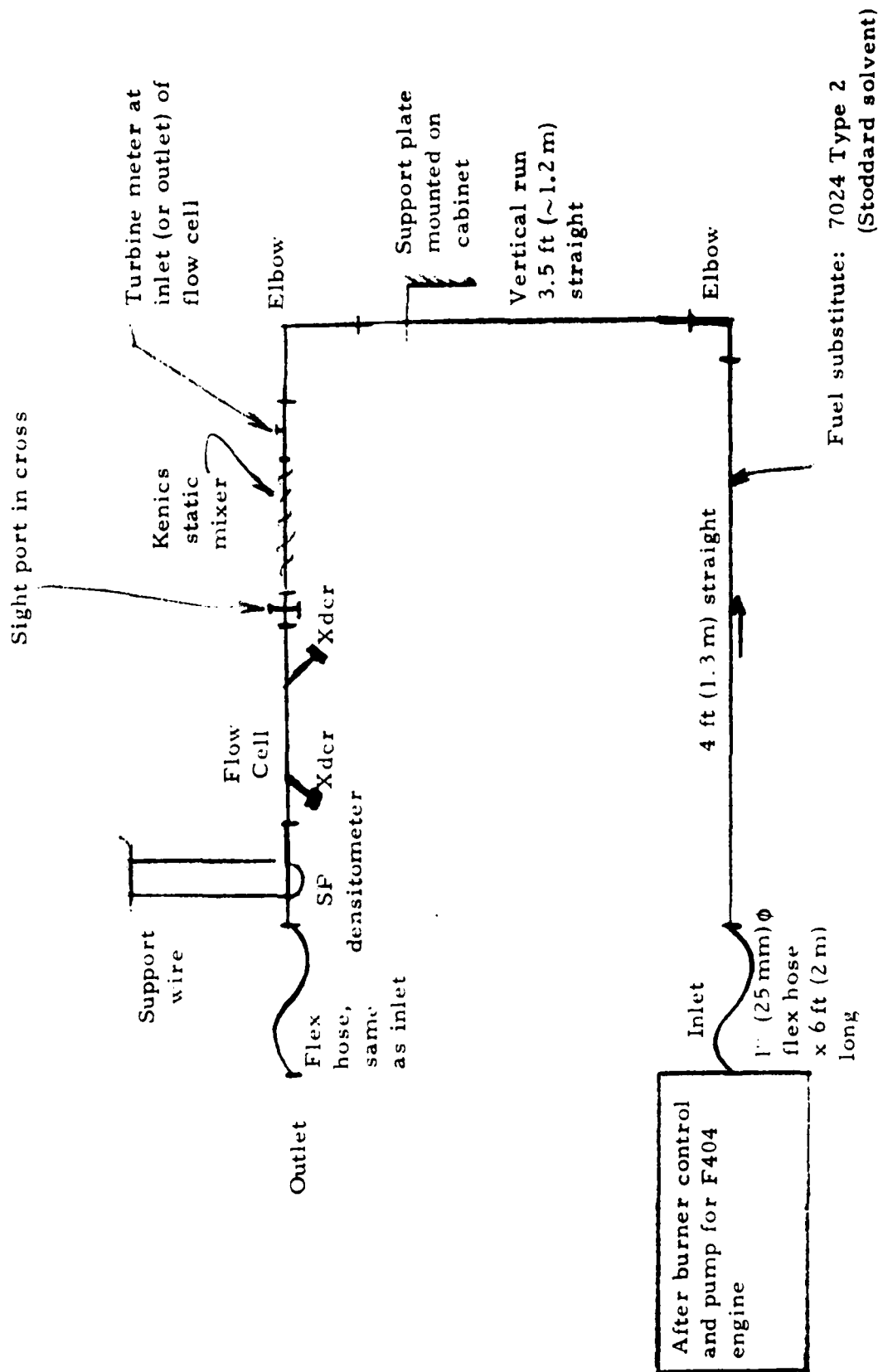


Fig. 26. Schematic of test at GE-Lynn, March 1980

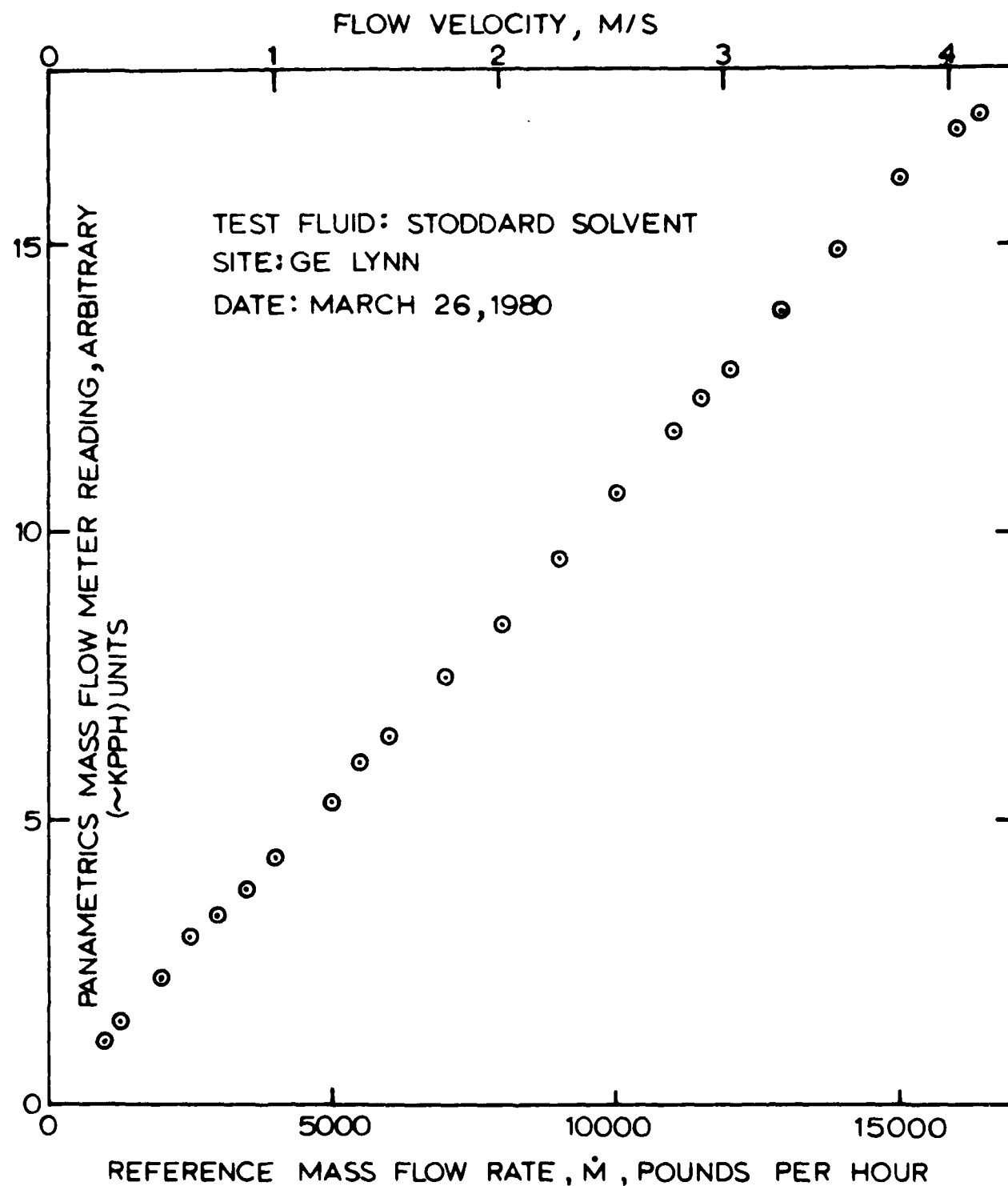


Fig. 27. Mass flow rate calibration data using fuel substitute. Reference \dot{M} obtained using Cox ANC-24, S/N 23803, calibrated from 990 to 59000 pounds per hour, accuracy $\pm 1/4\%$ of reading.

Flow cell type: 25x25 mm square zigzag. Transducer Frequency = 2 MHz.

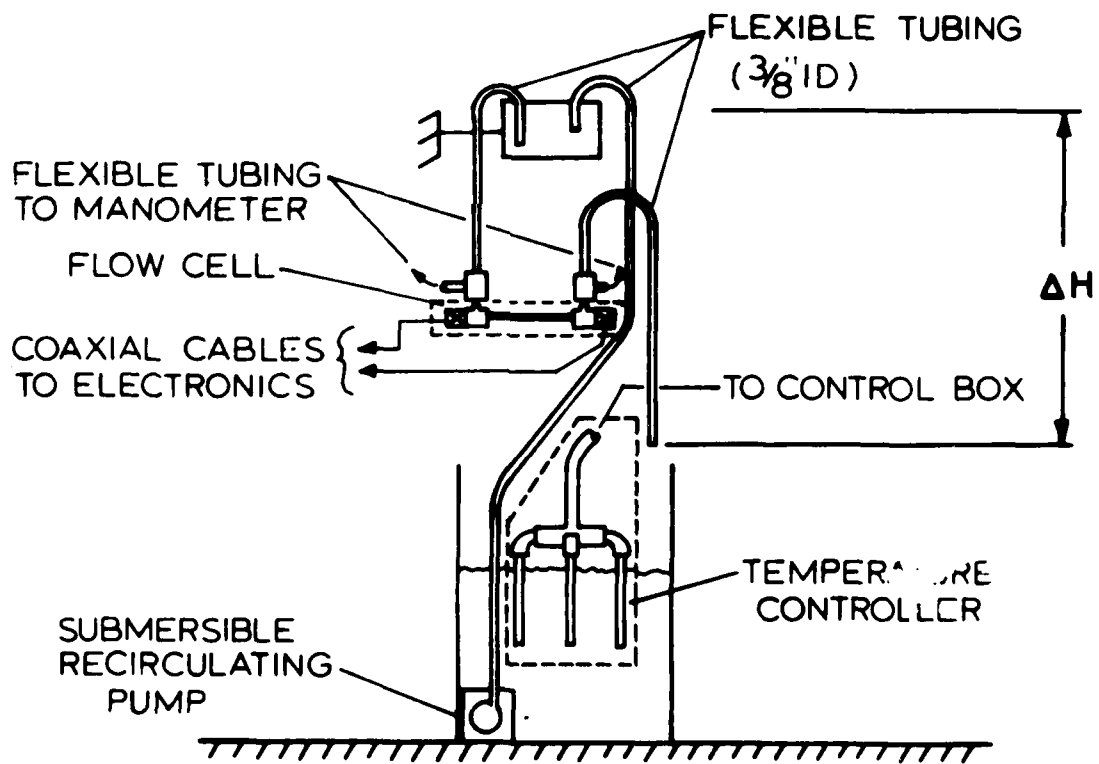


Fig. 28. ΔH flow loop with offset flow cell used in 10-day repeatability test.

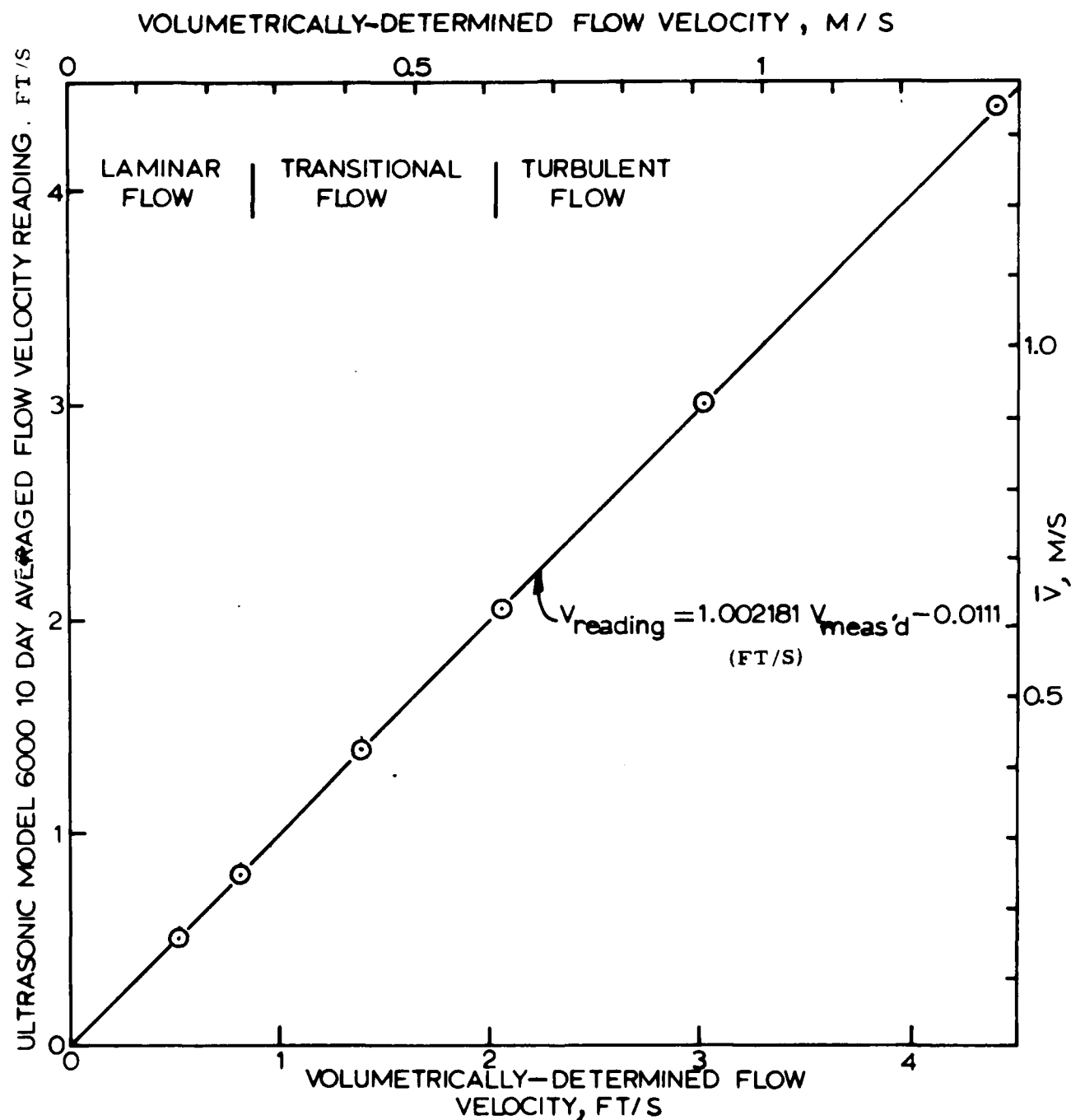


Fig. 29. Data for 10-day repeatability test, using water in offset flow cell, July 1980. ID = 7.9 mm. L = 132 mm. P = 168 mm, $t_w = 1 \mu s$. At the maximum V, $\sigma = 0.2\%$ of reading; at minimum V, $\sigma = 2\%$ reading.

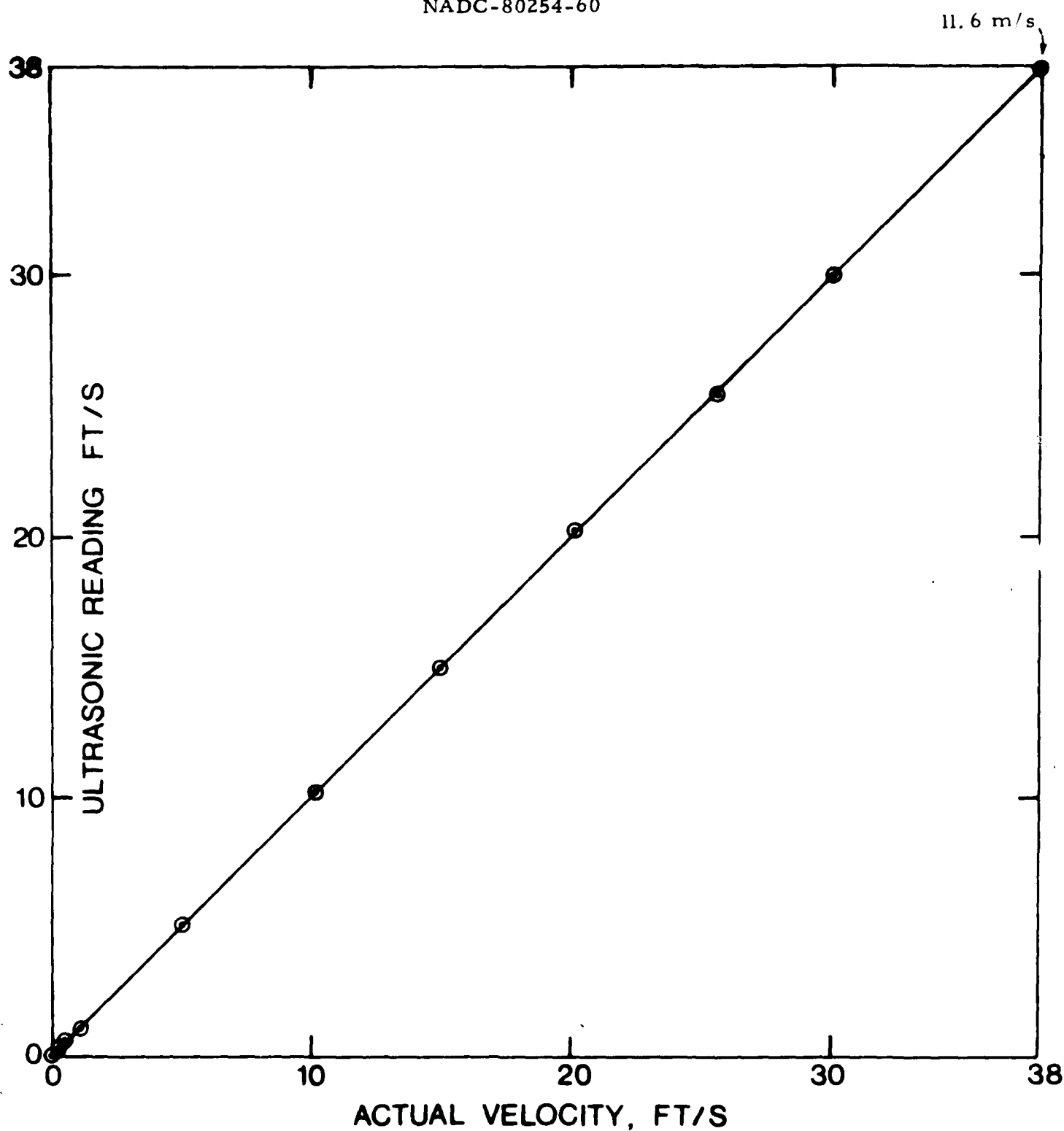


Fig. 30. Water calibration test data obtained by the Foxboro Company, Foxboro, MA, on 23 and 24 September 1980.

Flow cell type: same as previous figure. Above data obtained after subjecting cell and transducers to Mil Spec vibration test 5 to 2000 Hz and up to 20 g/s.

APPENDIX A. OBJECTIVES/EXTRACTS FROM NADC STATEMENT
OF WORK

3. Requirements

- 3.1 Fuels: The transmitter must be capable of the mass flow rates of JP-4 and JP-5 aviation fuels and all mixtures thereof without manual calibration.
 - 3.1.1 Fuel Temperature Range: The flowing fuel temperature range may vary from -38°C to $+150^{\circ}\text{C}$.
 - 3.1.2 Fuel Substitution: An approved commercial fluid of higher flash point but same specific gravity may be used for test and calibration.
 - 3.1.3 Contaminated Fuel: The transmitter shall be operated as specified in sec. 4. 10. No degradation in subsequent accuracy tests shall be evidenced or damage observed upon inspection.
- 3.2 Mass Flow Rate Range: The transmitter shall be capable of accepting a flow rate range and transmitting signals analogous to flow rates of 100 PPH to 25,000 PPH.
- 3.3 Accuracy: Over the flow range stated in item 3. 2, the transmitter accuracy shall be $\pm 5\%$ of point at low end of flow range and linearly improving to $\pm 0.5\%$ of point at 3,000 PPH. Then it shall remain at this value over the rest of the flow range to maximum flow (25,000 PPH).
- 3.4 Hysteresis: Upscale and downscale readings shall agree to within $\pm 0.3\%$ of each other.
- 3.5 Repeatability: Repeatability is here defined as the capability of reproducing, at successive points in time, the same signal output for the same mass flow input.

The variations shall not exceed:

- ± 2 PPH at low end of flow range
- ± 3 PPH at test point of 3,000 PPH
- ± 15 PPH at test point of 15,000 PPH
- ± 25 PPH at test point of 25,000 PPH

- 3.6 Response Time: The transmitter shall be capable of being rapidly slewed from 500 to 25,000 PPH and having its output come to within $\pm 1\%$ of final steady-state value in two seconds.
- 3.7 Signal Output Format: The transmitter signal output shall be: a 0 to 5 volt square wave with a frequency directly proportional to mass rate of flow (\dot{M}) and further shall be compatible with the requirements of MIL-STD-1553 for multiplex operation.
- 3.8 Vibration: The transmitter and any associated signal processing circuitry shall be capable of meeting the accuracy requirements of 3.3 while under vibration at room temperature as in sec. 4.9.
- 3.9 Power: The transmitter shall be designed and built to accept 28 volts D. C. as defined by MIL-STD-704.
 - 3.9.1 Optional Power Requirement: In addition, the design, but not the present fabricated product, shall incorporate the option of being able to operate on 400 Hz, 115 volt power as defined by MIL-STD-704.
- 3.10 Desired Design Attributes
 - 3.10.1 Wiring: To consist of not more than 4 conductors, 2 for power, 2 for signal. Signal and power common shall not be carried on the same conductor. Design should incorporate the option for optical signal transmission.
 - 3.10.2 Flow Connectors: All fluid transmitting connectors shall be of the quick disconnect type, sized to accommodate those flow rates cited herein and stressed to withstand pressures to 1600 PSI.

4. Acceptance Tests and Evaluation

- 4.1 The contractor shall prepare and submit to the Navy a comprehensive program of test procedures designed to verify the performance requirements of section 3.

- 4.2 The contractor shall then conduct tests to verify the performance requirements of section 3. In addition to contractor-performed tests the equipment will be examined and tested by the Navy.
- 4.3 Test Instrumentation: For the purpose of verifying the output performance requirements a commercially-available frequency-type or counter-type meter may be used.
- 4.4 Fuel Temperatures and Densities: Fuel temperature shall vary, as required, over the range specified in 3.1.1. Fuel densities shall vary over the range taken by the minimum density of JP-4 at high temperature and the maximum density taken by JP-5 at low temperature.
- 4.5 Accuracy: Accuracy tests shall first be performed at room temperature. These tests shall be repeated at the specified fuel temperature extremes with an allowable variation from the established room temperature error of not more than $\pm 10\%$ of that error for any position in the flow range.
- 4.6 Hysteresis: The transmitter shall be subjected to a series of runs to verify the hysteresis requirements. Room temperature accuracy tests shall be run at increasing flow rates from minimum to maximum. Master transmitter vs test transmitter readings shall be taken at intermediate points moving up through the flow range. The flow shall be decreased and master vs test transmitter readings again taken at the same flow points as indicated by the master. Upscale and downscale readings of the test transmitter shall be within $\pm 0.3\%$ of each other for any flow rate.
- 4.7 Repeatability: Not less than ten room temperature accuracy tests shall be run, each separated from the previous by one day in time. The day to day variations shall not exceed:
- ± 1 PPH at extreme low end of flow range
 - ± 3 PPH at test point of 3,000 PPH
 - ± 15 PPH at test point of 15,000 PPH
 - ± 25 PPH at test point of 25,000 PPH

Several intermediate test points in addition to the above shall also be recorded.

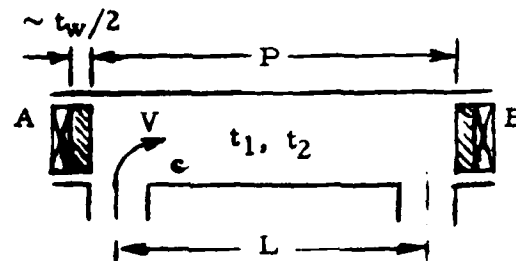
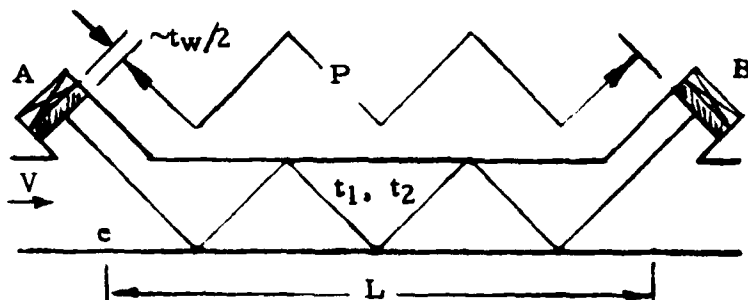
- 4.8 Response Time: The response time test shall be the measurement of the capability of the transmitter to track a step change in flow rate due to the activation of a quick opening valve.
- 4.9 Vibration: The transmitter shall be tested for accuracy while under vibration. This shall be done for a selected mass flow rate in the 7,000 to 15,000 PPH range. The vibration test shall be performed according to MIL-STD-810 method 514.1 as required by MIL-E-5007D para 4.6.2.3.9 except that the maximum temperature test shall be deleted.
- 4.10 Contaminated Fuel Test: A room-temperature accuracy test shall be run continuously for 300 hours at maximum flow rate with fuel having contaminants of the size, nature and quantity shown in Table X of MIL-E-5007D.

APPENDIX B. LIST OF MATHEMATICAL SYMBOLS

a	constant
A	area
b	constant
c	sound speed
C	polarizability
f	frequency
K	meter factor
L	axial projection of path in flowing liquid
\dot{M}	mass flow rate
N	multiplier
P	path length in liquid
Q	volumetric flow rate
Re	Reynolds number
t, T	transit times
V	flow velocity
\bar{V}	area average flow velocity
w	window (subscript)
Z	acoustic impedance
α	attenuation coefficient; thermal expansion coefficient
ϵ	dielectric constant; error
σ	standard deviation
Δ	difference
ρ	density
ν	kinematic viscosity

APPENDIX C. DERIVATION OF V EQUATIONS

Let the zigzag and straight velocimeter geometries be represented as follows:



Let P = path length in fluid.

L = axial projection of effective path in flowing fluid.

t_w = total time delay in window, shim, wedge, buffer, impedance matcher, etc. + reciprocal electrical delays including cables and circuit components, i.e., all non-fluid delays.

t_z = time difference, upstream minus downstream, measured at zero flow; or the difference between t_1 and t_2 measured at steady (non zero) average flow velocity V and constant sound speed c , for transposed cables, that is,

$$t_z = (t_1 - t_2)_{CA} - (t_1 - t_2)_{CB} \approx (t_1 - t_2)_{\text{no flow}} \approx \Delta_1 - \Delta_2$$

Δ_1 = electrical + nonreciprocal path delays in configuration 1 (A transmits).

Δ_2 = electrical + nonreciprocal path delays in configuration 2 (B transmits).

t_1 = transit time measured when A transmits

t_2 = transit time measured when B transmits

$$\Delta t = t_2 - t_1$$

If the system were reciprocal, and if there were no electrical delays, then at a flow velocity V ,

$$\Delta t = t_2 - t_1 = \frac{2LV}{c^2} \quad (1)$$

where

$$c = 2P / (t_1 + t_2 - 2t_w) \quad (2)$$

Therefore
$$V = \frac{c^2 \Delta t}{2L} = \left(\frac{2P^2}{L} \right) \frac{t_2 - t_1}{(t_1 + t_2 - 2t_w)^2} \quad (3)$$

If the system is not reciprocal,

$$V = \frac{2P^2}{L} \frac{(t_2 - \Delta_2) - (t_1 - \Delta_1)}{[(t_1 - \Delta_1) + (t_2 - \Delta_2) - 2t_w]^2} \quad (4)$$

which if desired, may be rearranged as

$$V = \frac{2P^2}{L} \frac{t_2 - t_1 + \Delta_1 - \Delta_2}{(t_1 + t_2 - \Delta_1 - \Delta_2 - 2t_w)^2} \quad (5)$$

If the system is reciprocal, $\Delta_1 = \Delta_2 \equiv \Delta$ and

$$V = \frac{2P^2}{L} \frac{t_2 - t_1}{(t_1 + t_2 - 2\Delta - 2t_w)^2} \quad (6)$$

The transmitter is programmed to transmit an equal number of times in each configuration. The times for these transmissions to occur are Nt_1 and Nt_2 . By counting cycles from a 10 MHz clock during each phase-locked configuration, counts proportional to t_1 and t_2 are obtained. The μP is programmed to manipulate these counts according to Eq. (5). * Provided V and c are constant, resolution is improved by making N large. The upper limit on N is imposed by whichever of the following is smallest:

- (a) Max interval in which V or c is constant;
- (b) Half the required response time (e. g. , 1/2 of 2 sec in present contract);
- (c) Max no. of counts that can be accumulated, $\frac{c}{f}$ clock frequency.

* If the system turns out to be reciprocal, then Eq. (6) would be used automatically. Note that if cable lengths were 100 ft, $2\Delta \approx 250$ ns. Assuming $t_1 + t_2 \approx 250 \mu s$, neglecting the cable delays would introduce an error in V of 0.2%. However, for cable lengths less than 10 ft, and $P > 6$ inches, Δ could be neglected, because its contribution to errors in V would be $< 2\Delta / t_1 = 25 \text{ ns} / 100 \mu s = 0.025\%$.

APPENDIX D. FLOW VELOCIMETER ELECTRONICS

This appendix relates in general to ultrasonic flowmeters. More particularly, it relates to "Model 6000" circuitry for precise determination of the differences in transit time of ultrasonic wave propagation upstream and downstream within a fluid flowing in a conduit.* Jet propulsion fuels such as JP-4, JP-5 or their mixtures, flowing in a flow cell or spoolpiece, are of prime concern.

One method of determining the velocity of flow of fluids within a conduit utilizing ultrasonic wave transducers has been to place a pair of transducers apart in the direction of flow and to determine the difference in propagation time of ultrasonic waves between these transducers in the upstream direction and the downstream direction. The flow velocity of the fluid, V , adds to the sound velocity c in the downstream direction and subtracts from it in the upstream direction. One effective technique for ultrasonically measuring sound speeds, and hence flow, is known as the sing-around method. In this method an ultrasonic wave is initiated at one of the transducers and is transmitted to the other transducer. Upon receiving this transmitted ultrasonic wave, the second transducer generates an electrical signal, which is used to again trigger the propagation of an ultrasonic wave from the first transducer. This process is repeated and the repetition frequency of the output signals from the first transducer then corresponds to the transit time of ultrasonic waves passing from the first transducer to the second transducer. When the same technique is used with respect to ultrasonic waves propagated in the opposite direction, a pair of frequencies result. The difference between the frequencies Δf is proportional to the flow velocity of the fluid.

One problem with the singaround technique is that of rapidly and accurately measuring a small difference in frequency. Other problems arise from reverberation effects in the conduit or fluid or ultrasonic transducers themselves, rendering it still more difficult to obtain a correct measure of Δf . Additionally, the presence of nonfluid path delays such as delays due to buffer rods between the transducers and the fluid leads to inaccuracy in interpreting Δf in terms of V .

The delivered equipment avoids the above problems as follows.

Broadly speaking, in the standard Panametrics Model 6000 Ultrasonic Flowmeter, a special phase locked loop (PLL) technique accurately determines the flow velocity. In this approach, as in the singaround approach, a pair of transducers are placed apart in the direction of flow. An ultrasonic wave is initiated at one transducer. Its reception at the other transducer locks the half-period of a voltage controlled oscillator

*Pedersen, N. E., Bradshaw, J. E., Matson, J. E. and Lynnworth, L. C., Ultrasonic Flowmeter, U.S. Patent (1981); ser. no. 086402 (Oct. 1979).

to the transit time. The transit time for waves transmitted in the opposite (upstream) direction is similarly locked onto. The difference in half-periods then provides for a highly accurate measure of flow velocity, capable of compensating for nonfluid delays, as well as for reverberations and ringing within the spoolpiece (transducers, or fluid).

For a typical ultrasonic flowmeter configuration employing reciprocal transducers, the flow velocity V along the interrogated fluid path P may be computed from the times of flight t_1 and t_2 measured between the two transducers:

$$V = \frac{c^2 \Delta t}{2L} = \frac{2P^2}{L} \frac{t_2 - t_1}{(t_1 + t_2 - 2t_w)^2} \quad (1)$$

where L = axial projection of path in the flowing fluid, and t_w = sum of all nonfluid path delays (e. g., windows in front of transducers, cable delays, electronic delays).

Equation (1) given for V above is an approximation that is applicable to the extent that $V^2 \ll c^2$.

The flow velocity V may be converted to \bar{V} , the area averaged flow velocity, by utilizing area averaging cells or other means.

To understand how the present PLL method differs from a conventional singaround method, note that in the Model 6000, the transit time between transducers and the half period of one cycle of the output of a voltage controlled oscillator (VCO) is compared. The resultant difference signal is used to control the VCO until, after repeated ultrasonic transmissions, the frequency of the VCO is such that its period is equal to twice the transit time of the ultrasonic waves.

In this arrangement it is the output from the VCO which can initiate the repetition pulses of ultrasonic waves from the transducer. In fact, the period of the VCO need not be equal to twice the transit time between transducers, but may instead be made proportional to it so that the VCO is operating at either a higher frequency (so that its cycle period is a precise rational fraction of the transit time between transducers) or may be operated at a lower frequency (so that its cycle period is an exact multiple of this transit time). In this technique, however, it is not the frequency which is measured, but rather the elapsed time of a number of cycles of the VCO. This is accomplished by generating at a relatively high repetition rate a train of clock timing pulses (e. g. 10 MHz), at least one order of magnitude higher than the interrogation frequency, and measuring the total accumulated number of these timing pulses over the integer N periods of the VCO output. This technique substantially reduces the error in determination of the flow of velocity, for a given clock frequency (say 10 MHz).

If response time is unimportant, the number of periods, N , can be selected to be a convenient, large fixed integer, say 1024. This value is appropriate for the measurement of the flow of many liquids having sound speeds ranging between 300 and 3000 m/s, or gases having sound speeds from, say, 100 to 1000 m/s. For faster response, a small N is selected, e. g., 32, 64, or 100. In contrast to certain earlier methods wherein N was adjusted to compensate for variations in sound speed, the present invention compensates for sound speed through synchronism (pulse repetition period proportional to time of flight) and instead uses a generally fixed N as a means for optimizing response time and resolution.

DESCRIPTION OF PREFERRED EMBODIMENTS

Figure D1* shows one form of a flow cell with transducers 4a and 4b coupled to buffer rods 3a and 3b which are installed in threaded nipples 2a and 2b welded to the pipe 1. The transducers are cable-connected to flowmeter electronics 14. The transducers are cable-connected to flowmeter electronics 14. The pipe 10 has an inside diameter D , an area $A = \pi D^2/4$, and provides an axially-projected path length L between the wetted ends 5a and 5b of the buffer rods, and a fluid path P along tilted diameters. The fluid at rest has a sound speed c , and flows at a velocity V . The pipe 10 may also be penetrated by thin rod waveguides connected to torsional mode sensors 6a and 6b. Sensor 6b is encased in a hermetically sealed sheath 7. Pipe wall penetrations are sealed by compression fittings 8 which are of conventional design and so are not detailed. The purpose of the optional torsional sensors is to sense fluid density and/or temperature. However, they are not discussed any further in this appendix.

In Figs. 2a and 2b, there are shown several timing diagrams. Those in Fig. 2a pertain to upstream ultrasonic interrogation waveforms, while those in Fig. 2b pertain to the downstream interrogation. The timing diagrams illustrate the interrogation repetition rate at which ultrasonic waves are emitted from the transducers 4a and 4b as well as timing pulses employed to measure the period of these interrogation signals over several cycles. Turning to Fig. 2a the square wave of audio frequency f_{a1} represents the repetition rate for upstream interrogation, whose period t_1 is to be measured. To achieve high accuracy, the system employs a clock frequency f_c which is in the ultrasonic range, i. e., $f_c \gg f_{a1}$. The number of clock pulses counted during t_1 is $t_1 f_c \pm 1$. To reduce the fractional error due to the ± 1 uncertainty, f_c can be increased or the count can be extended for a longer time than t_1 , for example, for Nt_1 , where N is an integer greater than 1, and usually much greater than 1. In this illustration, by way of example, $N = 2$, so that the counting interval $T_1 = 2t_1$. If the same counting multiplier N is used in downstream interrogation, then $t_1 - t_2$ can be determined by counting at the f_c rate for intervals T_1 and T_2 .

*Figures D1-5 cited in this appendix are all contained at the end of this appendix, and are not to be confused with the figures from the main text.

By choosing a large N , the ± 1 uncertainty in the measured count is rendered insignificant. The time required to make such measurements, again, is $N(t_1 + t_2)$ or some multiple of this time if more than one pair of interrogations upstream and downstream are averaged. If a given time is allotted to making a V determination, as may be imposed by dynamic flow considerations and a corresponding short response time, there are several ways that the ± 1 uncertainty associated with the single clock tick of frequency f_c might be reduced. These ways include: use a clock of higher f ; use 2 clocks of slightly different frequencies f_{c1} and f_{c2} in a vernier mode; or use but one clock, but supplement it with an analog interpolation circuit.

In Fig. D3 there is illustrated in block diagrammatic form suitable circuitry for the flowmeter electronics illustrated in Fig. D1. In the circuit of Fig. D3 VCO 20 provides its output to a divide circuit 22, with the divided output from the VCO being provided simultaneously to a configuration switch 24 and to a one-shot multivibrator 26, as well as to one input of a phase detector 28. The output from the one-shot 26 is provided through multiplexer 30 to either of two amplifiers 34 and 36. The output of amplifier 34 is coupled to the upstream transducer 4a and the output of amplifier 36 is coupled to the downstream transducer 4b. The output of the one-shot multivibrator 26 is also connected to delay circuit 38 whose output feeds automatic gain control amplifier 40 in receiver 41 and a comparison zero crossing detector 44. The inputs to the automatic gain control amplifier 40 are received from either amplifier 46 coupled to the output from transducer 4a, or from amplifier 48, coupled to the output from transducer 4b. The output from the zero crossing detector becomes an input to the phase detector 28. The output from the one-shot multivibrator 26 is provided as a reset signal to the phase detector 28.

The output from the phase detector 28 is coupled through differential integrator 50 to a multiplexer 52 at the control input of the VCO 20. Multiplexer 52 provides a switching function to couple either one of two capacitors 56 or 58 to the control input of VCO 20.

Typically a 10 MHz clock 60 is coupled through logic circuit 62 to either upstream 24 bit counter 66 or downstream 24 bit counter 68. The outputs from the counters 66 and 68 are coupled through a buffer stage 70 to a computer (not shown).

The operation of the circuit of Fig. D3 is best understood in conjunction with the timing diagrams of Figs. D4 and 5. In operation the VCO 20 provides an output signal illustrated in Fig. 4 in which the down-going edge of the waveform after passing through divider 22 (which for purposes of this initial discussion will be considered to have a dividing factor of one) triggers one shot multivibrator 26 which produces the transmit pulse. The same waveform edge provides a signal to a flip-flop circuit, FF_1 and FF_2 , resetting them

in the phase detector 28. The transmit pulse is passed to multiplexer 30, which depending upon which control signal it is receiving from the configuration switch 24, may pass that signal from the one shot multivibrator 26 to amplifier 34 to initiate an ultrasonic pulse from transducer 4a. Or, in the other mode, it passes that same pulse through amplifier 36 to transducer 4b to initiate an ultrasonic pulse in the opposite direction. Configuration switch 24 operates to change the state of the entire circuit to operate in one mode to determine the time period t_1 for upstream interrogations. Or, in the other mode it determines the time period t_2 for downstream interrogations. The quantity by which the divide circuit 22 divides the output from the VCO 20 defines the number of cycles N for which the transit time is measured. Thus the configuration switch 24 switches back and forth between upstream and downstream, counting every N cycles from the VCO 20.

The operation of the overall circuit of Fig. D3 is to control the VCO such that it is operating at a frequency which is equal to $1/2$ the system frequency, where the system frequency is defined as the frequency whose period equals the time of flight of an ultrasonic pulse from one transducer to the other. Basically, this is accomplished by detecting the zero crossings of received pulses in the zero crossing detector 44 and supplying them to a flip-flop circuit, FF_2 in the phase detector 28. This phase detector determines which came first, the rising edge of the FF_1 output or the rising edge of the received frequency FF_2 output. This phase detector 28 then provides an output pulse, whose width is the difference in the arrival time of the two edges, to either the plus or minus input of the differential integrator 50. It is the output of this differential integrator 50 applied through multiplexer 52 which is the frequency-controlling input to the VCO 20.

As the width of the phase detector output pulse approaches zero, the VCO frequency will approach half of the system frequency and the circuit becomes locked with the VCO output frequency tracking the system frequency. Since the phase detector is always reset at the same time that the falling edges of the transmit and receive frequencies are generated, it will always phase detect the succeeding two edges which are the 50% duty cycle point of the transmit frequency and the zero crossing detected output of the received pulse. This ensures that the entire circuit will not lock on harmonics of either the receive or transmit frequencies and that every interrogation of the flow will yield correction information. This feature provides for very fast tracking of the system frequency (which it will be understood changes with changes in the flow velocity) and enables non 50% duty cycle frequencies to be phase detected.

The circuit operating in this fashion usually disregards transducer ringing signals because the 50% duty cycle halves the pulse repetition frequency, compared to a traditional singaround. This means that the time between transmits is exactly twice the time of flight, allowing twice the time for the ringing to decay.

In order to cancel the effects of triple or multiple transit reflections of the ultrasonic waves, or unusually long ringdown times (e. g., in buffer rods) the circuit may be configured to skip a number M of transmitted ultrasonic pulses to thereby allow enough time for multiple transits to die out while maintaining the VCO at exactly $1/2$ the system frequency. This is accomplished by utilizing the divider 22 for a relatively high number M of cycles. Thus, after the 50% duty cycle edge of the transmit frequency and the received edge of the received frequency have been compared, another transmit pulse to the transducer is not initiated and therefore the flip-flops FF_1 and FF_2 are not reset until M cycles have passed. This is allowable because the phase detector will only operate on the two succeeding edges following the reset pulse. See Fig. D5. Dividing by $M \geq 2$ is called a skip mode.

For longer ultrasonic path lengths the time between the detected pulses increases and storage of the corrected VCO input voltages is mandated. This is accomplished by the differential integrator 50 which uses high impedance field effect transistor switches to keep capacitor leakage low. The storage capacitors 56 and 58 are alternatively switched into the circuit, depending upon whether the measurement mode is upstream or downstream, as will be explained below.

With increased conduit diameters, the effects of reflections and ringing become small enough due to beam spreading attenuation or sound absorption so that operation in the skip mode is not required. In this case, upon receiving the ultrasonic signal (zero crossing), a new transmit can be immediately initiated. At the same time a counter is incremented so that a total of N increments is used to accumulate N samples of the time of flight, whereas in the PLL incrementing a counter on each receive for N increments will yield $2N$ samples (in twice the time for equal times of flight) of the time of flight. The number N is implemented by selecting a fixed divided output of divider 22. By dividing the VCO frequency directly, the regular mode and the skip mode will both yield the same number of times of flight for a given divisor.

As previously indicated, the output of the divide circuit 22 is used to toggle the configuration switch 24, changing the overall circuit from an upstream counting mode to a downstream counting mode. The output of the configuration switch 24 is indicated in one mode as a straight arrow and in the second as an arrow with a small circle. Throughout the circuitry this convention is applied so that the configuration of the multiplexers 30 and 52, as well as that of the logic circuit 62 and the gating of amplifiers 46 and 48 are all shown as controlled by the toggle output from the configuration switch 24. The output of the configuration switch 24 applied to the logic circuit 62 operates to gate the oscillator clock 60 away from the upstream 24 bit counter 66 to the downstream 24 bit counter 68. The numbers in these counters can then be used by a computer to compute the velocity of flow V . By switching

the multiplexer 52, the configuration switch 24 switches the capacitor used on the output from the differential integrator 50 and therefore allows one set of capacitors (each of the capacitors 56 and 58 is actually a pair of capacitors) to hold the control voltage for the upstream operation, and the other set of capacitors 58 is used to hold the control voltage for the downstream operation.

Any errors associated with the switching in and out of these capacitors and the subsequent need of a number of cycles to recharge the capacitors to the correct value are eliminated as follows. The Model 6000 only gates on the oscillator clock 60 to the counters for a particular number of counts at the end of a number of cycles of the VCO. In fact, any number of cycles of transmits can be ignored by these counters. The computer will divide by only the number of cycles actually used to gate on the counters. Such a method allows the circuit to well establish its operating frequency before the counters are employed.

The S P electronics produces a voltage which is linearly related to ρ in the range of 1.5 to 6.5 volts. The output of the S P electronics is connected to a Teledyne analog to digital converter. The A/D converter upon command of microprocessor performs a conversion of input voltage to digital format and then signals the computer that the conversion is complete. The computer commands and receives a conversion for every flow sample. Using the formula for the S P output, the computer converts the digital code of the A/D first to a voltage and then to a value of density in lb/gal (this is part of its program). The computer also has calculated the flow velocity from the latest upstream and downstream transit times (t_1 , t_2). It then multiplies the velocity times the cross sectional area of the cell (a number that is stored in its permanent memory), and finally multiplies that result by the density obtained from the conversion. The data point is then output to the output devices.

The logic circuit referred to on p. D-4 consists of three flip flops and a few logic gates. Their purpose is to steer the 10 MHz clock to one counter or the other depending upon the state of one of the flip flops, whose state is changed every time the configuration switch is changed. The other two flip flops are used to signal the computer that a count has been completed, so that the computer can: 1) read which counter is ready (the state of the first flip flop); 2) read the counter; and 3) reset the counter for the next interval.

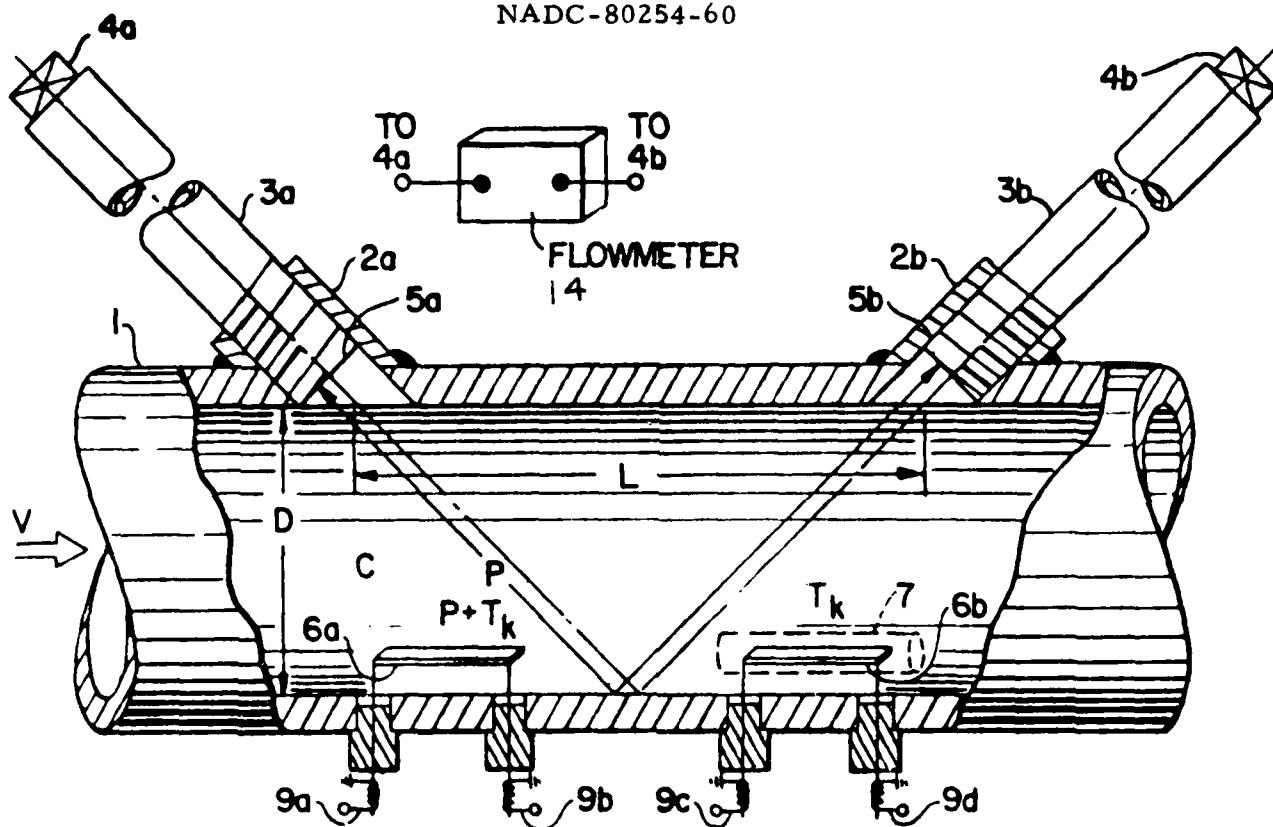


Fig. 1

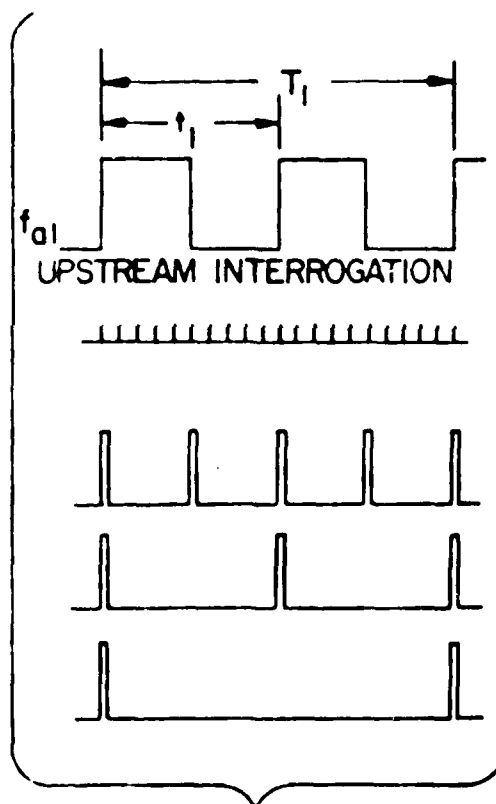
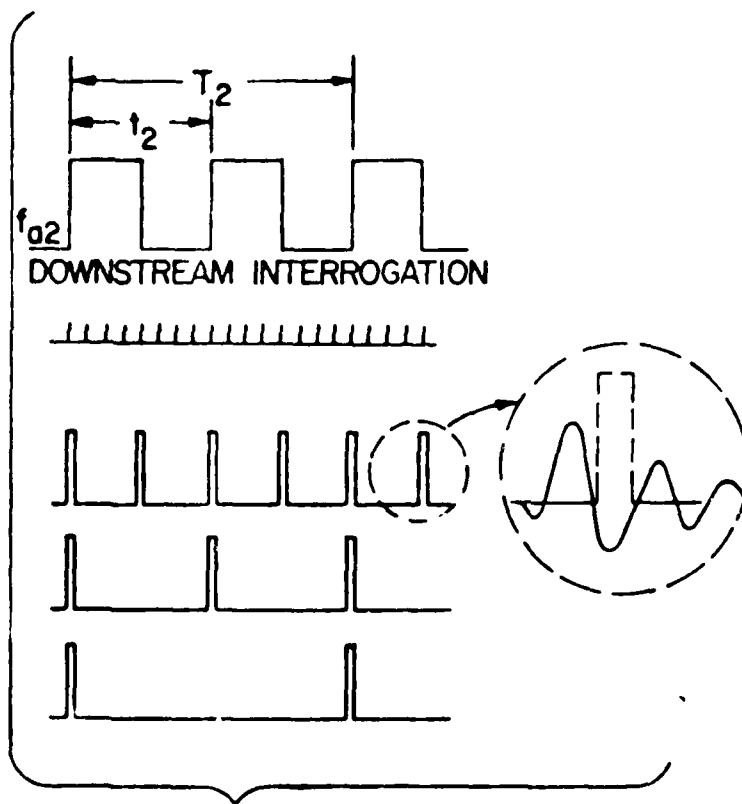


Fig. D2a



D-8 *Fig. D2b*

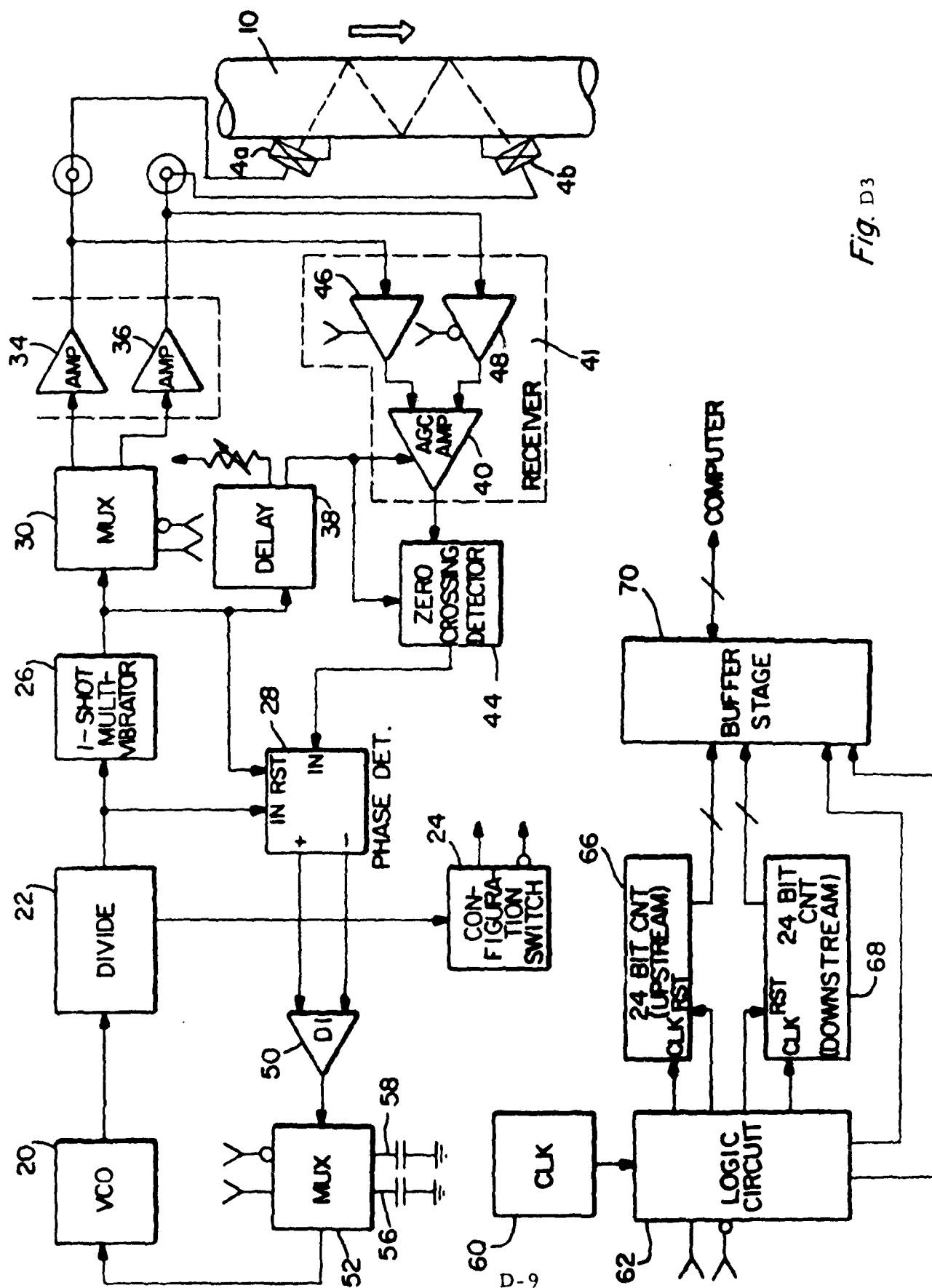


Fig. D3

AD-A104 364

PANAMETRICS INC WALTHAM MASS
ADVANCED FUEL FLOWMETER FOR FUTURE NAVAL AIRCRAFT.(U)
JUN 81 L C LYNNWORTH, N E PEDERSEN

F/G 21/4

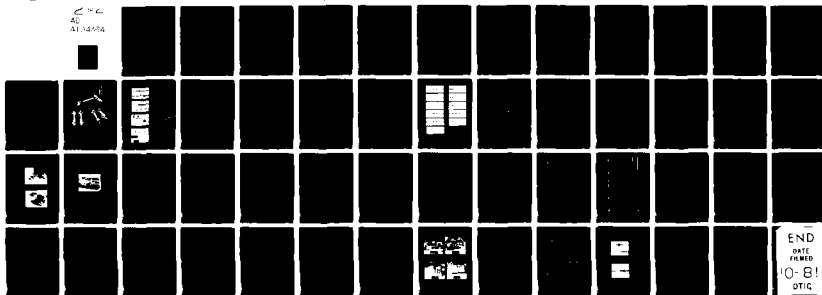
N62269-78-C-0069

NADC-80254-60

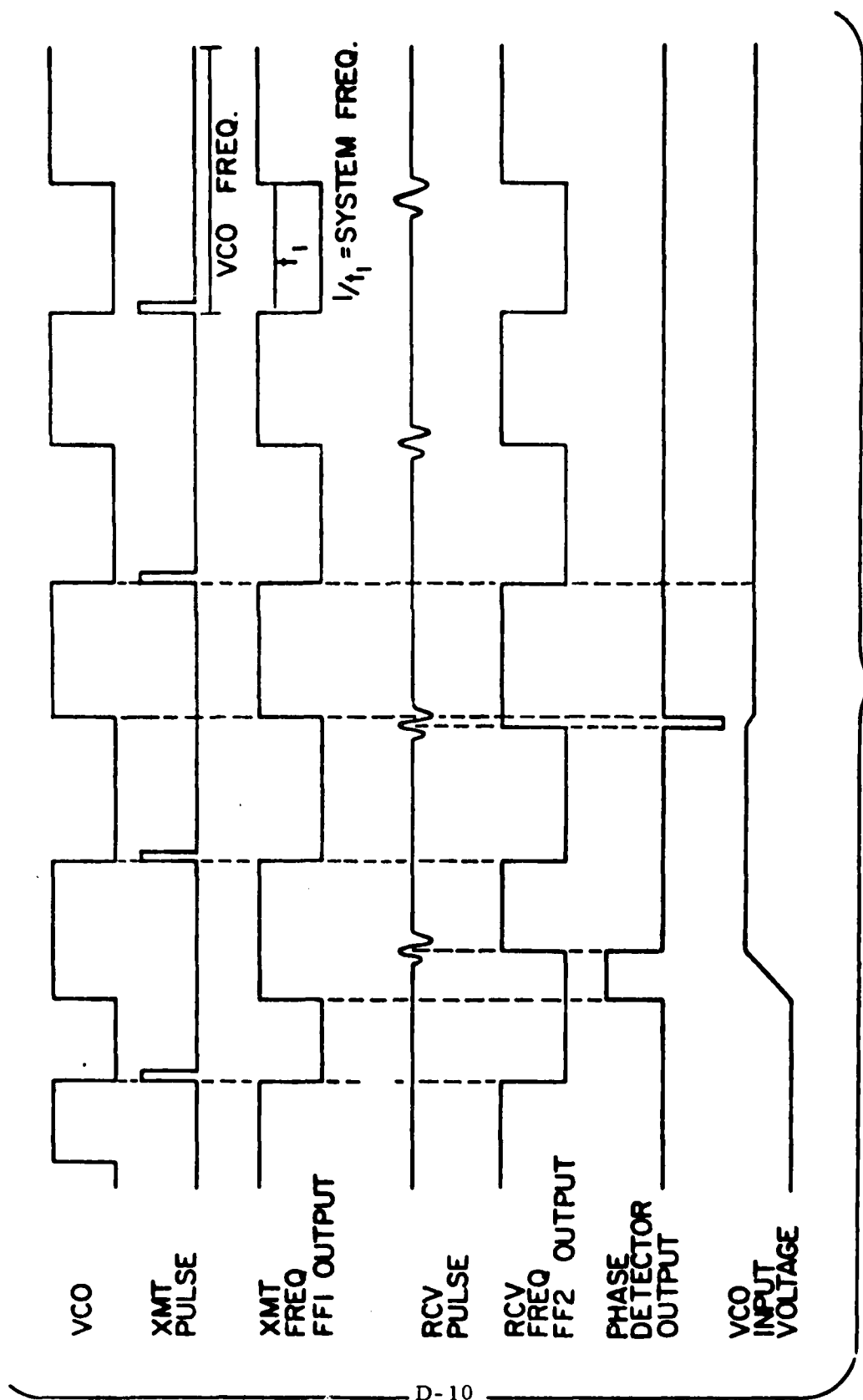
NL

UNCLASSIFIED

ALC
ALC
ALC



END
DATE
FILMED
10-81
DTIC



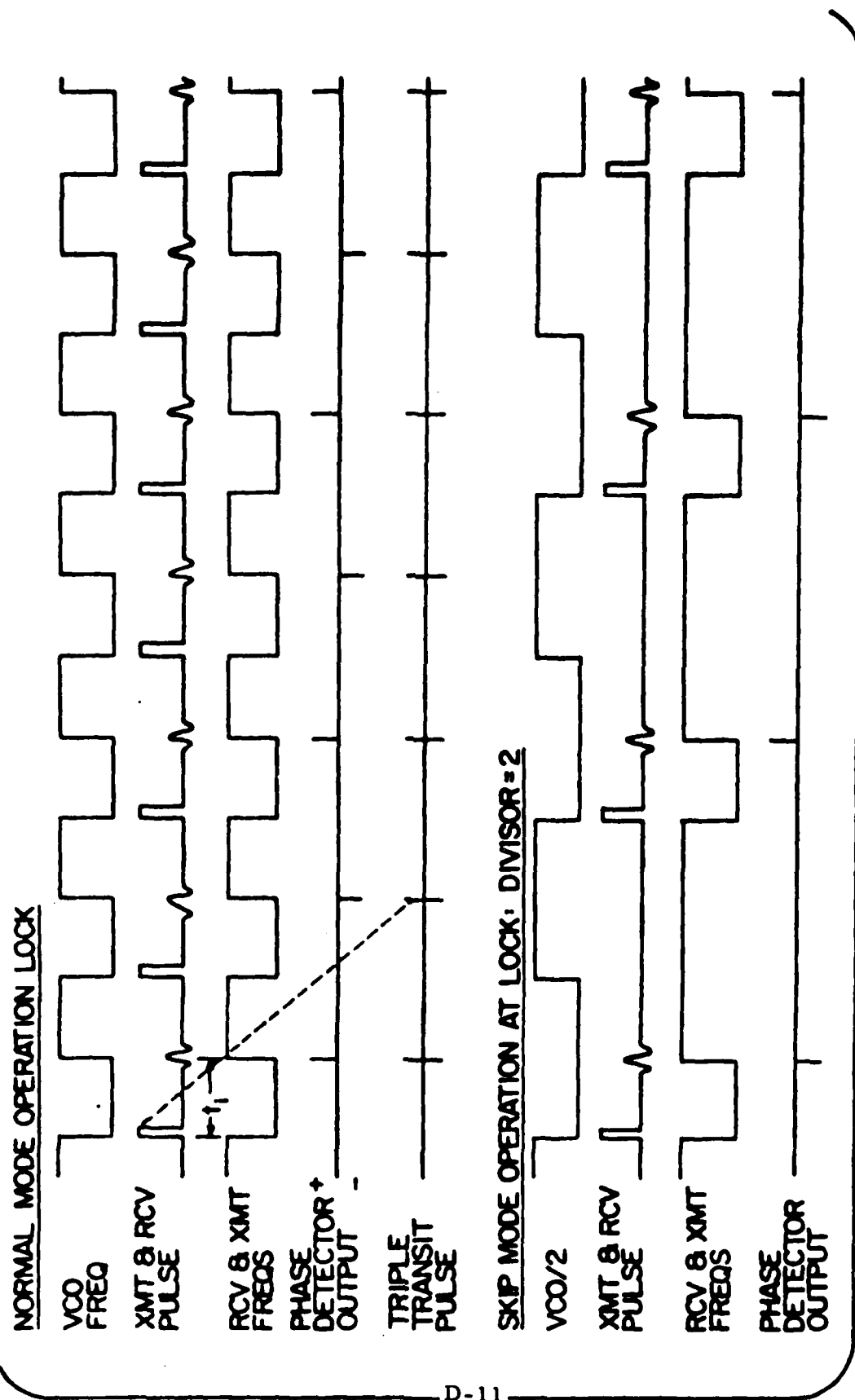


Fig. D5

APPENDIX E, RESPONSE TIME TEST DATA
(DATA OBTAINED WHILE FLOW
VELOCITY CELL WAS UNDER
X-AXIS 20 g DWELL AT
2000 Hz, 17 SEPT. 1980, ATL)

Valve closed to
zero flow

Flow reduced to 2 ft/s
by closing valve one turn

Flow resumed to maximum available rate

1 minute

Valve opened
by three turns

6 seconds

Flow reduced from 2.5 to 1 ft/s

100 mV

Cell
under
vibration
test

Cell
at
rest

APPENDIX F: EXTRACT FROM NASA RFP

EXHIBIT "B"

DESIGN GUIDELINES AND SPECIFICATIONS

1. Measurand and method of measurement - Fuel mass flow (both mass flow and total mass flow accumulated) shall be measured either directly, or by using a composite system of separately measuring volumetric flow and fuel density, or by measuring a combination of quantities from which mass flow can be calculated. For a flowmeter system that measures volumetric flow, the preferred method of measuring density is to use a densitometer rather than a correlation between density and temperature. The reason is that fuels that are within the MIL specifications can still show variations between batches that can produce uncertainties up to $\pm 1/2$ percent in density when determined by a temperature measurement. This uncertainty exceeds the contract goal.
2. Types of fuels - Fuels of interest are JP-3, JP-4, JP-5, JP-8 (Type A-1) and Type A.
3. Flow range - Typical ranges of fuel flow between engine full power and idle are between 50:1 to 100:1 depending on whether or not the engine has an afterburner. The absolute value of full scale flowrate varies with engine thrust; but for the purpose of this contract, a flowmeter with a nominal full scale of 6.3 l/s (40,000 lb/hr) and a 50:1 operating range is of primary interest. A full scale range of 0.5 l/s (3000 lb/hr) is also of interest and shall be considered.
4. Pressure - Flowmeters are subjected to high pressures because they are usually located downstream of the fuel pump. Operating pressures up to 7000 kPa (1000 psi) shall be considered. Flowmeter bodies shall be hydrostatic pressure tested to 1.5 times the maximum operating pressure.
5. Pressure drop - At maximum fuel flow the maximum pressure drop across the flowmeter shall be 68 kPa (10 psi).
6. Fuel temperature - The flowmeter shall be capable of operating over a fuel temperature span from -55°C to 130°C .
7. Ambient temperature - The flowmeter shall be capable of operating over an ambient temperature span from -55°C to 130°C .
8. Accuracy - The total error band for mass flow measurement shall be no greater than 0.25 percent of reading. The project goal of the error band is 0.1 percent of reading.

9. Resolution - The maximum value of resolution of fuel flow measurement at 1/50 of full scale shall be 0.25 percent.

10. Ambient pressure - The flowmeter and signal conditioning electronics are usually located in unpressurized regions of the aircraft. The units shall be capable of satisfactory operation in an external pressure environment between 100 kPa and 7 Pa (15 to 0.001 psi).

11. Vibration Characteristics - The flowmeter shall be capable of satisfactory operation in the following vibration - frequency envelope: ± 1.2 mm (5 to 14 Hz), ± 1 g (14 to 23 Hz), ± 0.45 mm (23 to 90 Hz), and ± 15 g (90 to 2 kHz).

12. Size and Weight - Because of space limitations associated with flight applications, the flowmeter shall fit within the cylindrical envelope outlined by the AN fitting nuts (MS-33656) associated with the nominal fuel line tube size for the flow range specified in paragraph 3 of Exhibit "B". A protrusion from the side of the flowmeter is acceptable but shall be no larger than a volume of the following dimensions: 3 fuel line tube diameters long, 2 fuel line tube diameters high, and $3/4$ tube diameters wide. The maximum length of the flowmeter including end connections (see paragraph 19 of Exhibit "B") shall be 8 fuel line tube diameters. The maximum size of the signal conditioning, which may be located remotely from the flowmeter, shall be 1000 cm³. The maximum weight of the flowmeter assembly including any required valves and manifolds (but not including signal conditioning) shall be 5 kg.

13. Material - Wetted parts of the flowmeter shall be compatible with the fuels listed above and at the pressures and temperatures listed above without suffering corrosion, brittleness, seal leakage, or other degrading properties.

14. Response - Time constant of the flowmeter shall not exceed 25 ms.

15. Failure mode - Because the safety of the aircraft is of paramount importance, any failure of the flowmeter shall not cut off fuel supply or otherwise interfere with proper engine performance.

16. Power - The flowmeter and signal conditioning (if required) shall operate on 28 V dc.

17. Output - The output (or outputs) of the flowmeter including signal conditioning (if required) shall be a voltage or frequency which is a single valued function of fuel mass flow or of quantities from which flow can be

computed. The output (or outputs) shall be compatible with digital processing techniques. The data processing of the output signal (or signals) is not considered part of this contract.

18. Pressure pulsations - The flowmeter performance shall be unaffected by maximum fuel line pressure fluctuations of ± 2 percent of the fuel pressure for frequencies of fluctuations above 10 Hz.

19. Mounting and position sensitivity - The flowmeter shall have AN Series 37⁰ male flared tube (MS-33656) end connections. Flowmeter performance shall be unaffected by changes in operating attitude.

20. Overrange capability - The flowmeter performance shall be unaffected after being subjected to a fuel flow of 125 percent of full scale.

21. Calibration - It is likely that insitu calibration of the flowmeter in the aircraft will not be done because of the complexity of such a procedure. However, the flowmeter, including identical flight fuel system upstream and downstream tubing sections, shall be calibrated as an assembly on a flow stand of sufficient precision to determine flowmeter accuracy.

APPENDIX G. CLAMP-ON AND OFFSET ALTERNATIVES FOR THE FLOW VELOCIMETER

The V portion of the electronics may be easily adapted to flow cell configurations other than the delivered square-holed sleeve. As mentioned in the body of this report in connection with Figs. 9, 10 and 12, two such alternatives are the clamp-on and the offset. The main features of these alternatives are compared with the square-holed sleeve in Table G1.

Table G1. Comparison of Three Flow Cell Designs.		
Type	Main Advantages	Main Disadvantages
Clamp-On	Ease of installation on existing pipe; ease of maintenance; no cost for cell (except for clamp).	Inaccuracy due to profile uncertainty and wall-borne noise; L usually small when D is small.
Offset	100% of flow is area-averaged for $b \leq D \leq 30$ mm; resolution improved in proportion to L; $L \approx P - D$; low cost.	ΔP , end effects due to offset geometry; installation must avoid gas entrapment.
Square-Holed Sleeve	100% of flow is area-averaged without need for offset.	Expensive; $P > \sqrt{2} L$; installation must avoid gas entrapment.

Clamp-On (Externally Mounted) Transducers

Externally-mounted transducers do not penetrate the pipe wall. These wedge-type angle beam transducers, Fig. G1, typically provide low-velocity (c_1) oblique incidence waves (e.g., vertically polarized shear at an angle of incidence $\theta_1 = 60^\circ$) which are coupled to the pipe's exterior. If the pipe wall thickness W is large compared to the wavelength λ_2 therein, the preferred wave in the wall is also shear, and of velocity c_2 . If the wedge and pipe are made of the same material, $c_1 = c_2$.

If the wedge and wall are made of elastically dissimilar materials, and in particular if the wedge is a relatively low-speed material compared

to the pipe, and further, if the pipe wall is not too thick, (e. g., W comparable to $\lambda_{2\text{Lamb}}$) a quasi-Lamb wave may be launched in the wall at the refracted angle $\theta_2 = 90^\circ$. In other words, $c_1/\sin\theta_1 = c_2/\sin 90^\circ$. The analysis of this problem and the implementation of its solution are simplest if c_1 is not a function of temperature. Hence, an "isopaustic" wedge is preferred in which $c_1 < c_{2\text{Lamb}}$ for the pipe and low-speed Lamb wave mode of interest.

In the delivered system, the V portion of the electronics may be modified for use with clamp-on transducers of the type described above. One simple form of this solution is adequate only to the extent that the profile is developed, $L = \text{constant}$ and $v = \text{constant}$. This v constraint means Re is a function of V only, and so the meter factor K can be programmed as follows: $K_{\text{laminar}} = 0.7500$, $K_{\text{transitional}} = 0.84$, $K_{\text{turbulent}} = 1/(1.119 - 0.011 \log Re)$.

Derivation of clamp-on equations corresponding to Lamb or SV waves in the wall follow.*

Table G2. Typical values for clamp-on parameters when obliquely incident wave is a vertically polarized shear wave, for Lamb and SV waves in the wall and notation.

Parameter	Lamb Wave in Wall	SV Wave in Wall
θ_1 , deg	60	60
θ_2 , deg	90	60
θ_3 , deg	45 to 60	20 to 30
c_1 , m/s	1500 to 2000	3000
c_z , m/s	~ 2000	~ 2500
c_3 , m/s	1000 to 2000	1000 to 2000
t_1 , μs	20	20
t_2 , μs	$(L-S)/c_z$	$(L-S)/c_z$
t_3 , μs	P/c_3	P/c_3
P	$D/\cos\theta_3$	$D/\cos\theta_3$
L	$D \tan\theta_3$	$D \tan\theta_3$
W	Comparable to λ	Large compared to λ

*These derivations are based on models, Fig. G1, in which a multiplicity of equal-delay paths exist between the transducers, such that constructive reinforcement occurs for a range of transducer spacings. The equal-delay concept is based in part on observations reported by L. C. Lynnworth in the 1979 Ultrasonics Symp. Proc., pp. 376-379, IEEE Cat. No. 79CH1482-9SU (1979).

Table G2. (cont'd)

<u>Special Notation for Clamp-On Derivations</u>	
\bar{t}	average transit time, or one-way transit time at no-flow
c_z	axial projection of sound speed in pipe wall
t_1	delay outside pipe
t_2	delay along pipe wall
t_3	delay in fluid
S	spacing between intersections of transducer centerlines and pipe exterior
c_1, θ_1	incident sound speed and angle of incidence
c_3, θ_3	refracted sound speed and angle of refraction in fluid
D, L, P, W, z	dimensions as shown in illustration, Fig. G1.

Lamb waves in wall

Snell's Law states:

$$c_1 / \sin \theta_1 = c_2 / \sin \theta_2 = c_3 / \sin \theta_3 \quad (G1)$$

The refracted wave in the wall propagates at the velocity $c_2 = c_1 / \sin \theta_1$.

Assuming t_1 is measured by butting the probes (angle beam transducers) with the transducer centerlines aligned, and with \bar{t} measured as the average transit time $[(t_{up} + t_{down})/2]$, one may write

$$\bar{t} = t_1 + t_2 + t_3 \quad (G2)$$

$$\text{Now } t_2 = \frac{S-L}{c_z} = \frac{S-D \tan \theta_3}{c_1 / \sin \theta_1} \quad (G3)$$

$$\text{and } t_3 = \frac{P}{c_3} = \frac{D \sin \theta_1}{c_1 \sin \theta_3 \cos \theta_3} \quad (G4)$$

$$\text{Therefore } \bar{t} - t_1 = \frac{(\sin \theta_1) (S-D \tan \theta_3)}{c_1} + \frac{D \sin \theta_1}{c_1 \sin \theta_3 \cos \theta_3} \quad (G5)$$

or
$$\frac{c_1(\bar{t} - t_1)}{D \sin \theta_1} - \frac{S}{D} = \frac{1}{\sin \theta_3 \cos \theta_3} - \tan \theta_3 = \cot \theta_3 \quad (G6)$$

Thus,
$$\theta_3 = \cot^{-1} \left[\left(\frac{1}{D} \right) \left(\frac{(\bar{t} - t_1) c_1}{\sin \theta_1} - S \right) \right] \quad (G7)$$

and
$$V = c_3^2 \Delta t / 2L \quad (G8)$$

where $c_3 = (c_1 / \sin \theta_1) (\sin \theta_3)$, $L = D \tan \theta_3$, $\Delta t = t_{\text{upstream}} - t_{\text{downstream}}$ and $\bar{V} = KV$ where K = meter factor. The volumetric flow rate is $Q = \bar{V}A = \pi D^2 \bar{V} / 4$. The mass flow rate is $\dot{M} = \rho Q$, where ρ = density.

SV Waves in Wall

This derivation is similar to the Lamb wave case, the principal difference being the "refracted" wave in the relatively thick wall zigzags at an effective velocity in the z direction given by $c_z = c_1 \sin \theta_1$, assuming for simplicity that wedge and wall have identical shear wave velocities.

As before, one may write for Fig. G1 (c),

$$\bar{t} = t_1 + t_2 + t_3 \quad (G2')$$

and
$$t_3 = \frac{D \sin \theta_1}{c_1 \sin \theta_3 \cos \theta_3} \quad (G4')$$

but now
$$t_2 = \frac{S - L - x}{c_2 \sin \theta_2} = \frac{2W}{c_2 \sin \theta_2} = \frac{S - L - x}{c_1 \sin \theta_1} = \frac{2W}{c_1 \sin \theta_1} \quad (G3')$$

where $x = S - L - 2W \tan \theta_2$ and $L = D \tan \theta_3$

Therefore
$$\bar{t} - t_1 = \frac{S - D \tan \theta_3 - x}{c_1 \sin \theta_1} + \frac{D \sin \theta_1}{c_1 \sin \theta_3 \cos \theta_3} + \frac{x \sin \theta_1}{c_1} \quad (G5')$$

or
$$\frac{c_1 \sin \theta_1}{D} (\bar{t} - t_1) - \frac{S}{D} \sin^2 \theta_1 = \sin^2 \theta_1 \cot \theta_3 + \frac{W}{D} \sin 2\theta_1 \quad (G6')$$

or

$$\frac{c_1}{D \sin \theta_1} (\bar{t} - t_1) - \frac{S}{D} = \cot \theta_3 + \frac{2W}{D} \cot \theta_1 \quad (G6'')$$

After solving this equation for θ_3 , one proceeds to calculate c_3 , L , V , \bar{V} , Q and \dot{M} as before.

Offset Flow Cell

The delivered transducers, or others of similar design, may be installed in tees connected at the ends of a section of pipe or tubing (Fig. 12). The effective interrogation length L is very nearly proportional to the length of the section between the tees. Hence, this cell design offers an economical way to achieve high resolution. For example, in the delivered system, $L \approx 10$ cm. An order-of-magnitude increase in L is achieved with a 1-m long pipe section. The repeatability in V corresponding to $L = 1$ m may be determined from the nomogram, Fig. 21, or from the equation

$$\Delta V = c^2 \Delta t / 2L$$

where we take the electronic repeatability to be $\Delta t = 1$ ns and, for example, $c = 1500$ m/s. Hence

$$\Delta V = (2.25 \cdot 10^6) (10^{-9}) / 2 \approx 1 \text{ mm/s.}$$

If this offset design were to be utilized with the delivered system, the main electronic change would be in the constants prom, in which the new L , P and A (area) would have to be entered. The upper limit on L is imposed either by space constraints or by attenuation.

For the offset axial flow cell, or for any other conduit of circular cross section, the volumetric flow rate Q may be graphed as a function of duct inside diameter D and area averaged flow velocity \bar{V} as in Fig. G2.

For small engine applications or other situations where there is not enough axial length between existing ports to install a standard axial offset flow cell, a folded path flow cell may be considered. By routing the flow oblique or orthogonal to the initial flow direction, opportunities may be created to achieve a large enough L to obtain the required Δt , and thereby obtain the required sensitivity to flow. Two examples of folded path offset flow cells are shown in Fig. G3.

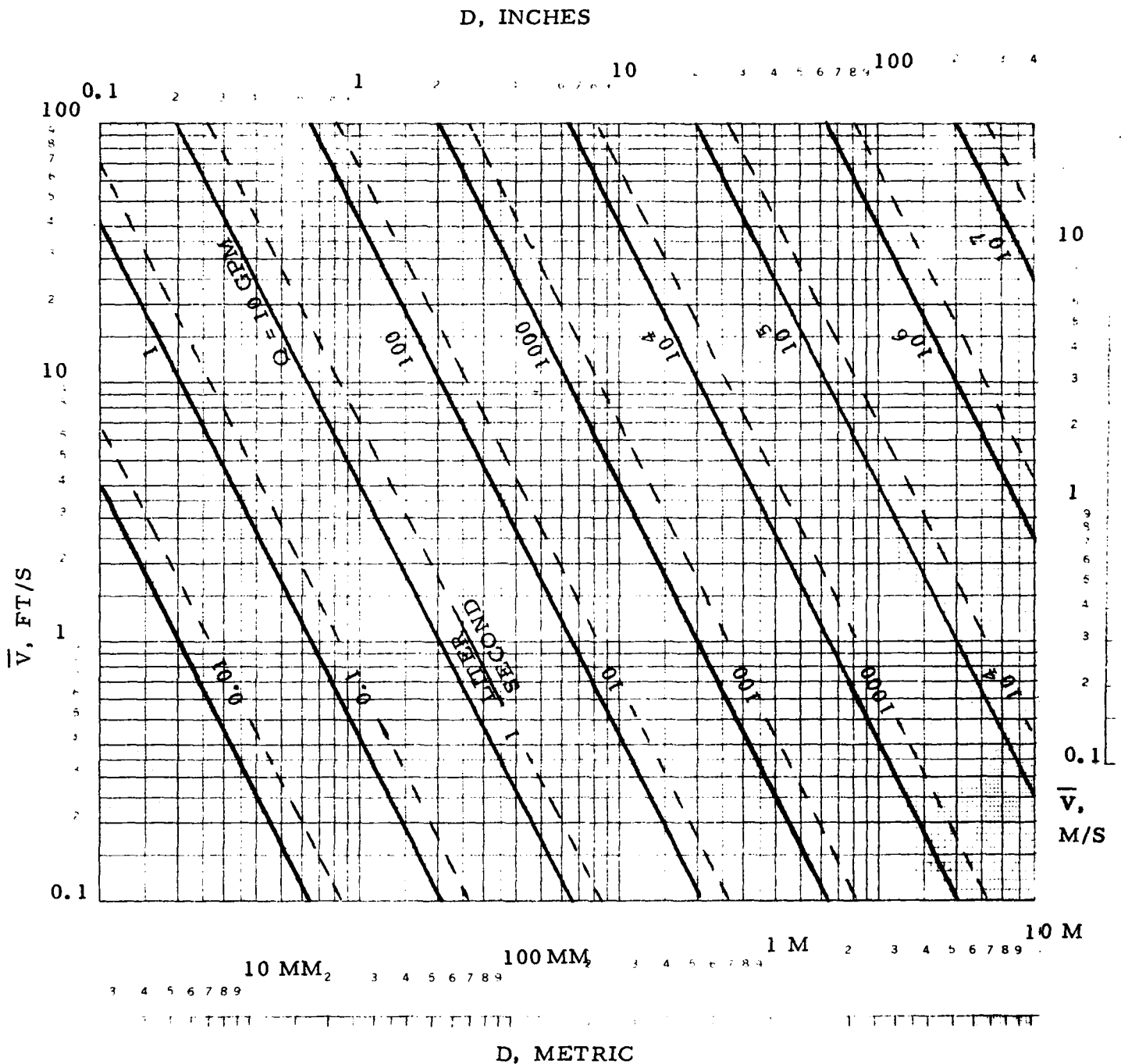


Fig. G2. Volumetric flow rate Q in gpm and liters/s as a function of D and \bar{V} . It may be of interest to note that \bar{V} (ft/s) $\approx 0.4Q/D^2$ for D in inches and Q in gpm. If Q is in liters/second and D is in cm, $V = 0.4Q/\pi D^2$ m/s $= 1.27Q/D^2$ m/s.

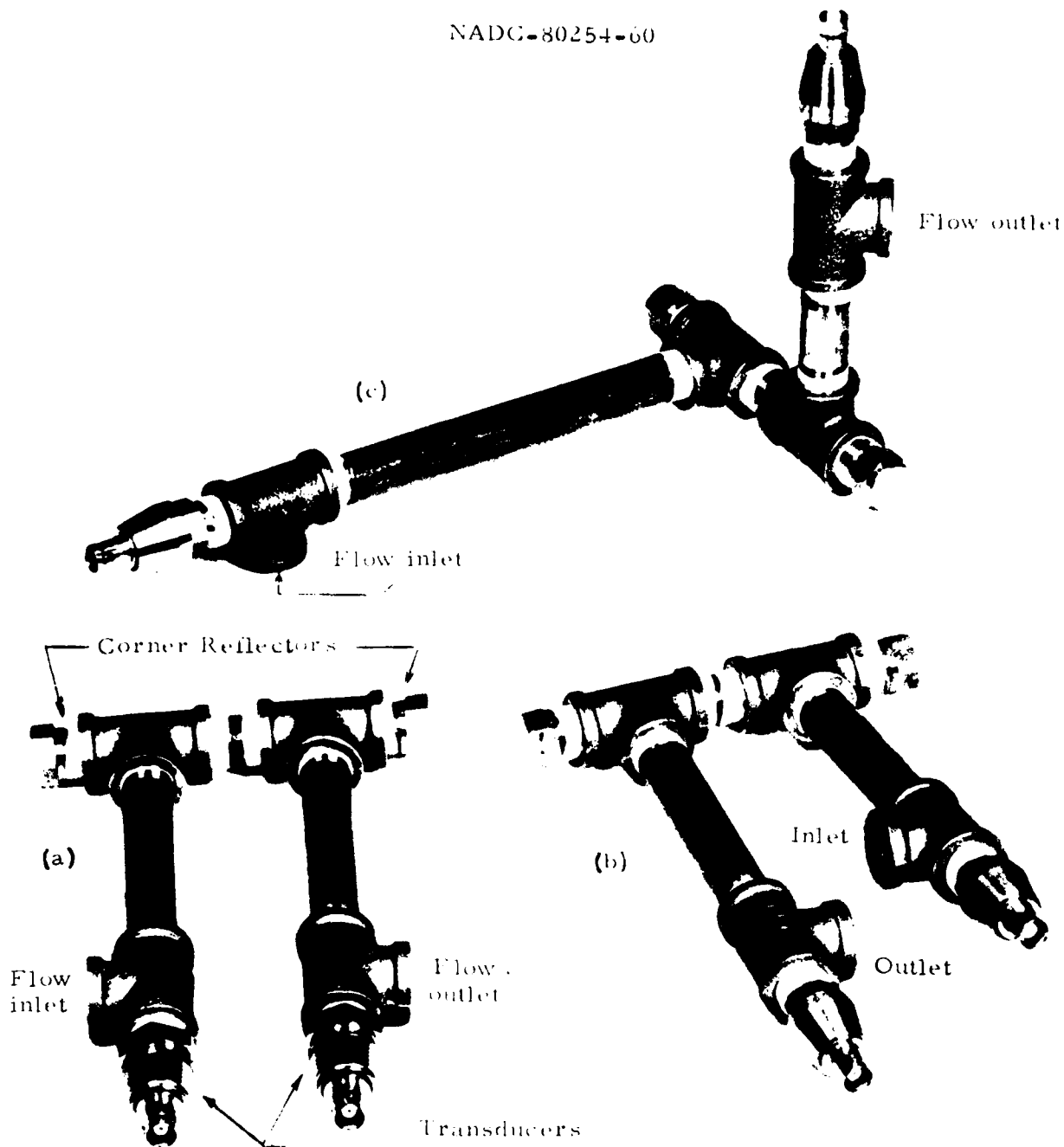
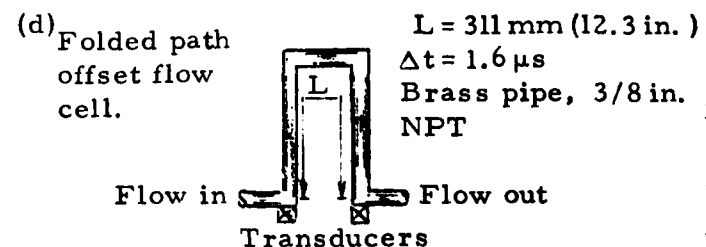
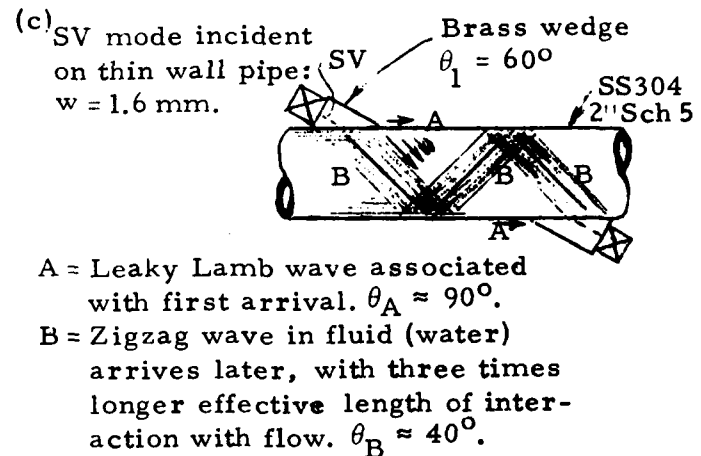
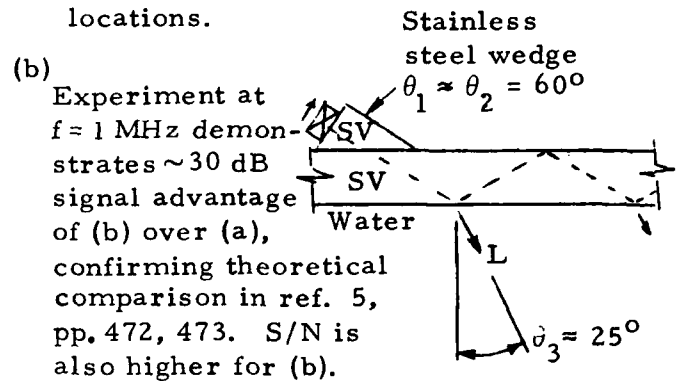
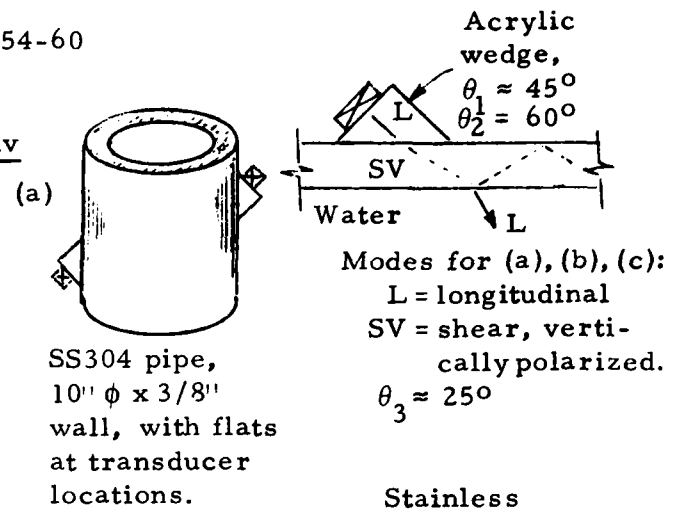
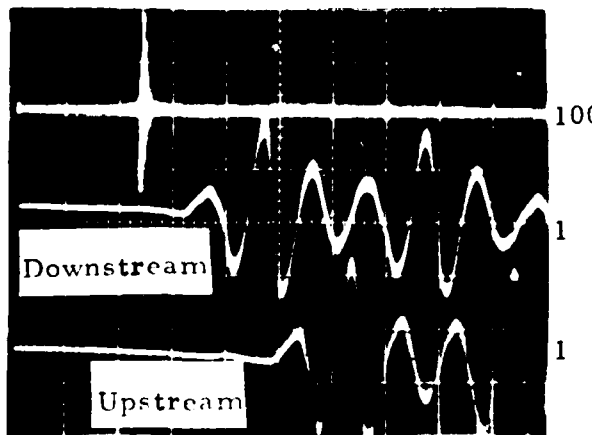
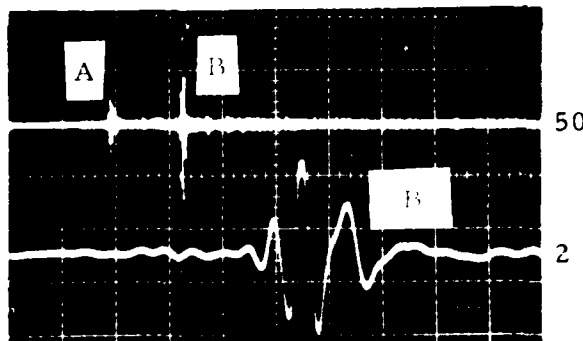
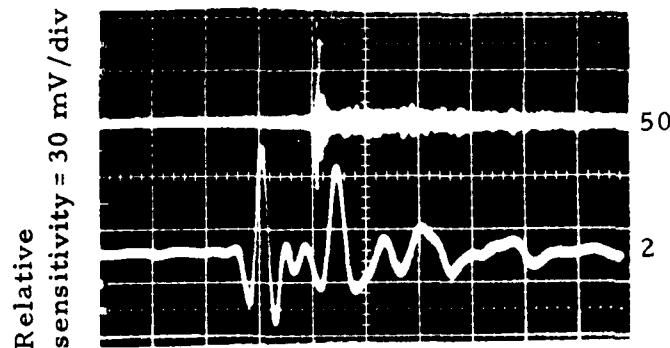
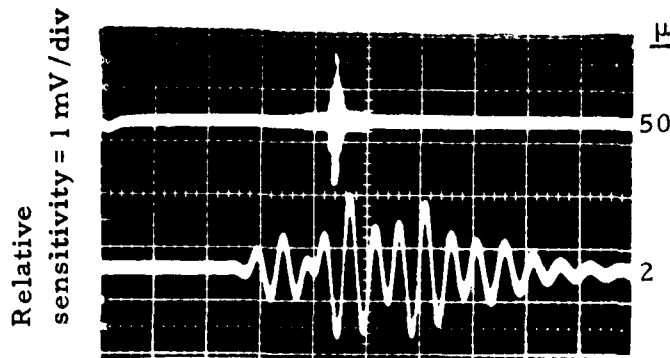


Fig. G3. Folded path offset flowmeter configurations enable flow to be interrogated ultrasonically in at least two noncolinear conduit segments. (a) Symmetrical design: axes of all conduit segments lie in one plane; adjacent segments are orthogonal; two main parts of folded path are parallel, spaced apart a distance X , of equal length ($Y_1 = Y_2 \gg X$) and orthogonal to aligned inlet and outlet axes. (b) As in (a) except: axes not all in same plane; inlet and outlet ports are "reversed" and misaligned slightly, enabling the distance between ports X_p to be as small as the conduit inside diameter D . (c) Unsymmetrical, nonplanar design uses skewed segments of unequal length ($X \neq Y_1 \neq Y_2$) to adapt to arbitrary configuration of inlet and outlet ports. In the folded path configurations shown, the effective interrogation path length L exceeds the distance between inlet and outlet ports.



Waveforms at $V = 6$ m/s (20 ft/s) for configuration of Fig. G3 (a).

Fig. G4. Oscillograms for several clamp-on and offset geometries at 1 MHz, using water as the test fluid. (a), (b) Comparison of wedge material and incident mode. (c) Thin wall pipe interrogated with SV. (d) Folded path cell.

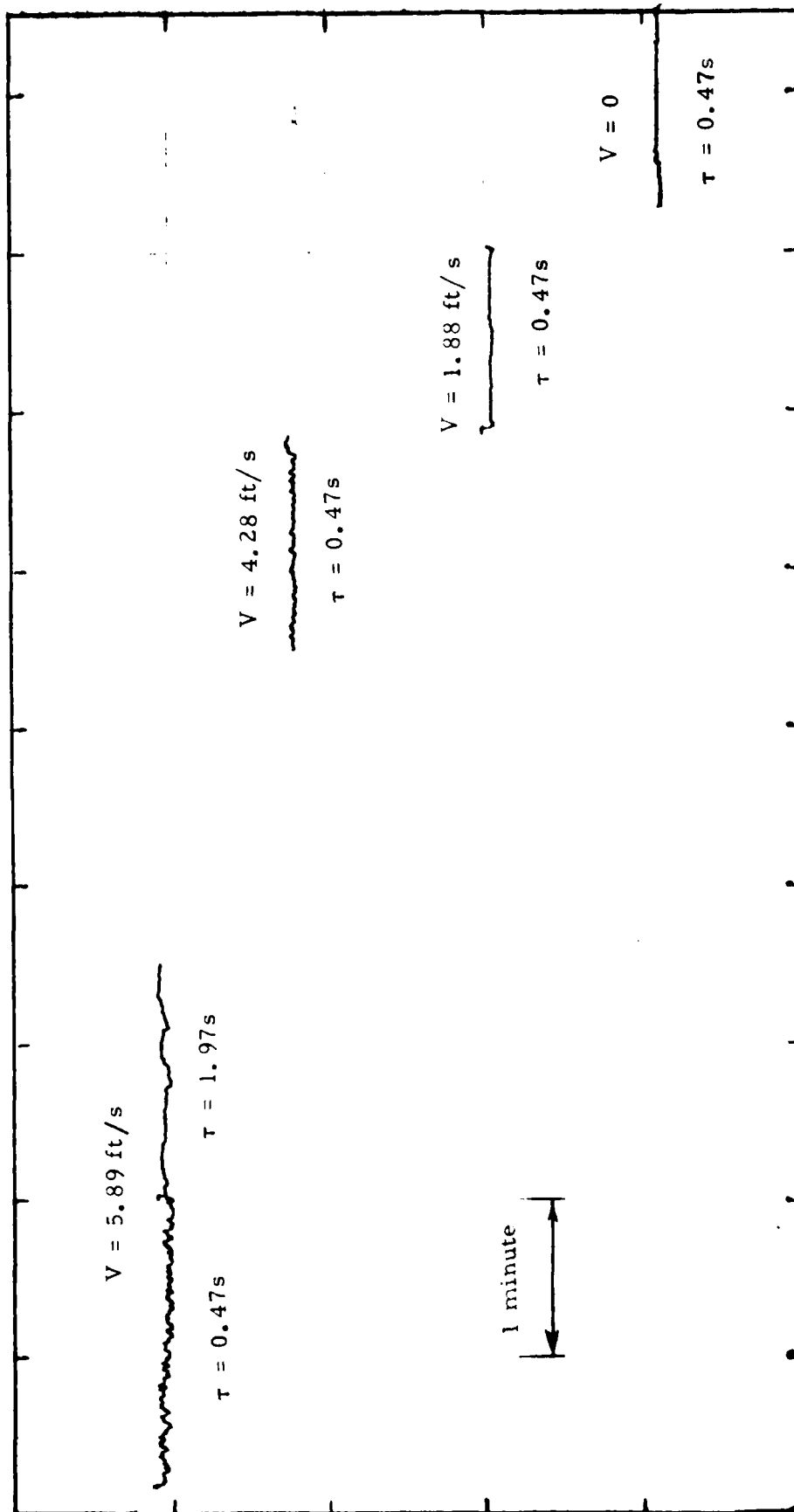


Fig. G5. Chart recording showing jitter as a function of flow velocity V and as a function of the RC time constant τ of the analog output ($I = 4$ to 20 mA) of a Model 6000 ultrasonic flowmeter. The cell used in this test was the axial offset type, using the ΔH flow loop of Fig. 28, p. 73.

Table G3. Jitter observed in offset flow cell of Fig.28, measured by Model 6000 ultrasonic flow velocimeter. Date of test: 16 April 1981.

VELOCITY OF FLOW, FT/S	5.89		4.28	1.88	0
TIME CONSTANT, SECONDS	1.97	0.47	0.47	0.47	0.47
ANALOG OUTPUT CURRENT, I, MILLIAMPERES	7.15	7.18	6.28	5.01	4.06
	7.16	7.17	6.29	5.01	4.06
	7.15	7.18	6.30	5.01	4.06
	7.15	7.16	6.29	5.01	4.06
	7.15	7.17	6.28	5.01	4.06
	7.14	7.14	6.29	5.01	4.06
	7.13	7.13	6.28	5.01	4.06
	7.12	7.13	6.27	5.01	4.06
	7.13	7.12	6.30	5.01	4.06
	7.12	7.11	6.28	5.01	4.06
AVERAGE OF 10 READINGS	7.14	7.15	6.286	5.01	4.06
STANDARD DEVIATION (σ) OF ABOVE 10 READINGS	.014	.026	.00966	0	0
$\frac{\sigma}{I}$, %	0.20	0.36	0.15	0	0

APPENDIX H. HYDROSTATIC PRESSURE TEST REPORT

INSPECTION REPORT

CUSTOMER <i>Dynametries</i>			ENGINEER <i>T. C. Tro</i>			S.O. <i>78377</i>		
Dwg. No. <i>Contract No</i>		Rev.	Desc.				Item	
<i>N62269-78C-0069</i>		<i>—</i>	<i>Zig Zag Flow Cell U.S. Navy</i>					
Operation <i>Hydro</i>		Quan. Rec. <i>1</i>	Accept <i>1</i>	Reject.	Inspector <i>J.E. Thompson</i>		Date <i>8/18/80</i>	

REMARKS:

*Hydro Tested at 1500 P.S.I. Held for
one hour at pressure.*

No Apparent leaks noted.

*Artesian Industries Inc
James E. Thompson G.E.M.*

SUMMARY:

H-1

NEXT OPERATION:

APPENDIX I. TEMPERATURE TEST DATA

<u>Date</u>	<u>Transducer Temp., °C</u>	<u>Echo Amplitude mV</u>	<u>Oscillogram I -</u>	<u>Remarks</u>
26 Aug. 1980	23	1580	1	Start test
	-40	1470	2	-0.6 dB
	+150	1480	3	--
	+175	1500	4	--
2 Sept. 1980	25	1500	5	Resume test
	-196	1400	6	--
	-196	700	7	0.5 hr dwell
	-196	750	8	2.5 hr dwell
3 Sept. 1980	-100	850	9	> 10 hr dwell at T < -100°C
	-83	1100	10	-3 dB
	-55	1200	11	-2 dB

Notes: -196°C achieved in liquid nitrogen
 -100°C achieved after liquid nitrogen evaporated
 High temperature achieved in environmental chamber
 -40°C, -55°C, -83°C in environmental chamber

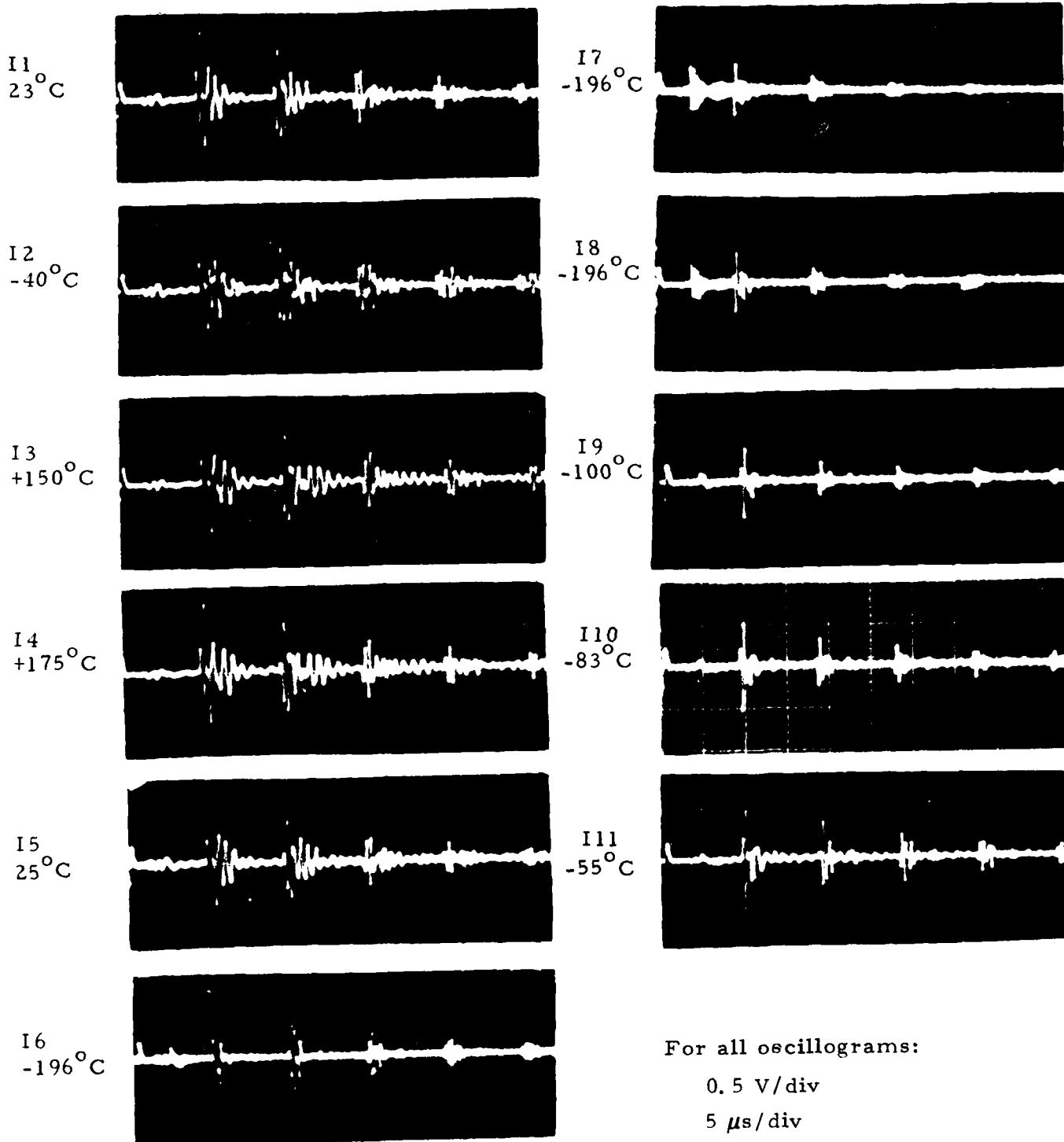


Fig. I 1-11. Oscillograms of transducer temperature test from -196°C to $+175^{\circ}\text{C}$. Acceptable performance was required from -38 to $+150^{\circ}\text{C}$. Figures I1, I2, and I3 show that this was achieved. The other oscillograms show performance during and after exposure to temperatures beyond the -38 to $+150^{\circ}\text{C}$ required.

APPENDIX J.

Test Report No. T-2248-11No. of Pages 13**Report of Test on**ZIG-ZAG FLOW CELLSINE VIBRATION TESTING

for

PANAMETRICS**Associated Testing Laboratories, Inc.**Wayne, New Jersey 07470
Burlington, Massachusetts 01803Date September 18, 1980

	Prepared	Checked	Approved
By	S. Fratto	R. Montvitt	E. E. Kulcsar
Signed	<i>S. Fratto</i>	<i>R. Montvitt</i>	<i>E. E. Kulcsar</i>
Date	9-19-80	9-23-80	9-23-80

Administrative Data

1.0 Purpose of Test:

To subject the Flow Cell to sine vibration testing in accordance with MIL-STD-810C and the procedures of this report.

2.0 Manufacturer: Panametrics
221 Crescent Street
Waltham, MA 02154

3.0 Manufacturer's Type of Model No.: Zig-Zag Flow Cell: P/N
N62269-78-C-0069.

4.0 Drawing, Specification or Exhibit: MIL-STD-810C, Procedure I,
Part 1, Cat. B Equipment,
Curve L.

5.0 Quantity of Items Tested: One (1) (S/N 001)

6.0 Security Classification of Items: Unclassified

7.0 Date Test Completed: September 18, 1980

8.0 Test Conducted By: Associated Testing Laboratories, Inc.

9.0 Disposition of Specimens: Returned to Panametrics.

10.0 Abstract:

The Flow Cell was subjected to sine vibration testing as outlined in this report. There was no evidence of physical damage as a result of the testing.

Report No. T-2248-11

Page 1

Associated Testing Laboratories, Inc.

Wayne, New Jersey 07470
Burlington, Massachusetts 01803

LIST OF APPARATUS

<u>Item</u>	<u>Manufacturer</u>	<u>Model No.</u>	<u>Accuracy</u>	<u>Calibration Date</u>	<u>Calibration Date Due</u>
Sine Console	Associated Testing Laboratories, Inc.	--	±5% A ±2% F	7-14-80	10-14-80
Analyzer Console	Associated Testing Laboratories, Inc.	--	±5%	8-18-80	10-18-80
Charge Amplifier	Unholtz-Dickie	11MGS	±1%	8-13-80	11-13-80
Accelerometer	Endevco Corporation	2215E	±5%	6-23-80	9-23-80
Accelerometer	Endevco Corporation	2226C	±5%	7-18-80	10-18-80
Vibration System	Ling Electronics	335#1	N/A	Prior to Use	

Report No. T-2248-11Page 2**Associated Testing Laboratories, Inc.**

Wayne, New Jersey 07470

Burlington, Massachusetts 01803

VIBRATION TESTTEST PROCEDURE

The Zig-Zag Flow Cell was subjected to a vibration test in accordance with MIL-STD-810C, Method 514.2, Procedure I, Part 1, Cat. B Equipment, Curve L, as follows.

The unit was securely attached to a vibration test fixture which, in turn, was securely attached to the table of a vibration exciter. A control accelerometer was mounted to the fixture for controlling the input vibration amplitude of the unit. A monitor accelerometer was mounted to the unit for monitoring the vibration amplitude on the unit. The unit was then subjected to a resonance search over the frequency range of 5 to 2000 Hz at the levels in Table I below.

The unit was then subjected to 30 minute resonance dwells at the four most severe resonant frequencies which were determined using the above procedure. The resonance dwells were performed at the levels in Table I.

At the conclusion of the resonance dwells in each axis, the unit was subjected to vibration cycling over the frequency range of 5 to 2000 Hz at the levels in Table I. The frequency range of 5 to 2000 Hz and return to 5 Hz was traversed during a time interval of 20 minutes. The unit was subjected to a total of three hours of vibration per axis, including resonance dwell and cycling time.

Table I

<u>Frequency (Hz)</u>	<u>Amplitude</u>
5 - 14	0.1 inch d.a.
14 - 23	1.0g's
23 - 104	0.036 inch d.a.
104 - 2000	20.0g's

The above procedure was performed in each of three mutually perpendicular axes.

Report No. T-2248-11

Page 3

Associated Testing Laboratories, Inc.

Wayne, New Jersey 07470

Burlington, Massachusetts 01803

VIBRATION TESTTEST RESULTS

There was no evidence of physical damage noted as a result of the above testing. During the resonance search, the following resonant frequencies were determined: X Axis 1950; Y Axis 1425 Hz; Z Axis 1530 Hz and 1900 Hz. A resonance dwell was performed at the above mentioned frequencies for a period of 30 minutes. The Flow Cell was returned to Panametrics for further post test evaluation. X-Y plots generated from the above testing may be referred to in the appendix of this report.

Explanatory note added April 1981 by Panametrics concerning strip chart recordings on pages J-16, J-17:

The deflections recorded on pages J-16 and J-17 represent analog signals proportional to flow velocity V, as explained on p. 34. The excursions for the cell at rest are typically ± 1 minor division. For the cell under vibration, the same magnitude is observed except for the group of resonances observed near the graduation marked 2000 Hz, during each logarithmic sweep of frequency. At the resonances, the high noise interfered with the signal, causing erroneous V's to be indicated. Although not available at the time of these vibration tests in September 1980, later models of the flow velocimeter include better filtering and bad data rejection algorithms, which are designed to provide better noise immunity. The resonances themselves, however, need to be addressed in terms of mechanical design, to minimize their occurrence or strength, rather than rely on electronic or software remedies.

Associated Testing Laboratories, Inc.

Wayne, New Jersey 07470

Burlington, Massachusetts 01803

A P P E N D I X

A

Report No. T-2248-11

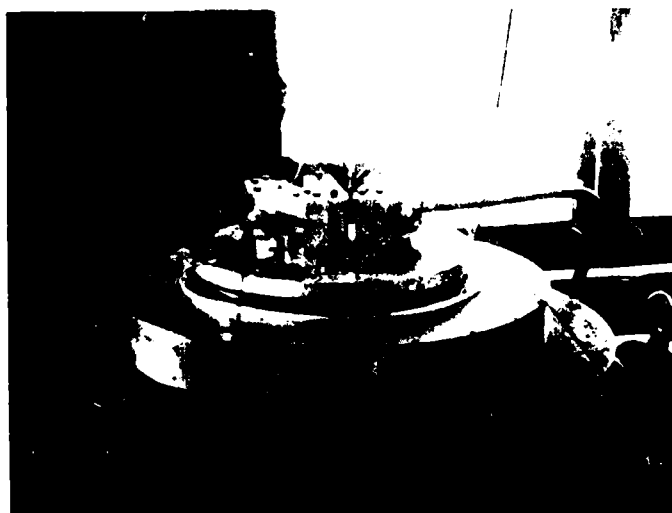
Page 5

Associated Testing Laboratories, Inc.

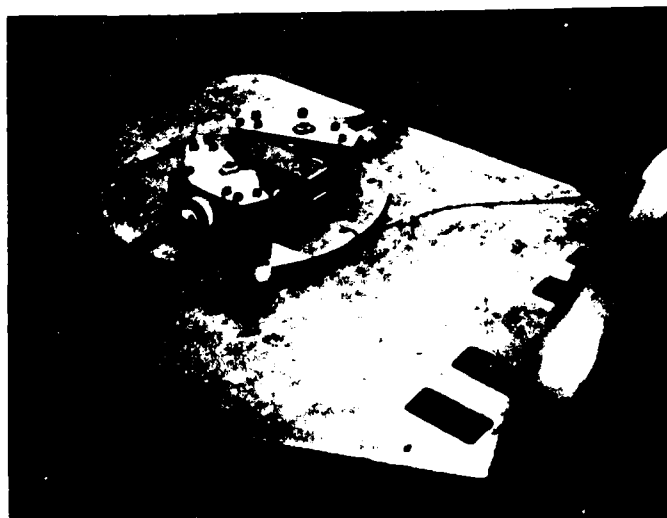
Wayne, New Jersey 07470
Burlington, Massachusetts 01803

PHOTOGRAPHS OF AXES DESIGNATION

X AXIS



Y AXIS



Report No. T-2248-11

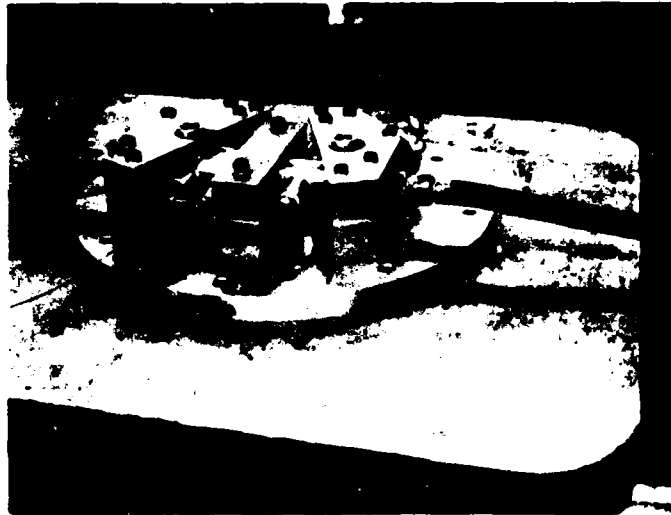
Page 6

Associated Testing Laboratories, Inc.

Wayne, New Jersey 07470

Burlington, Massachusetts 01803

PHOTOGRAPH OF AXIS DESIGNATION



Z AXIS

Report No. T-2248-11

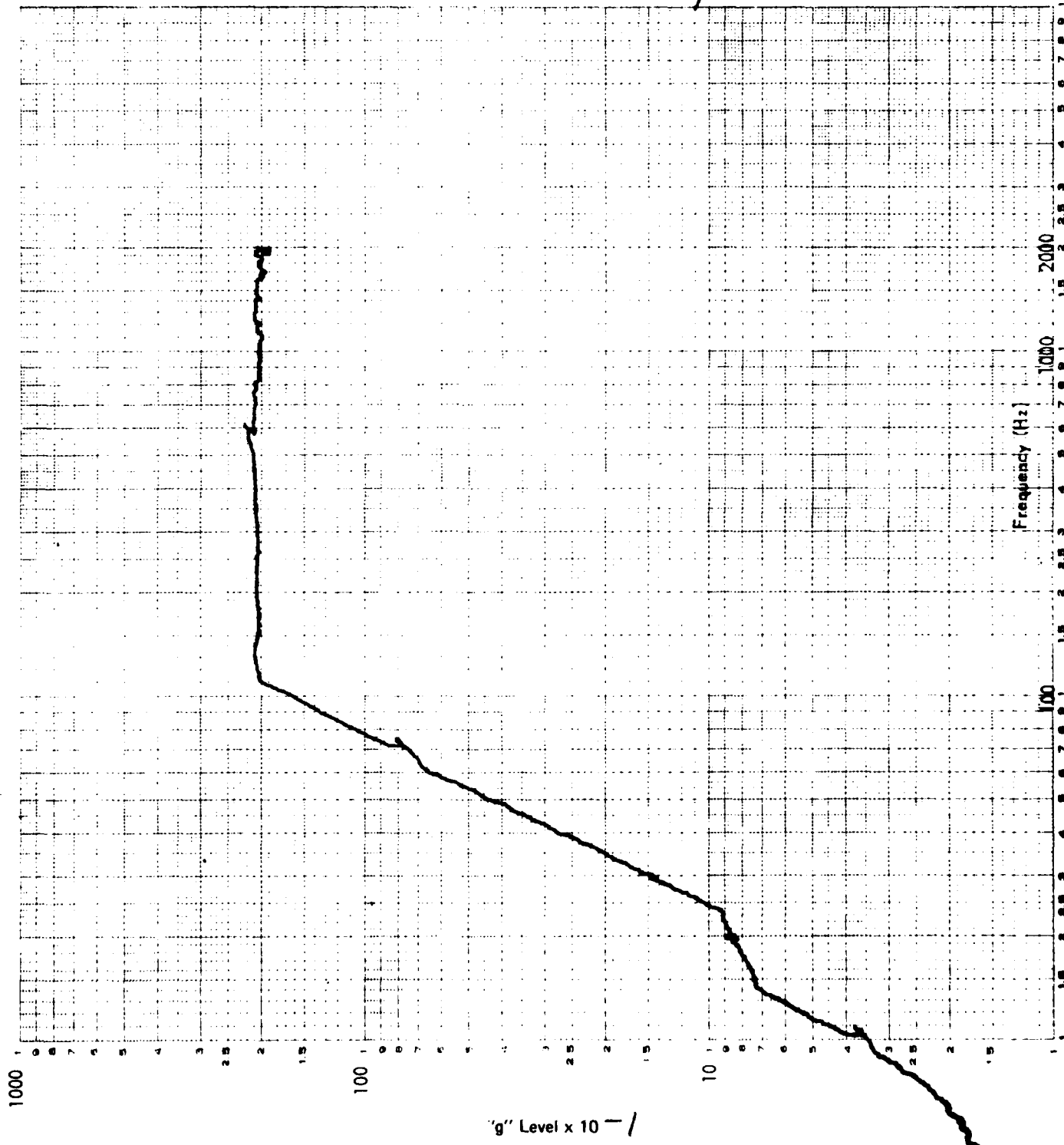
Page 7

Associated Testing Laboratories, Inc.

Wayne, New Jersey 07470
Burlington, Massachusetts 01803

NADC-80254-60
SINUSOIDAL VIBRATION ANALYSIS

Job Number T-2248 Customer Pencumotors Date 9-12-72
Specimen P N 262265 X-C-423 Specimen S N 001 Test Temp. Run
Axis X Control Technician S/E



"g" Level x 10⁻¹

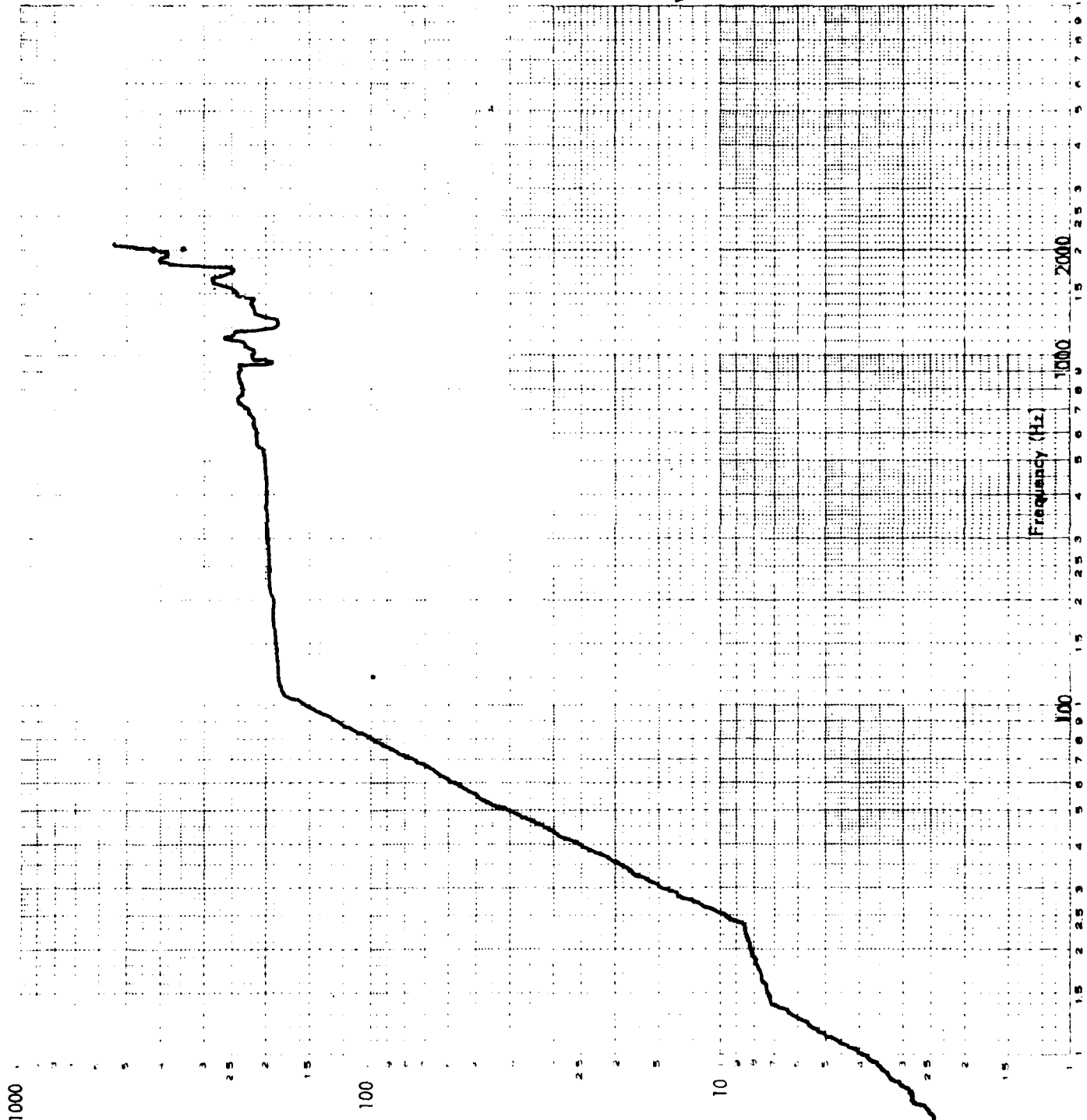
Report No. T-2248-11

Figure _____

Page 8

NADC-80254-60
SINUSOIDAL VIBRATION ANALYSIS

Job Number T-2248 Customer Pharmaceuticals Date 9-13-60
Specimen P NA62269-78-C-0069 Specimen S N 001 Test Temp. Room
Axis X horizontal Technician SJE



Report No. T-2248-11

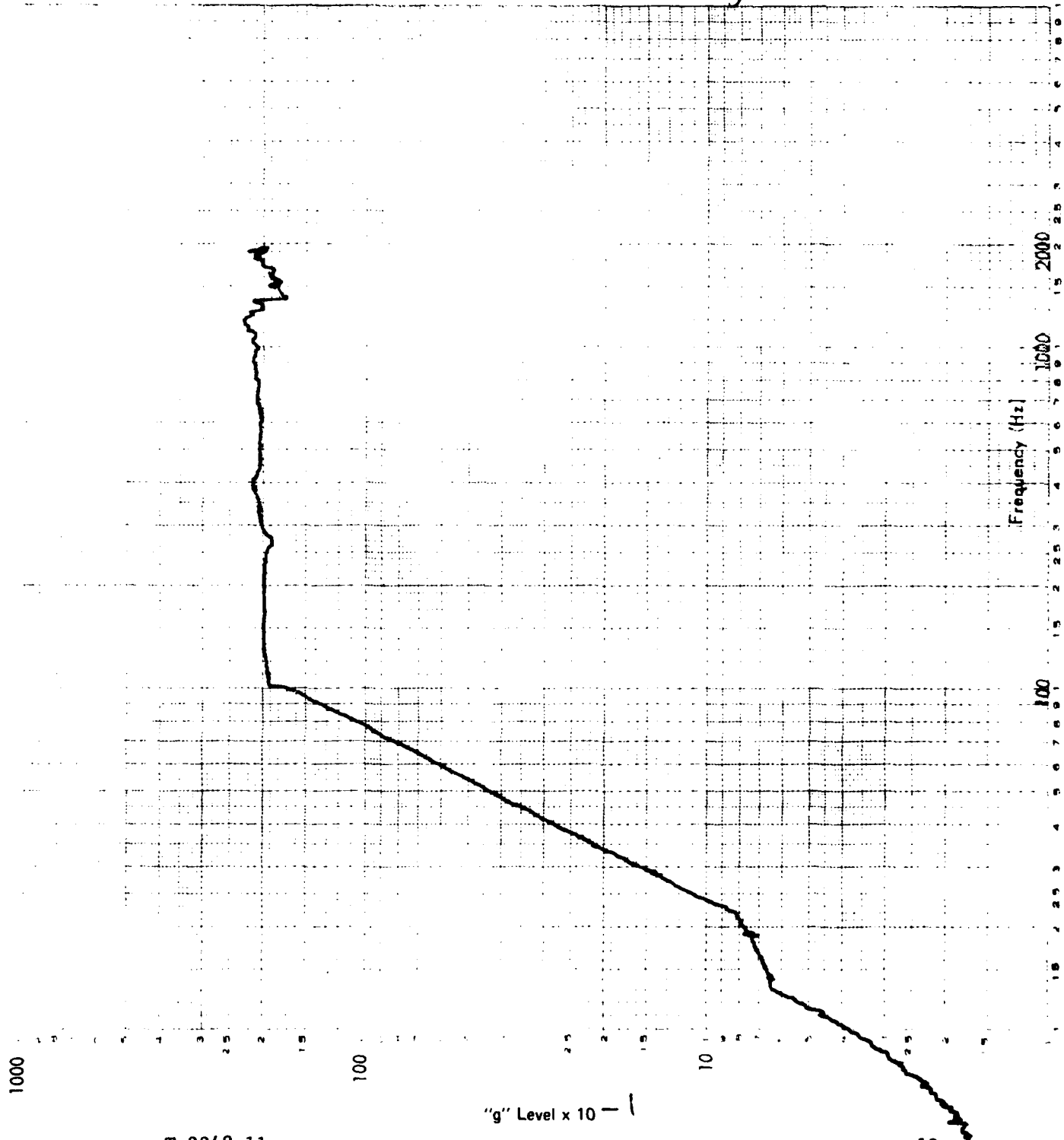
"g" Level x 10 -1
Figure _____

Page 9

ASSOCIATED TESTING LABORATORIES
Subsidiary of Waller Kiddle & Company, Inc.
KIDDE

NADC-80254-60
SINUSOIDAL VIBRATION ANALYSIS

Job Number 10244 Customer Pine & metrics Date 8-17-64
Specimen P N N6226 2 78-C-0005 Specimen S N 001 Test Temp. Room
Axis Y Centrif Technician SJF



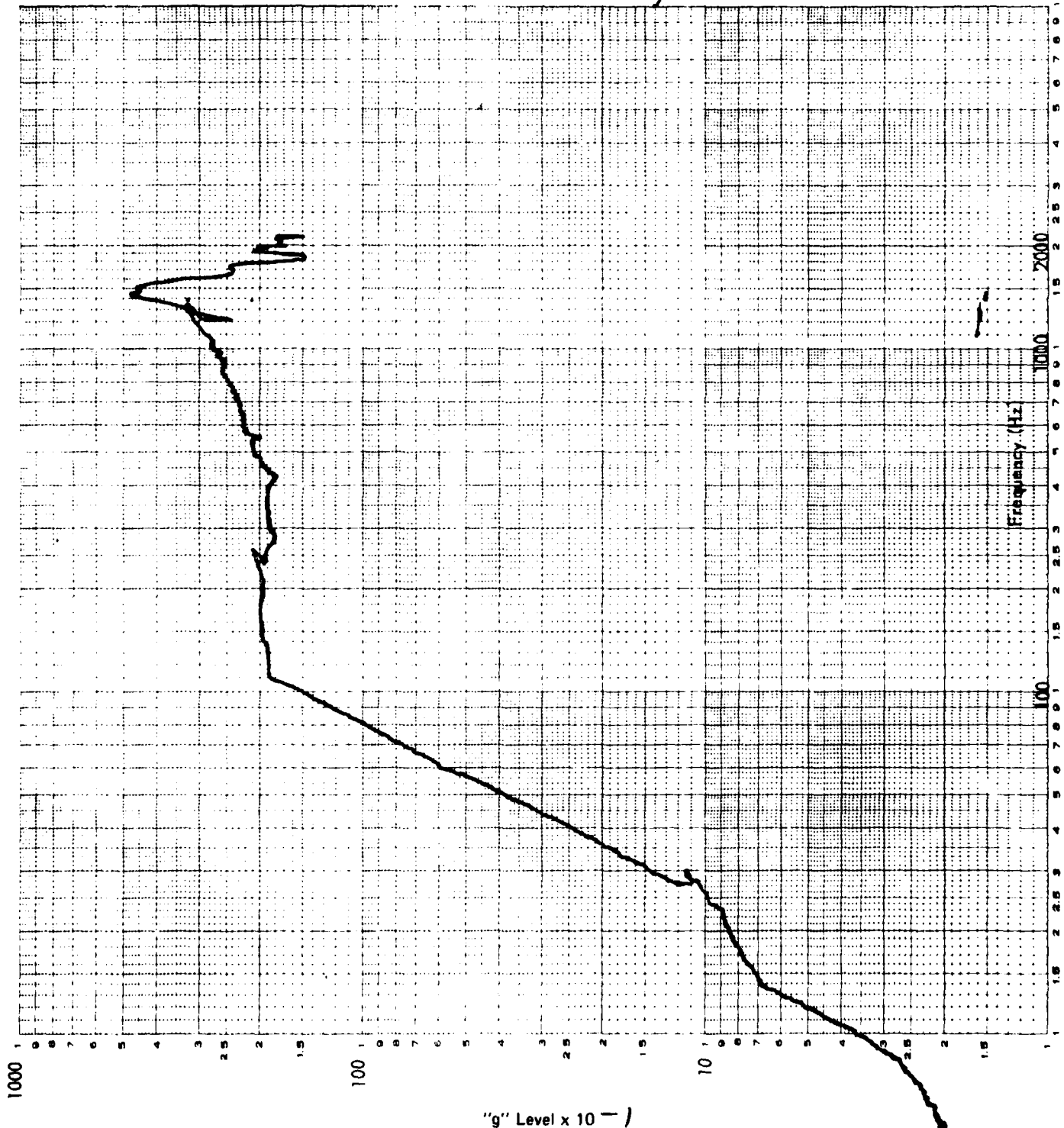
Report No. T-2248-11

Figure _____

Page 10

NADC-80254-60
SINUSOIDAL VIBRATION ANALYSIS

Job Number T-2248 Customer Panmetrics Date 9-17-64
Specimen P/N 26229-75C-2248 Specimen S N 601 Test Temp. Room
Axis Y Mark Technician SFF



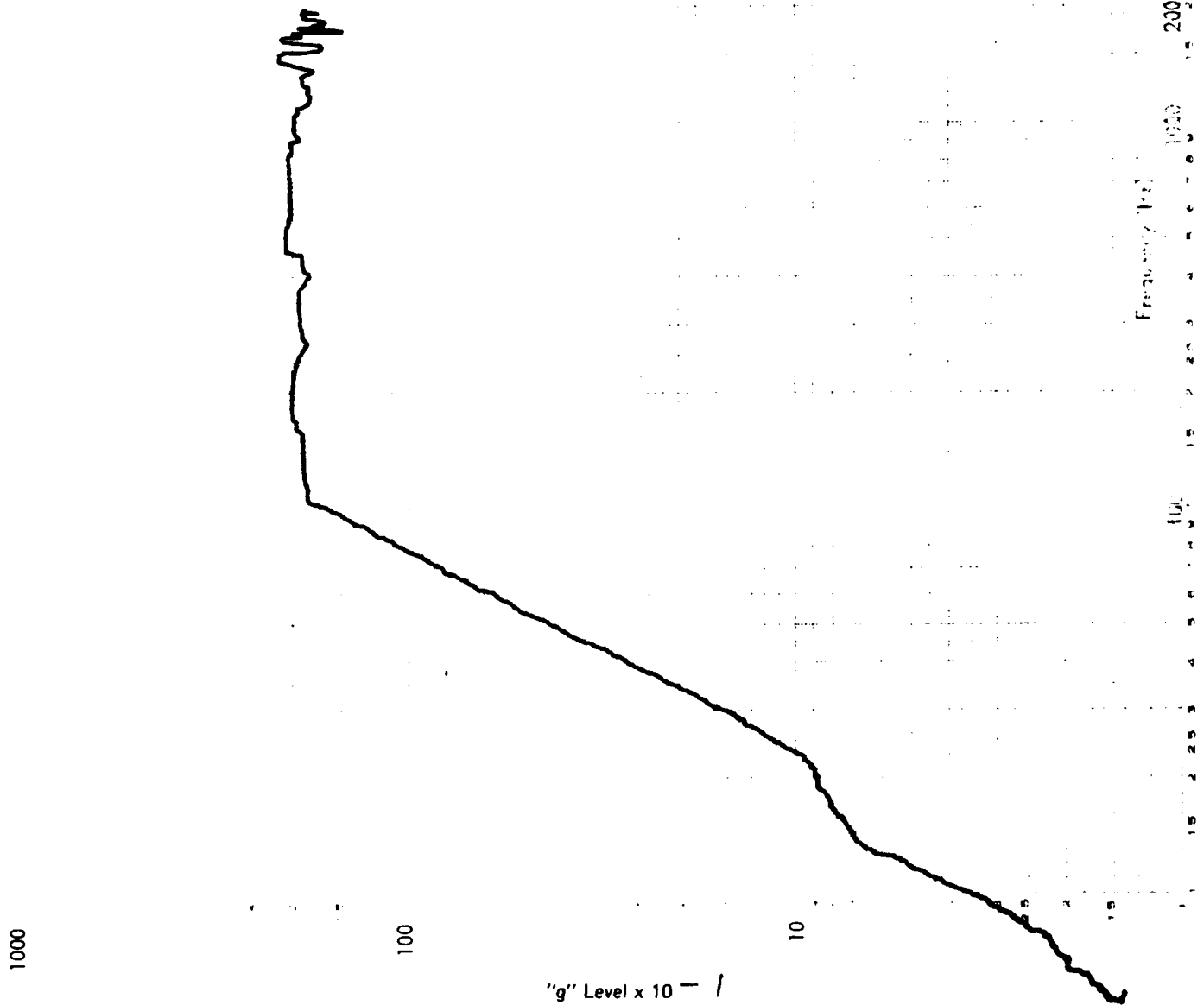
Report No. T-2248-11

Figure 11

Page 11

NADC-80254-60
SINUSOIDAL VIBRATION ANALYSIS

Job Number T-248 Customer Panometers Date 9/15/72
Specimen P N 22249-72-601-29 Specimen S N 001 Test Temp. Room
Axis Z Control Technician SJF



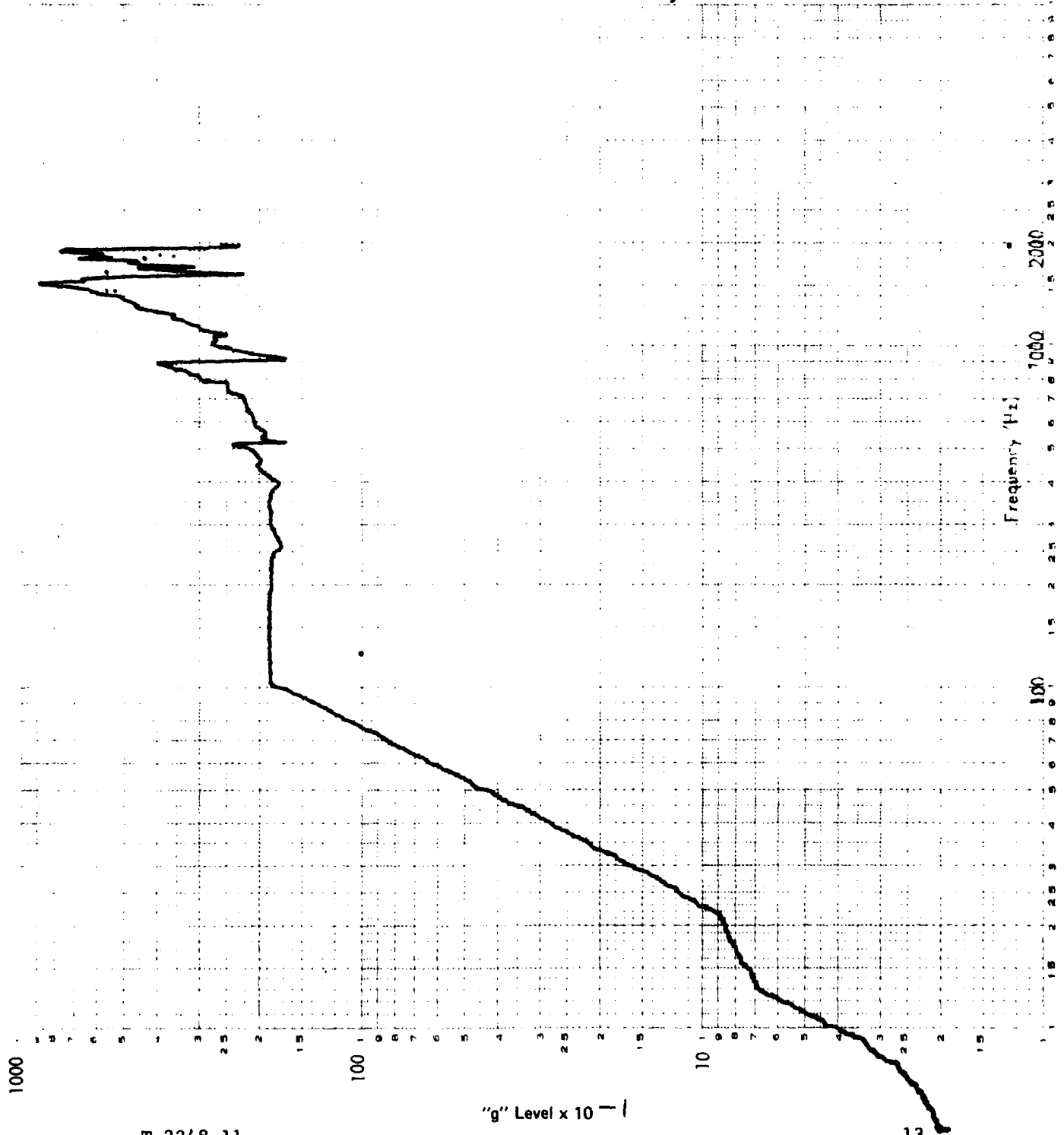
Report No. T-2248-11

"g" Level x 10⁻¹
Figure _____

Page 12

NADC-80254-60
SINUSOIDAL VIBRATION ANALYSIS

Job Number T-2248 Customer Pennametrics Date 9/18/70
Specimen P N 062164-2248-002 Specimen S N 001 Test Temp. Room
Axis Z Motion Technician S/F

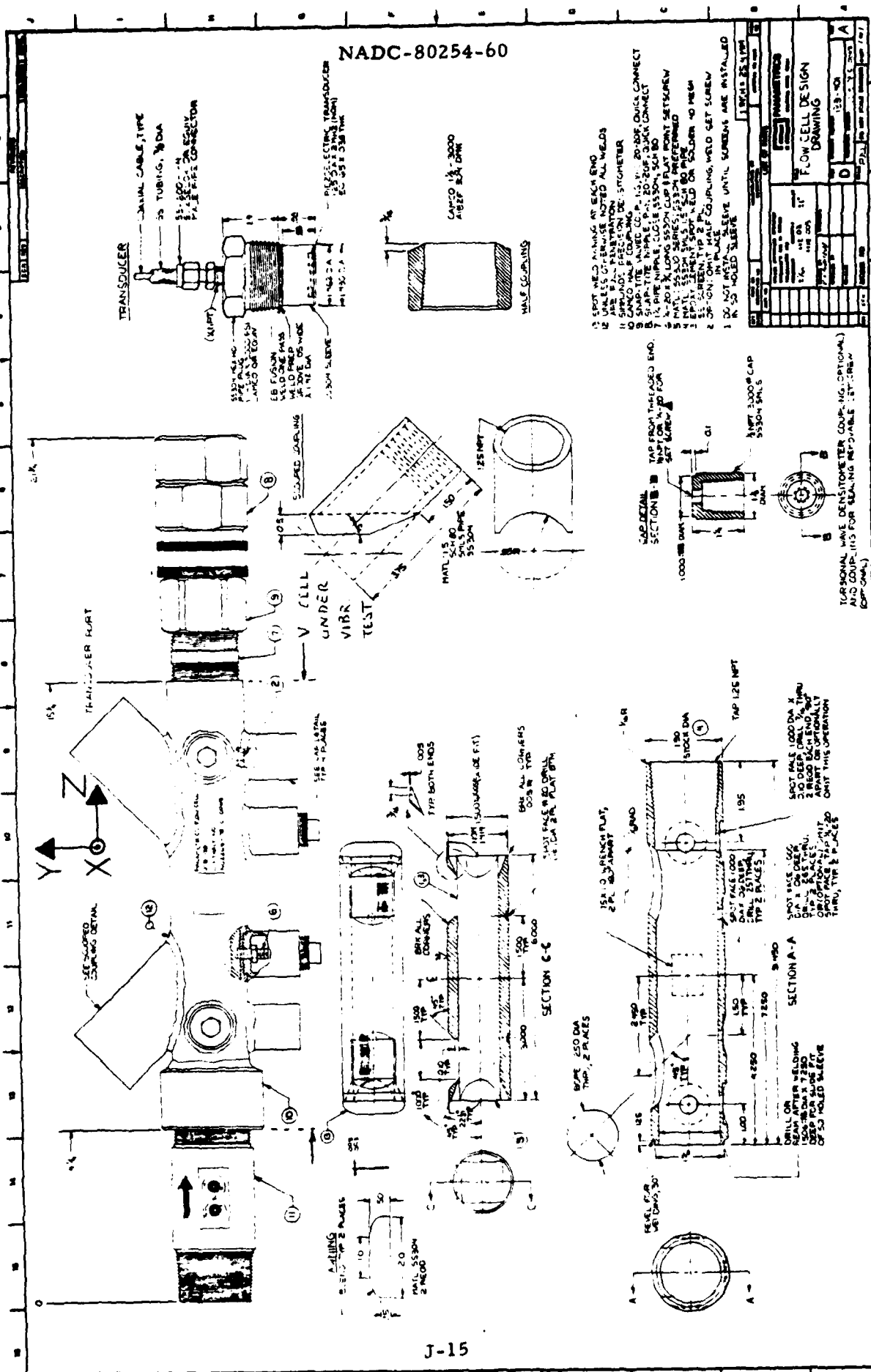


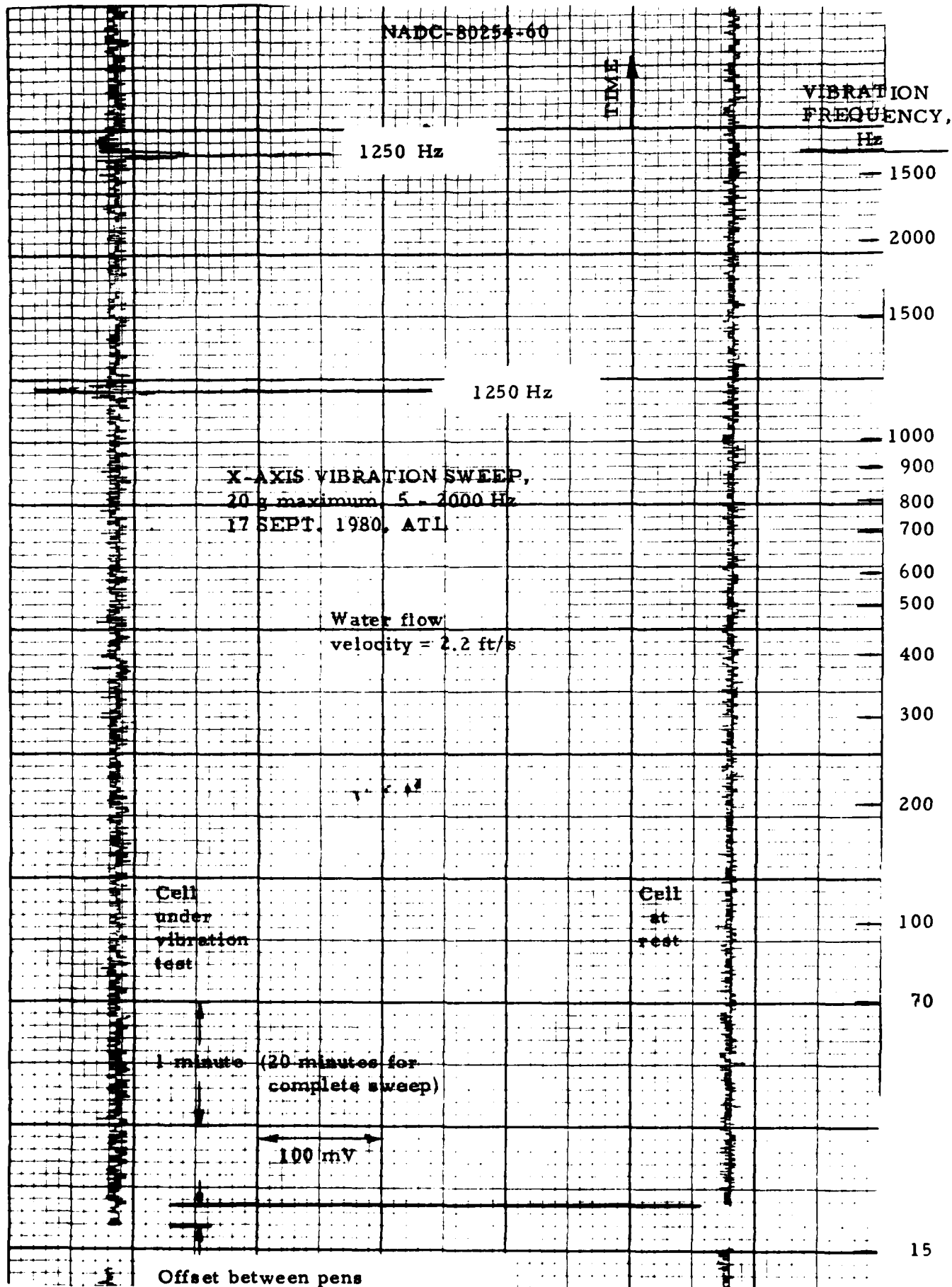
Report No. T-2248-11

Figure _____

Page 13

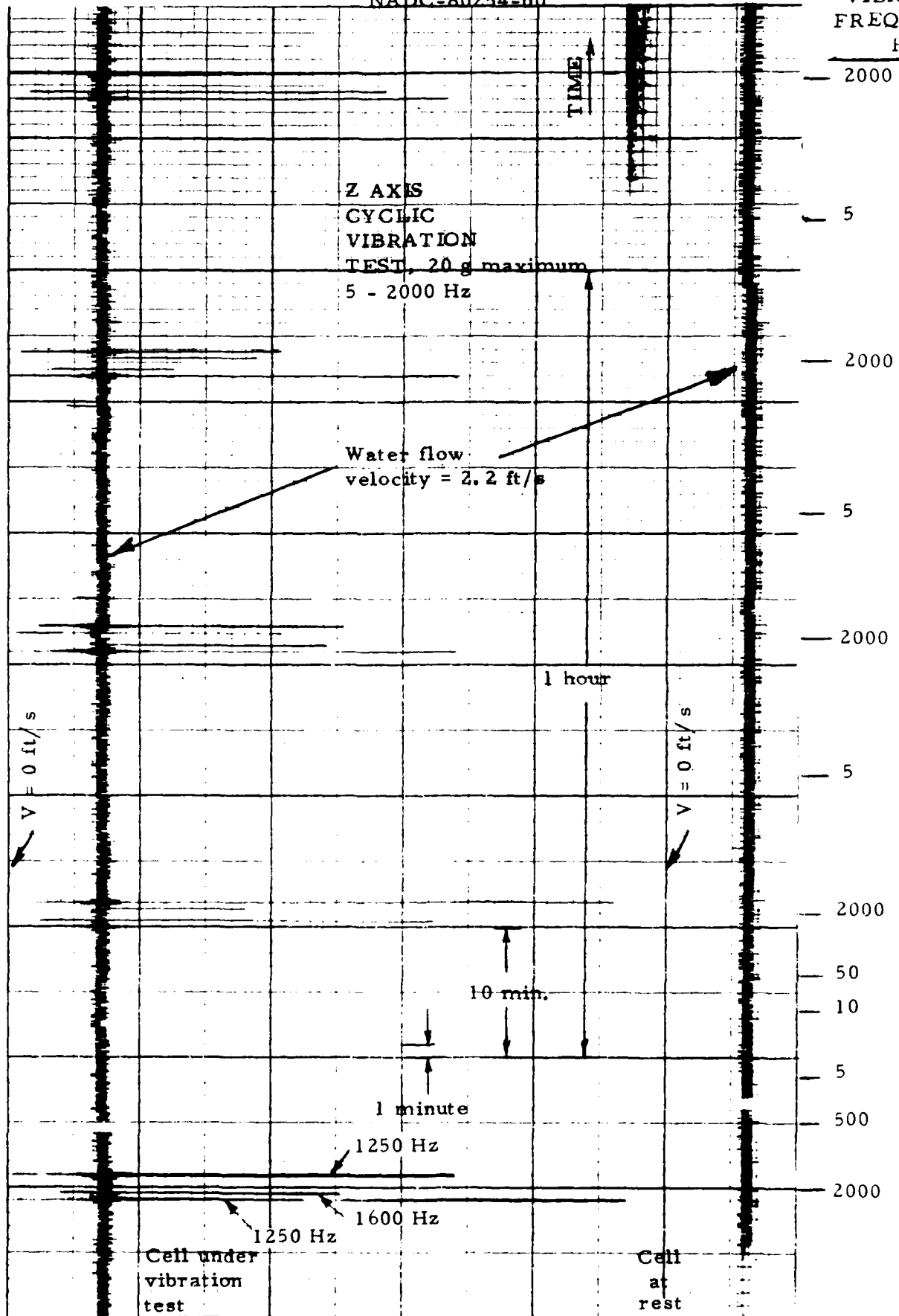
NADC-80254-60





HEWLETT-PACKARD 9280-0288

03



FURTHER COMMENTS ON VIBRATION TEST PROCEDURES AND RESULTS

1. Maximum Flow Rate

The maximum water flow rate through the cell was limited to 3 ft/s (~ 1 m/s) since, at ATL, the source was a city water pressure tap some 50 ft (~ 15 m) from the Ling vibration equipment. Garden hoses were used to bring water to the delivered cell to connect between this cell and the second cell at rest (distance about 10 ft or 3 m), and from the second cell to an outdoor drain. Thus, the total length of garden hose was 110 ft (~ 30 m).

2. Maximum g Load

On 4 and 5 September 1980 several preliminary vibration tests were conducted at ATL using three split collars as simple, low-cost mounts. These collars were bolted to the driver plate using three 1/2 in. - 13 steel bolts. During y-axis vibration, however, the bolts failed several times. Therefore, the mount was redesigned as shown in the ATL report photographs. Prior to bolt failure, the maximum vibration level sensed by an accelerometer on the cell was 140 g's.

It is noteworthy that the flowmeter transducers and electronics operated satisfactorily up to this 140 g level. Also, after the preliminary testing was terminated, the flow cell was disassembled and examined for internal failures. None were found. The cell was reassembled, remounted in the new fixture and subjected to the final vibration tests documented in the ATL report.

3. Vibration-Induced Noise

At a few discrete frequencies, not necessarily the major structural resonances, the noise exceeds the signal at the receiver transducer. This audio frequency noise "gets through" despite ultrasonic bandpass filtering, apparently by means of nonlinear mixing in the transducer element. The approach to eliminating this problem (as evidenced in the recordings on pp. J-16, J-17) would be to determine the source and modify its dimensions and/or its supports and damping.

APPENDIX K. FINAL SYSTEM TEST IN FUEL SUBSTITUTE 7024 BII

On 31 March 1981 and 1 April 1981, at GE, Lynn, Massachusetts, AETD Bldg. 40, Test Stand 76, the M system was tested in three runs covering flow ranges from 95 to 31,450 lb/hr.

The minimum flow rate was determined by the smallest available turbine flowmeter, whose calibration extended down to 114 lb/hr. The maximum was determined by the piping and sensor configuration, i.e., 31,450 lb/hr was the maximum \dot{M} achievable. In runs 1 and 2, the \dot{M} limit of $\sim 27,000$ lb/hr was imposed by the ANC 16 turbine sensor, which probably would have been damaged if higher \dot{M} rates would have been attempted. The high pressure boost pump used in these tests was manufactured by Roth, model No. 31 TEH 9479 BF (92 gpm, 250 psi, 760 TDH).

The fluid was 7024 BII, a fuel substitute commonly used in calibration tests. The Re ranged from ~ 100 to $\sim 10^6$, thereby covering laminar, transitional and turbulent regimes. Temperature ranged from 62.4 to 79.8°F. Pressure ranged from 20 to 220 psig. No vibration isolators, static mixers or flow straighteners were used. See Fig. K1, which shows several views of the test arrangement and test equipment.

Table K1 lists the reference turbine flowmeters used for the three runs, their ranges, test dates and cell parameters. Table K2 lists all relevant data. Dual or multiple entries represent the extremes of turbine and ultrasonic variability at each flow rate, or difference in readings of two different turbine meters at a given flow rate. The apparent larger spread of ultrasonic values is attributed to the sound beam's inertialess response to turbulence, compared to the response of a turbine flowmeter which is smoothed by virtue of the turbine's mass and readout means.

The spread of ultrasonic values, or jitter, has been reported previously by Pedersen et al. (1977)* and independently by Schmidt (1980).** Schmidt's chart recordings demonstrate that the jitter decreases markedly as the integration or averaging time increases from, say, 1 s to 10 s to 100 s, in crude oil clamp-on tests in a 24 inch pipeline. Pedersen et al., quantified the decrease in standard deviation as a function of integration time interval, based on ultrasonic measurements along a 45° path in a 24 inch natural gas pipeline. Integration times were 0.5, 5, 50 and 500 minutes.

*N. E. Pedersen, J. E. Bradshaw, L. C. Lynnworth and P. R. Morel, 293-318, especially Fig. 7, in: L. K. Irwin (ed.), NBS Spec. Publ. 484, Proc. Symp. on Flow in Open Channels and Closed Conduits (1977).

**T. R. Schmidt, Clamp-On Ultrasonic Flowmeters - Application Considerations and Field Test Results, Proc. ISA 1980 Conference, pp. 111-126, ISA, ISBN 87664-491-4, C.I. 80-510 (Oct. 1980).

Schmidt has suggested (private communication, April 1981) that ultrasonic measurements in a more nearly axial direction than his clamp-on geometry allowed, ought to be less responsive to the radial components of turbulence, and hence steadier. This is probably true. However, in tests with the axial offset flow cells used in the present programs, e.g., the ΔH tests, jitter increased as V increased. This jitter may have been mainly due to inlet and outlet turbulence near the tees, which had no flow straighteners or other flow control surfaces in the acoustic path. Perhaps the use of vanes or tubes, especially in the offset path near the inlet (as suggested by Fig. 11) will prove helpful in reducing turbulence and the associated jitter. (See pp. G-10, G-11 for axial path jitter test data.)

The reference \dot{M} is computed by the Cox system based on a selected turbine sensor and the measured fluid temperature. Uncertainty is stated to be 1/2% of reading, presumably three standard deviations. Because different turbine sensors were used in each run above 600 lb/hr, the difference between the ultrasonic \dot{M} and the reference \dot{M} is not the same in each run.

From the raw \dot{M} data it is clear that the ultrasonic \dot{M} readout is proportional to the actual \dot{M} as measured by the various turbine sensors. The constant of proportionality was determined by comparing the averages of all the valid ultrasonic data shown in column 4 of Table K2. The \dot{M} values of column 4 are plotted versus the corresponding average turbine \dot{M} in Fig. K2. In this plot, representing three runs covering \dot{M} from 95 to 31,450 lb/hr, the results are evidently linear with respect to full scale flow. Deviations from linearity, expressed as percent of reading, are largest in the bottom tenth of the meter's range, i.e., below 3000 lb/hr (Table K3).

Table K2 also lists the flow velocity \bar{V} , computed from the Cox \dot{M} , fluid temperature T , pipe area A , and specific gravity $SG = 0.767 - 0.000435(T - 70^\circ F)$. $\bar{V} = Q/A$; $Q = \dot{M}/\rho = \dot{M}/62.4 SG \text{ cu ft/hr} = 1.998 \times 10^{-3} \dot{M}/SG \text{ gpm}$. \bar{V} was also measured ultrasonically in a vertical axial offset flow cell built from a 1 inch schedule 40 pipe x 12 inches long and two tees, with transducers at each end. These transducers had buffers (similar to those in the zigzag cell) to prevent gas trapped in the top tee from blocking the acoustic wave. The corrected ultrasonic V is plotted versus \bar{V} calculated from the turbine data in Fig. K3. Remarks on linearity are similar to remarks for the zigzag cell. For both cells, no hysteresis, temperature, pressure or drift effects were observed.

Besides the numerical data of Table K2, oscillographic data showing waveforms for the zigzag and axial offset cells are of interest (Fig. K4). These waveforms illustrate several aspects of the ultrasonic measurements, such as basic time intervals t_1 , t_2 and $\Delta t = t_2 - t_1$; waveform stability in the zigzag cell at the maximum flow rate achievable in the test stand for the given piping configuration (31,450 lb/hr); waveform jitter in the offset

cell (without flow control surfaces) as observed between 18,000 and 25,000 lb/hr. The similarity and stability of the upstream and downstream waveforms and high signal to noise ratio for the zigzag cell at all flow rates in these \dot{M} tests (maximum flow velocity $V_{\max} = 26.2$ ft/s or 8 m/s in the 1 inch square hole) indicates that the present design is usable to even higher flow rates. (The Foxboro water flow tests previously demonstrated that flows up to at least 38 ft/s (11.6 m/s) could be covered with the present 1 inch square hole zigzag design.)

By comparing the raw ultrasonic \dot{M} and turbine \dot{M} data for 7024 BII, one can generate correction factors which comprise a look-up table linearization algorithm. This was programmed into the delivered equipment. This algorithm serves a function equivalent to the dynamic profile compensation program that the model 6000 velocimeter uses in conventional tilted diameter interrogations. For example, when the beam diameter d is much less than the duct diameter D and if the turbulent profile follows the universal velocity distribution law:

$Re \leq 2000$	$K = 0.750$
$2000 < Re < 4000$	$K = 0.840$
$Re \geq 4000$	$K = 1/(1.119 - 0.011 \log Re)$

Table K1. Turbine flowmeter and ultrasonic flow cell parameter data.

<u>Cox turbine flowmeter</u>	<u>Date used</u>	<u>am or pm</u>	<u>Run no.</u>	<u>Range, pph</u>
ANC 8-6, S/N23030	31 March 1981	am & pm	1 & 2	114 to 2280
ANC 16, S/N 10382	31 March 1981	pm	2	600 to 24,000
ANC 24, S/N23803	31 March 1981	am	1	990 to 59,000
ANC 24, S/N23801	1 April 1981	am	3	990 to 59,000

<u>Ultrasonic cell</u>	<u>L mm</u>	<u>P mm</u>	<u>A mm²</u>	<u>t_w μs</u>	<u>X mm</u>	<u>Flow axis orientation</u>
Square hole zigzag	102	274.3	651.6	10	30	Horizontal
Axial offset	353.3	404.8	557.6	6.5	20	Vertical

Table K2. Test data for run 1, using 7024 BU fluid. Site: GE - Lynn, AETD, Bldg. 40, Afterburner Control Stand No. 76. Date: 31 March 1981, a.m.

Mass Flow Rate M Data and Calculations				Fluid Property Data			Flow Velocity V in Axial Offset Flow Cell				
Cox Turbine, lb/hr		Panametrics, lb/hr		Difference Between Averages %	Pressure psig	Temp. of °F	Specific Gravity	Calc. from Cox M and Temp. ft/s	Measured Ultrasonic Reading ft/s	Corrected Ultrasonic Reading ft/s	Difference %
M Extremes	Average of Extremes	Extremes	Corrected Average of Extremes (Col. 34.1.13)								
192	195	150	157	-19	30	76.35±.05	0.764	0.19	.23	0.203	+6.7
198		204							.22		
497	499	485	449	-10.0	20	78.00±.1	0.764	0.48	.55	0.486	+1.4
501		530							.53		
999	1002	1050	965	-3.7	20	79.45±.05	0.763	0.97	1.11	0.991	+2.2
1005		1130							1.09		
2981*	3010	1585	1475	-51	25	80.05±.05	0.763	2.93	1.59	1.450	-50.5
3038		1749							1.63		
5004	5008	5666	5051	+0.9	66	79.45±.05	0.763	4.87	5.34	4.865	-0.1
5011		5750							5.46		
10002	10021	11176	9983	-0.4	88	78.65±.05	0.763	9.74	10.6	9.64	-1.0
10040		11385							10.8		
17930	17955	19900	17681	-1.5	88	77.10±.1	0.764	17.43	18.6	17.12	-1.8
17979		20058							19.4		
9943	9962	11127	9944	-0.2	76	78.45±.05	0.763	9.68	10.6	9.685	0.0
9981		11346							10.9		
4949	4957	5583	5002	+0.9	85	78.95±.05	0.763	4.82	5.31	4.815	-0.1
4964		5720							5.38		
3004	3009	3351	3021	+0.4	80	79.20±.1	0.763	2.93	3.19	2.905	-0.8
3015		3477							3.26		
381.1	384	369	350	-8.9	51	79.75±.05	0.763	0.37	.43	0.414	+12.0
387.0		420							.49		
3074	3077	3433	3086	+0.3	99	80.	0.763	2.99	3.21	2.93	-1.9
3081		3540							3.30		

*Turbine sensor ANC 24, S/N 23803 was found to be defective during this first run. Post-test examination confirmed malfunction. Therefore in this run, data at actual flow rates between 990 and 2500 lb/hr are to be disregarded.

Table K2, continued. Run 2.

Mass Flow Rate M Data and Calculations				Fluid Property Data				Flow Velocity V in Axial Offset Flow Cell			
Cox Turbine, lb/hr	Parametrics, lb/hr			Difference Between Averages %	Pressure psig	Temp. of	Specific Gravity	Calc. from Cox M and Temp. ft/s	Measured Ultrasonic Reading ft/s	Corrected Ultrasonic Reading ft/s	Difference %
	Average of Extremes	Extremes (Col. 3+1.13)	Corrected Average of Extremes								
M Extremes	27020	30458	26862	-0.7	83	76.6	0.764	26.26	-	-	-
	27080	30250							-	-	-
24980	25000	27750	24668	-1.3	72	76.95±0.5	0.764	24.27	-	-	-
25020		28000							-	-	-
20180	20205	22546	20029	-0.9	54	77.35±0.5	0.764	19.62	21.0	19.3	-1.6%
20230		22720							21.8		
14980	15015	16806	14984	-0.2	130	77.15±0.5	0.764	14.58	16.1	14.5	-0.5
15030		17058							16.2		
10030	10040	11265	10051	+0.1	120	77.55±0.5	0.764	9.75	10.9	9.77	+0.2
10050		11451							10.8		
5020	5025	5715	5095	+1.4	130	78.05±0.5	0.763	4.88	5.43	4.92	+0.8
5030		5800							5.48		
3070	3080	3467	3117	+1.2	82	78.55±0.5	0.763	2.99	3.25	2.96	-1.0
3090		3578							3.33		
990	995	1067	981	-1.4	29	79.15±0.5	0.763	0.97	1.07	0.98	+1.0
1000		1151							1.10		
494.5	496	479	457	-7.9	24	79.55±0.5	0.763	0.48	.54	0.49	+2.1
496.5		554							.55		
208.3	210	263	216	+2.9	24	79.55±0.5	0.763	0.20	.24	0.221	+10.5
211.7		225							.25		
94.1	95	141	94	-1.1	25	79.45±0.5	0.763	0.09	.11	0.104	+15.1
96.1		71							.12		
257.1	258	239	272	-12.0	22	79.55±0.5	0.763	0.25	.29	0.266	+6.3
259.0		272							.30		
600	605	599	643	-10.2	56	79.4	0.763	0.59	.67	0.608	+3.1
610		628							.68		
1120	1125	1254	1135	+0.9	90	78.85±0.5	0.763	1.09	1.25	1.14	+4.6
1130		1311							1.29		
3080	3085	3489	3145	+1.9	48	78.45±0.5	0.763	3.00	3.25	2.96	-1.3
3090		3614							3.32		
6040	6060	6474	6146	+2.2	87	78.15±0.5	0.763	5.89	6.50	5.91	+0.3
6080		7129							6.62		
12060	12075	13518	12071	0.0	100	77.8	0.764	11.72	13.0	11.76	+0.3
12090		13761							13.1		
22180	22200	24583	21420	-1.4	159	76.65±0.5	0.764	21.55	23.3	21.17	-1.8
22220		24957							23.7		

Table K2, continued. Run 3.

Mass Flow Rate M Data and Calculations				Fluid Property Data				Flow Velocity V in Axial Offset Flow Cell			
Cox Turbine, lb/hr		Panametrics, lb/hr		Difference Between Averages %	Pressure psig	Temp. °F	Specific Gravity	Calc. from Cox M and Temp. ft/s	Measured Ultrasonic Reading ft/s	Corrected Ultrasonic Reading ft/s	Difference %
M Extremes	Average of Extremes	Extremes	Corrected Average of Extremes (Col. 3+1.13)								
0		-40 -90	-65		-						
11540	11548	13016	11621	+0.6	29	64.5	0.769	11.14	12.3	11.13	-0.1
11550		13248							12.4		
31430	31450	35270	31336	-0.4	100	62.4	0.770	30.30	-	-	-
31470		35550							-		
25430	25455	28533	25386	-0.3	158	64.05±0.5	0.770	24.52	-	-	-
25480		28839							-		
24010	24020	27020	24023	0.0	168	64.25±0.5	0.770	23.14	-	-	-
24030		27284							-		
20980	21000	23568	20984	-0.1	194	64.45±0.5	0.769	20.25	22.0	20.14	-0.6
21020		23855							22.7		
19030	19045	21402	19045	0.0	204	64.7	0.769	18.37	20.2	18.38	0.0
19060		21639							20.6		
15930	15965	17899	15997	+0.2	214	65.15±0.5	0.769	15.40	17.3	15.54	+0.9
16000		18255							17.2		
11100	11110	12509	11197	+0.8	115	66.15±0.5	0.769	10.71	11.3	10.77	+0.5
11120		12796							12.1		
3980	3975	4507	4028	+1.3	98	67.35±0.5	0.768	3.84	4.32	3.87	+0.6
3970		4596							4.26		
6960	6950	7907	7065	+1.7	99	67.55±0.5	0.768	6.71	7.41	6.71	0.0
6940		8060							7.49		
13550	13565	15344	13650	+0.6	87	67.15±0.5	0.768	13.11	14.5	13.11	0.0
13580		15506							14.6		
16890	16940	19058	16967	+0.2	125	66.8	0.768	16.37	18.2	16.53	+1.0
16990		19288							18.5		
23000	23020	25795	22965	-0.2	122	66.35±0.5	0.769	22.20	23.9	22.03	-0.8
23040		26106							25.0		
28000	27975	31397	27917	-0.3	109	65.85±0.5	0.769	27.00	-	-	-
27930		31694							-		
29440	29010	32404	28861	-0.5	112	65.5	0.769	27.47	-	-	-
29030		32822							-		
29060	30090	33643	29944	-0.4	92	65.2	0.769	29.93	-	-	-
30040		33416							-		

NADC-80254-60

Table K2, continued, Run 3.

25740	25755	28892	25725	-0.1	115	65.15±0.5	0.769	24.84	27.2	24.19	-2.6
25770		29245							26.5		
24190	24200	27221	24181	-0.1	120	64.95±0.5	0.769	23.34	24.9	22.93	-1.8
24210		27427							26.0		
26920	26930	29939	26609	-1.2	145	76.35±0.5	0.764	26.15	-	-	-
26940		30196							-	-	-
18210	18220	20366	18130	-0.5	187	76.6	0.764	17.69	19.7	17.61	-0.5
18230		20608							19.4		
9100	9110	10262	9163	+0.6	220	77.3	0.764	8.84	9.82	8.87	+0.3
9120		10445							9.86		
1540	1535	1647	1527	-0.5	110	78.25±0.5	0.763	1.49	1.68	1.53	+2.7
1530		1805							1.71		
630	635	635	594	-6.5	115	78.4	0.763	0.62	.72	0.644	+3.9
640		706							.71		
1970	1975	2194	1999	+1.2	110	78.5	0.763	1.92	2.13	1.94	+1.0
1980		2323							2.18		
19960	19970	22274	19811	-0.8	112	77.05±0.5	0.764	19.39	21.2	19.28	-0.6
19980		22497							21.6		
25870	25885	28755	25550	-1.3	152	76.05±0.5	0.764	25.13	-	-	-
25900		29000							-	-	-
7980	7990	9000	8044	+0.7	140	77.3	0.764	7.76	8.61	7.78	+0.3
8000		9179							8.66		
3060	3065	3469	3130	+2.1	149	77.9	0.764	2.98	3.27	2.97	-0.3
3070		3605							3.33		
720	725	767	732	+1.0	62	78.35±0.5	0.763	0.70	.79	0.71	+1.4
730		886							.78		
336	337	319	304	-9.8	32	78.55±0.5	0.763	0.33	.38	0.35	+6.1
338		368							.39		

Table K3. Rms deviation from linearity expressed as percent of reading.*

Range of M, lb/hr	Run 1	Run 2	Run 3	Average
0-2999	11.77	6.22	-	7.91
3000-5999	0.68	1.69	1.3	1.29
6000-8999	-	1.63	1.7	1.66
9000-11999	0.32	0.43	0.71	0.51
12000-14999	-	0	0.6	0.6
15000-17999	1.5	0.2	0.2	0.77
18000-20999	-	0.75	0	0.65
21000-23999	-	1.4	0.16	0.82
24000-26999	-	1.27	0.08	0.90
27000-29999	-	0.7	0.41	0.53
30000-32999	-	-	0.4	0.4

* Different turbine sensors, each normally accurate to $\pm 0.5\%$ of reading, were used above 600 lb/hr in each run. See Table K1.

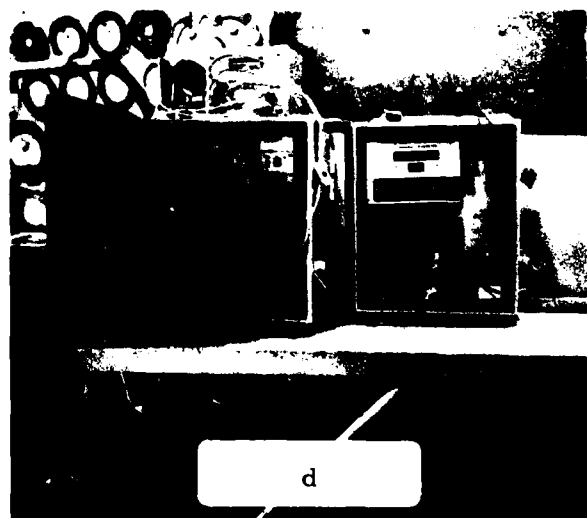
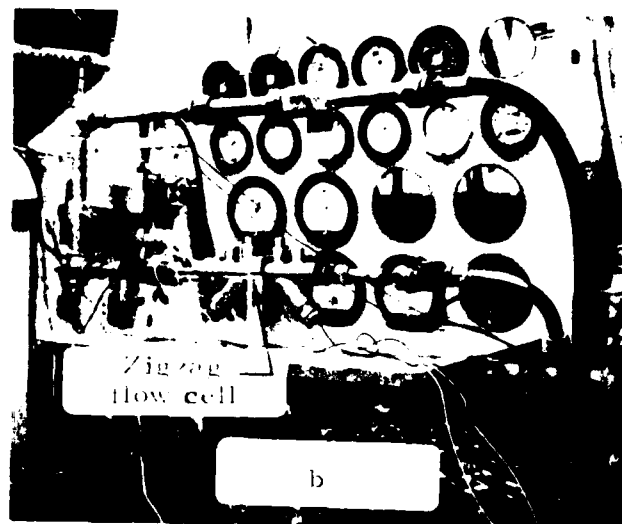
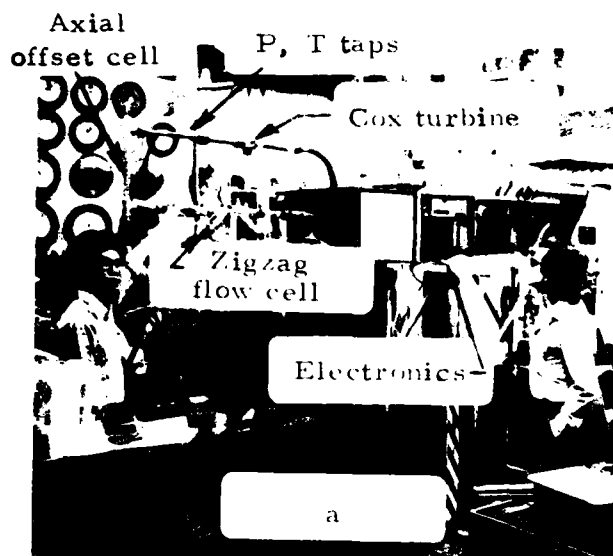


Fig. K-1. Mass flowmeter under final fuel substitute (7024 B II) test at GE-Lynn. (a) General view. (b) Close-up of flow cell, other sensors and piping. (c) Operator reading mass flow rate. (d) Close-up of mass flow rate instrument (left) and volumetric flow rate instrument associated with vertical axial offset cell. Dates of test: 31 March and 1 April 1981. Photos courtesy of General Electric, Lynn, MA.

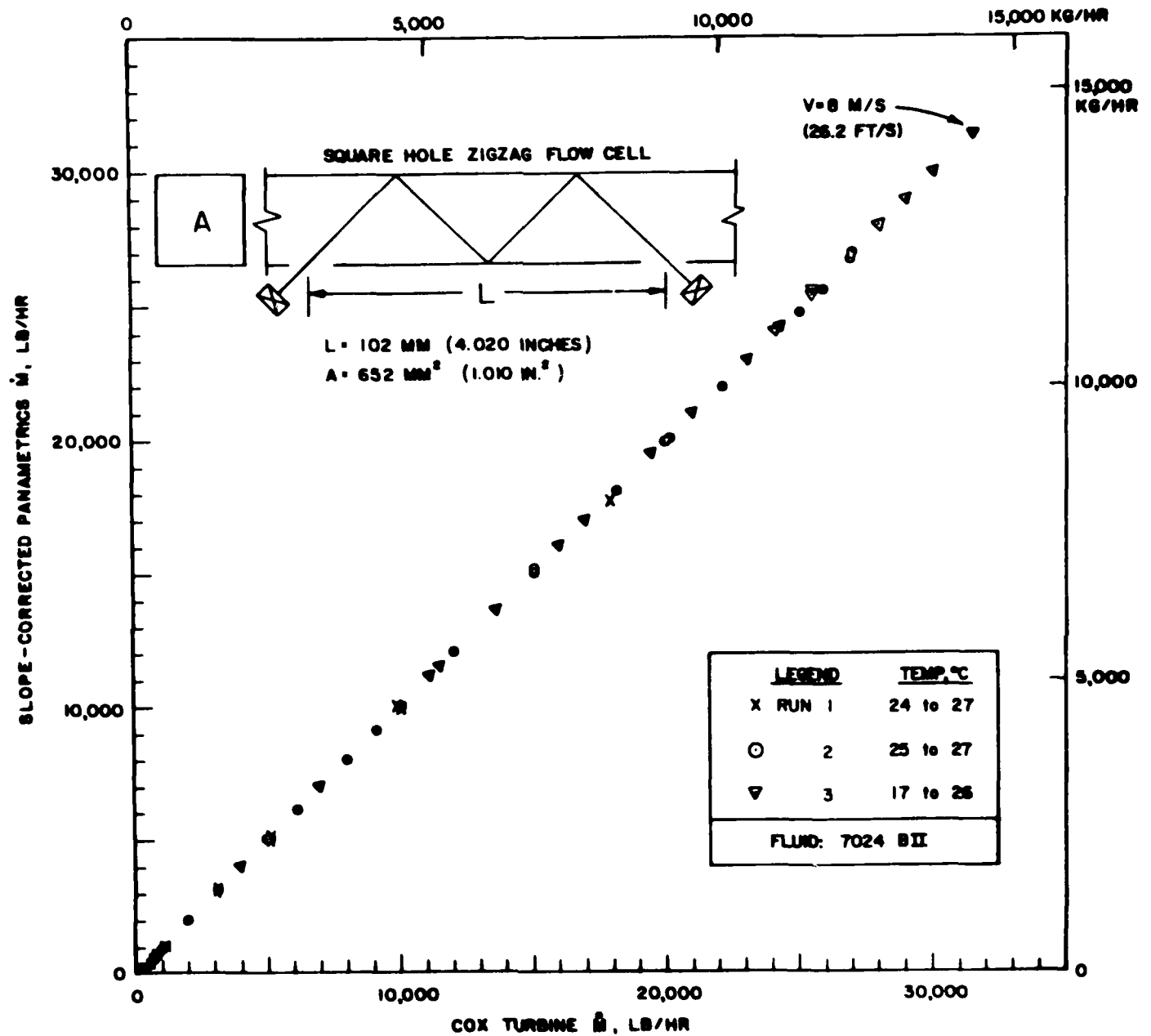


Fig. K2. Corrected Panametrics mass flow rate (\dot{M}) versus Cox turbine flowmeter mass flow rate, runs 1, 2 and 3. Dates of tests: 31 March and 1 April 1981. Site: GE-Lynn.

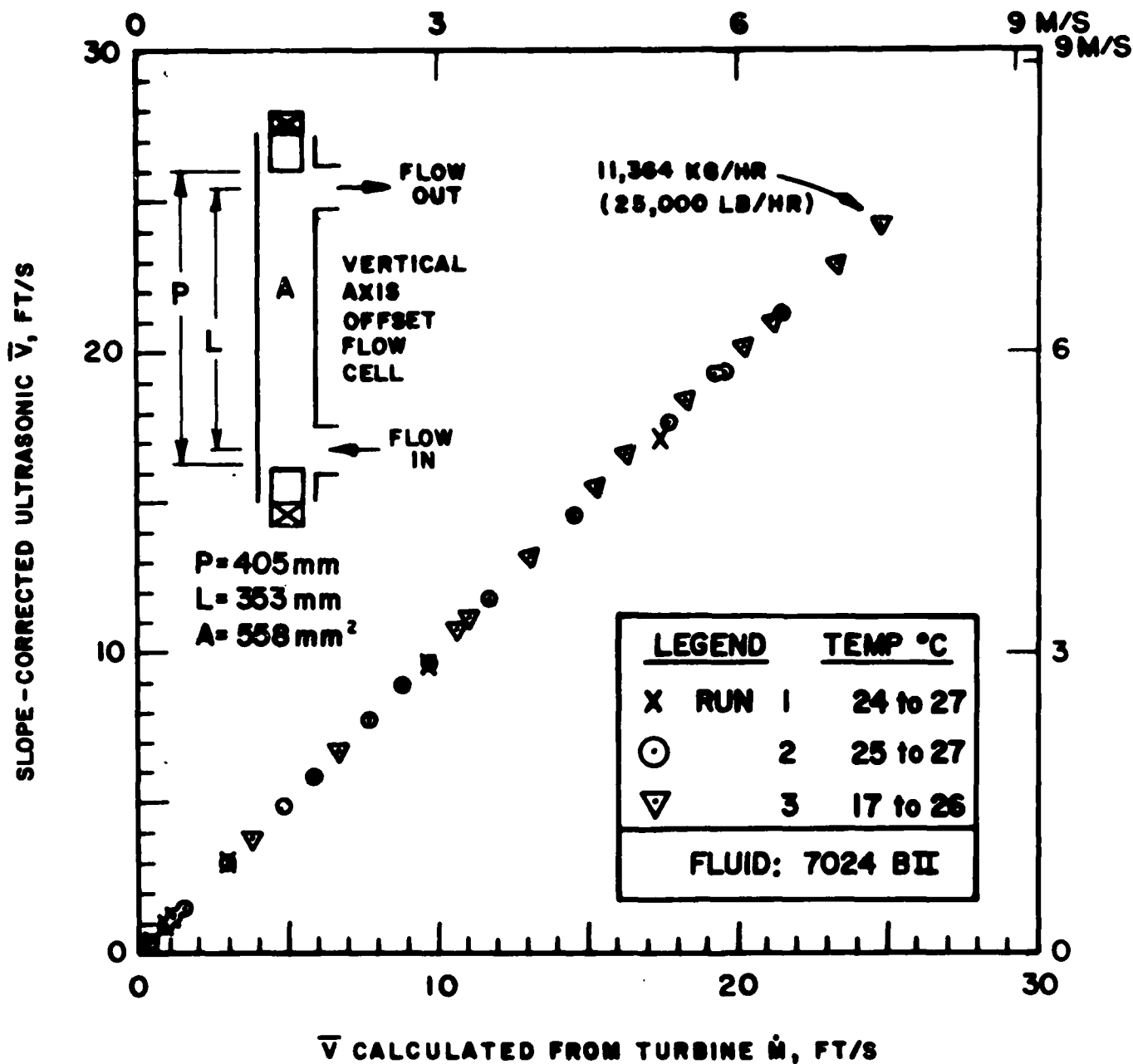
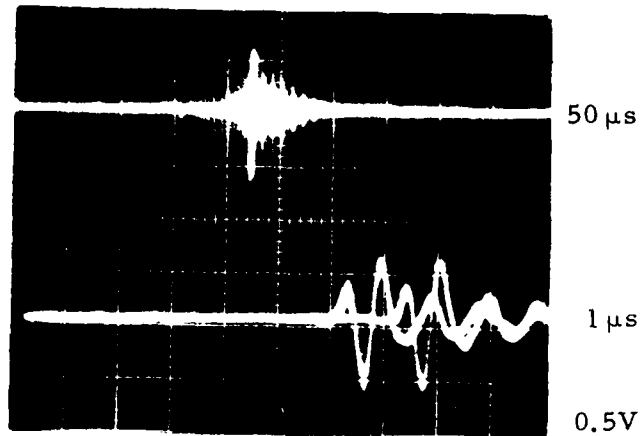


Fig. K3. Corrected ultrasonic \bar{V} versus value calculated from turbine flowmeters. Dates of tests: 31 March and 1 April 1981. Site: GE-Lynn.

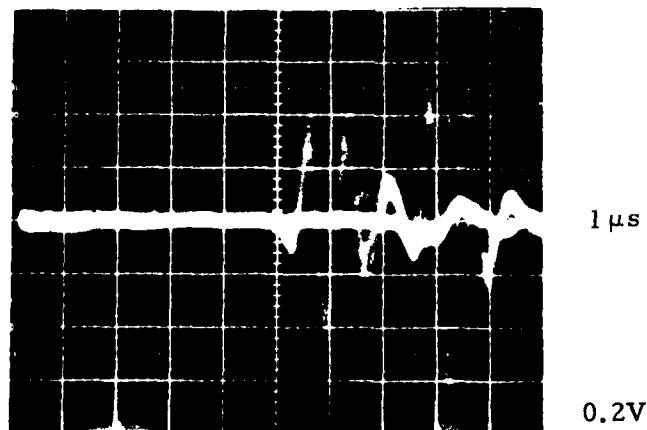


Cell: Zigzag square hole

$\dot{M} = 31,480$ pph
(14,309 kg/hr)

$t = 220 \mu s$; $\Delta t = 1.2 \mu s$

$T = 62.4^\circ F$



Cell: Axial offset

$\dot{M} = 18,000$ pph
(8182 kg/hr)

$t = 300 \mu s$; $\Delta t = 2.3 \mu s$

Fig. K4. Oscillograms of received ultrasonic signals in zigzag and offset cells, using 7024 BII fluid at GE-Lynn. Date of test: 31 March 1981.

NAVY CALIBRATION CORRECTION

The following procedure has been implemented in the software of the Navy flowmeter to correct the flow measurement using calibration data: *

$$V_{\text{corrected}} = V \times K_i$$

where

$$V = \frac{2 \times P^2}{L} \times \frac{(T_{\text{up}} - T_{\text{down}})}{(T_{\text{up}} + T_{\text{down}} - 2 T_w)^2}$$

$$V_i < V < V_{i+1}$$

<u>i</u>	<u>V_i</u>	<u>K_i</u>
1	0	1.000
2	.2	.970
3	.4	.940
4	.6	.920
5	.8	.900
6	1.0	.890
7	1.2	.885
8	1.4	.880
9	1.6	.875
10	1.8	.868
11	2.0	.865
12	3.0	.850
13	4.0	.847
14	5.0	.847
15	6.0	.850
16	7.0	.855
17	8.0	.860
18	9.0	.862
19	10.0	.865
20	11.0	.867
21	12.0	.869
22	13.0	.870

*Calibration data obtained using 7024 BII fuel substitute at GE, Lynn, MA on 31 March and 1 April 1981. Data in NADC-80254-60.

APPENDIX L. NAVY MASS FLOWMETER INITIAL SET-UP.

1) The mass flowmeter consists of two electronic circuits. The first is the Simmonds Precision electronics associated with the SP densitometer cell. The second is the Panametrics' ultrasonic flowmeter associated with the zigzag flow cell.

2) SP connections:

a) The SP density flow cell has two connections on it. One is marked H and the other is unmarked. There are two cables that connect the cell to the SP electronics. The connectors are keyed at their connection to the electronics. The cable that connects to the noninsulated BNC connector connects to the connector labeled H at the cell. The cable connection at the cell for H also has a length of white shrink tubing over it which the other cable does not. Both cables that interconnect the cell and electronics are white and both must be connected for correct operation.

b) The connection of the SP electronics to the flowmeter electronics is done with three single conductor cables. On the SP unit there are three binding posts labeled: +15 (RED), GND (BLACK) and OUTPUT (YELLOW). On the flowmeter electronics on the right side there is a 12 position double row terminal block (see Fig. 19). The bottom three terminals are labeled: +15V, ANALOG INPUT, and CIRCUIT GND. There are connections already on one row of the three terminals that connect into the flowmeter. The SP terminal labeled +15 connects to the flowmeter terminal labeled +15V, the SP terminal labeled GND connects to the flowmeter terminals labeled CIRCUIT GND and the SP terminal labeled OUTPUT connects to the flowmeter terminal labeled ANALOG INPUT.

3) The flowmeter to transducer connections are made with two coaxial cables. At the flowmeter the cables attach to the BNC connectors labeled XMTA/RCVB and XMTB/RCVA. At the flow cell the cables attach to the transducers with Microdot connectors. There is no preference for which cable attaches to which transducer unless the digital display is used. In this case the transducer located upstream with respect to flow through the flow cell is connected to the BNC terminal at the flowmeter labeled XMTB/RCVA, and the downstream transducer to the BNC connector labeled XMTA/RCVB.

4) The line power connections for the flowmeter are made on a 10 position, single row terminal block on the right side of the flowmeter. The bottom three terminals are used and are labeled N, L, and GND $\frac{1}{2}$. The 120 VAC connections are made to N and L while the earth ground connection is made to the GND terminal.